UV CURABLE POWDER COATINGS FOR THE FINISHING OF LEATHER

Xingsheng Jiang

Supervisors:
Prof. Geoffrey Edward Attenburrow
Dr. Jifeng Ding and Prof. Anthony Dale Covington

This thesis is submitted for the degree of Doctor of Philosophy at the University of Northampton

Division of Leather Technology, School of Applied Sciences
The University of Northampton
UK

Year of submission: 2007

UNIVERSITY OF NORTHAMPTON
PARK LIBRARY
ACC. No. 10352462
CLASS NO. D675 · 25 JIA

Acknowledgements

I would like to take this opportunity to thank my supervisors, Prof. Geoff Attenburrow at the British School of Leather Technology, The University of Northampton and Dr. Jifeng Ding at the Division of Chemistry and Materials, Manchester Metropolitan University, who successfully applied to the EPSRC for financial support for the powder coating project and Prof. Anthony Dale Covington also at the British School of Leather Technology, for their guidance and help.

I must also thank and acknowledge Mrs Pat Potter and other technicians for help in the laboratories; Mr. Karl Flowers for his support for this research work in the tannery; Dr. Sujee Jayapalina and Dr. Paula Antunes for guidance on operating various instruments, and other staff of the British School of Leather Technology for help.

Thanks also to BLC Leather Technology Center for use of its facilities.

To:

My beloved

Mrs. Dongmin Liang

She left her loved doctor post for supporting my doctoral

degree of philosophy

Table of Contents

Abstract

A novel powder coating binder system based on UV-curable, semi-crystalline polyurethane acrylates has been developed for heat-sensitive and highly flexible substrates, such as leather. The developed powder coating film had good abrasion and adhesion properties. The concepts applied in this work were based on the adjustment and control of the degree of crystallinity of binders by three ways: (i) formulating different molecular weight monomers for random copolymerization, (ii) introducing functional monomer with pendant groups and (iii) cross-linking during curing. Amongst the three approaches explored in this work, a combination of branching and cross-linking was found most successful. A crystalline binder with cross-linkable pendant groups was employed as the powder coating main binder; this is the major difference from other work on powder coatings where amorphous resin alone or partially blended with a crystalline component are used as binders.

The preparation of UV curable powder coating binder resins and their properties, such as crystallinity, viscosity and tensile modulus and elongation to break have been studied by DSC, SEM, FTIR-ATR and DMTA methods. It was found that the polyurethane acrylate binders (made from DHBA, BEP, DEG and HDI etc.) are potentially useful for formulating novel powder coatings. The properties of the developed powder coating finished leather have been tested. Hot plating processes and an EMB application method for leather finishing have been discussed as well.

Nano-scale silica particles surface modified with acrylate has been studied, and their properties or properties of powder coatings formulated with the particles have been characterized. The powder coating rub fastness was improved by formulation with surface modified nano-scale silica particles.

Key words Powder coating; UV-curing; UV curable powder coating; Leather Finishing; Heat sensitive substrate; Semi-crystalline polymer; Polyurethane acrylate; Surface modified nano-scale silica; Hot-plating process.

Symbols and Abbreviations

A	absorbance
ABG	anti-bumping granules
AC	acryloyl chloride
AEDD	5-acryloyloxymethyl 5-ethyl 2,2-dimethyl 1,3-dioxolane
AHK	alpha-hydroxy ketone
BAPO	bisacylphosphine oxide
BDMK	benzyldimethyl ketal
BEP	2-butyl-2-ethyl-1,3-propanediol
BHB	2,2-bis(hydroxymethyl) butyric acid
BIA	biacrylate
C	crystallinity
CF	chloroform
ε-CL	ε-caprolactone
CP	cloud powder coating
DEG	diethylene glycol
DHBA	dihydroxymethyl butyl acrylate
DMA	dynamic mechanical analysis
DMPA	2,2-dimethylolpropionic acid
DMTA	dynamic mechanical thermal analysis
DSC	differential scanning calorimetry
E	Young's modulus
EAA	ethyl acetoacetate
EHDD	5-ethyl 5-hydroxymethyl 2,2-dimethyl 1,3-dioxolane
EMB	electro magnetic brush
etc.	et cetera
Exp.	experiment
FTIR-ATR	fourier transform infrared attenuated total reflection spectroscopy
G	shear modulus

G_d	cross-linking degree
GLY	glycerine
ΔH	heat of fusion
$\Delta H_{100\%}$	heat of fusion of the corresponding 100% crystalline polymer
h	hour
HDI	hexamethylene 1,6-diisocyanate
I	intensity of transmitted light
IEM	isocyanatoethyl methacrylate
IR	infrared
K_g	kilogram
m_d	the dry mass of the sample
MDF	medium density fibreboard
MDI	4,4′- methylene diphenylene diisocyanate
min.	minute
m_{iso}	the isolated mass of the sample
No.	number
PA	polyacrylics
PCL	polycaprolactone
PCL-530	PCL diol Mn=530
PCL-1250	PCL diol Mn=1250
PCL-2000	PCL diol Mn=2000
PET-EH	polyester-epoxy hybrid
PET-T	polyester-TGIC
POM	polarised optical microscope
PU	polyurethane
PUA	polyurethane acrylate
PTMA	polytetramethylene adipate
PVC	polyvinyl chloride
RPM	revolutions per minute
R_f	retention factor
SBB	sodium 2,2-bis(hydroxyl methyl) butyrate

SEM	scanning electron microscope
SMS	stable micro system
TEA	triethylamine
T_g	glass transition temperature
THAS	triethylamine hydrochloric acid salt
THF	tetrahydrofuran
TLC	thin layer chromatograph
T_m	melting temperature
TMP	trimethylolpropane
TPMA	3-(trimethoxysilyl)propyl methacrylate
TRA	triacrylate
TSA	*p*- toluene sulphonic acid
TSP	thermosetting powder coatings
UV	ultraviolet
UV-VIS	ultraviolet-visible
V	volume
VOCs	volatile organic compounds
vs.	versus
W	weight
σ	stress
λ	extension ratio
η	viscosity

Chapter I

Introduction to Powder Coatings and Literature Survey

1.1 Introduction

A powder coating is a solid coating formulation in the form of a fine powder. The formulation contains minor components such as colorants, flow agents and cross-linkers, in a matrix of the major binders. Each particle contains all ingredients of the formulation, which are well mixed. The powder is applied to the substrate surface and fused to form a continuous film by stoving at a temperature in the range 120-200°C, depending on the coating formulation [1]. There are two broad categories of powder coatings, thermosetting powder coating and thermoplastic powder coating; by far the major portion of the market (>90%) is for thermosetting types [2]. Powder coatings [3] are an economic, energy-efficient, and ecological or environmentally friendly surface coating technology.

The advantages and disadvantages of powder coatings [3-5], when compared to waterborne coatings, radiation-cured coatings and high-solids solvent-based coatings, are described as followings:

(i) Advantages

- *High utilization*. Efficient recovery of over-sprayed powder can enable utilization figures of over 95%. With typical solvent-based paints manually applied the utilization can be as low as 15%
- *No effluent disposal*. No paint sludge is produced, as arises from water-wash booths used to trap over sprayed liquid paint.
- *Solvent-free*. No environmental pollution; no solvent is required; No oven is required for the flash-off of solvents before curing; reduced fire risk; flameproof equipment is not necessary.
- *Reduced Energy consumption*. Powder coating saves on heating energy.

- *Wide range of finishes*. A wide variety of finishes is available which emulate the texture and hammer finishes achieved with liquid-based paints. Structured, wrinkled and metallic finishes are also possible together with antique finishes which are unique to powder coatings.
- *Ready to use*. No stirring, mixing or thinning is required as it may be with liquid paints. Some application equipment enables the powder to be fed directly from the box.
- *Ease of use*. Powder is far easier to apply than wet paint and less operator training is necessary.
- *One-coat application*. Thick films of 40-500μm can be applied in a single application.
- *Fewer rejects*. The ease of use of powder, both manually and with automatic application plant, gives a lower reject rate compared with wet paint. Rejects caused by damage after coating are also reduced due to the toughness of powder coatings.
- *Less space requirement*.
- *Reduced health hazards*. Reduced; there are no solvents or volatile materials to be inhaled.

(ii) Disadvantages

- *Higher production cost*. The manufacturing cost of powder coatings is relatively higher for the more complex preparing processes.
- *Thin film difficult*. It is difficult to get thin coating film (<35μm) by applying powder coatings.
- *Contamination*. The contamination of one powder with another is likely to be visible after curing. The common problems are the presence of foreign colors, and defects such as pinholes, caused by an incompatible resin
- *Color change*. To minimize contamination when changing color the utmost care is essential in cleaning the application equipment, spray booth and powder

recovery circuit. Thus, even with modern equipment specially designed for quick color changes, color change is not a rapid operation.

- *Powder adjustment on-site is not possible.* Wet paints can often be adjusted or tinted on-site. This is not possible with powder.
- *Explosive hazards.* While the absence of solvents eliminates the flammability problem, suspensions of powder in air can explode. So, the manufacturing and application facilities have to be designed to avoid powder explosions.
- *Materials limitation.* Since all major components must be solids, there is a smaller range of raw materials available to the formulator. Furthermore, it is not possible to make thermosetting powder coatings where the T_g of the final film is low.
- *Lack of flexibility of final film.* Most of thermosetting powder coatings in the market give rigid film.
- *Health hazard.* Fine powder itself is a health hazard if inhaled.

Powder Coatings Application Methods

(i) Basic powder coating application methods

There are four basic powder coating application methods [6, 7]: electrostatic spray, fluidized bed, electrostatic fluidized bed and flame spray.

Electrostatic spray [8] is one of the processes to apply powder coatings where an electrostatic potential is created between the part to be coated and the coating particles. It is the most commonly used powder application method. There are two commonly applied methods, one is the corona gun process, and the other is the tribo-charging gun process.

In the *corona gun process,* powder is pumped to a spray gun, a charging electrode in the gun is connected to a high voltage generator, and both produce an electric field in excess of the breakdown strength of air causing a corona discharge, which forms free

ions in front of the charging electrode. As powder particles pass through this region, they become charged and follow the electric field and the air currents to the profile, which is earthed. The corona gun is particularly suited to flat surfaces. Its advantage is the good wrapping effect by the powder due to the electrical field lines; its disadvantage is the poor penetration into recesses due to the Faraday cage effect.

In the *tribo-charging gun process* [9] the gun is made of a Teflon tube where the powder flows. Powders, which are less electronegative than Teflon, will be positively charged by friction. Different powders have different charge ability. Tribo-charging guns were developed to overcome drawbacks of corona guns, such as the Faraday cage effect, which can disrupt the powder surface and limit the coating thickness.

The *fluidized bed* method is similar to a dip tank. Powder particles are kept floating by an air stream. A preheated work piece is placed in the fluidized bed where the powder particles come in contact with the work piece and melt and adhere to its surface. Post heating is required to completely cure thermosetting powder coatings. This method is used for applying powder coatings with thickness ranges between 25 to 76 μm, and the substrates must be able to withstand temperature above 125°C.

The *electrostatic fluidized bed* method is similar in design to a conventional fluidized bed method. But the air stream is electrically charged as it enters the bed. The ionized air charges the powder particles as they move upward in the bed, forming a cloud of charged particles as it enters the chamber. No preheating of the work piece is required. This method is most suitable for coating small objects with simple geometry.

The *flame spray* method was developed for application of thermoplastic powder coatings. The powders are fluidized by compressed air and fed into a flame gun, where they are injected through a flame of propane, and the powder melts. The molten coating particles are deposited on the work piece, forming a film on

solidification. This technique is suitable for applying coating to most substrates, and also suitable for coating large or permanently-fixed objects.

(ii) New development in powder coating application methods

Electro Magnetic Brush (EMB) technology [10-12]: DSM resin company, in collaboration with Michael Huber Munchen company, developed the EMB spray equipment. In the EMB system, the idea is to create a medium in which the tone or powder coating particles can be transported onto substrate. Within the magnetic Brush development station, the powder coating particles are intensively mixed with so-called carrier particles, which can be seen as relatively large particles with an iron core that have been coated with Teflon. During this mixing process the powder coating particles are tribo-electrically charged against the carrier particles. Consequently, the powder coating particles adhere onto the carrier particles due to their opposite electrical charge. Within the container the developed system is transported to a rotating shell or drum, which has stationary magnets in its inside. Within the working range of the magnets the iron-cored carrier beads, to which the powder particles are attached, form a chain as directed by the magnetic field lines. This is the so-called Magnetic Brush of the Electro magnetic Brush development system. This process is a high speed powder coating application process, that has been developed to coat flat substrates, and the powder coatings can be applied in very thin layers.

Cloud powder coating application technology (CP): CP is a developing and semi-commercial system [12-15]. This process involves a gas flow injection chamber, a diffusion chamber and a coating chamber and a method for coating a substrate or target object. The injection chamber receives powder from the reservoir at a controlled rate and the powder particles are entrained by a gas flow within the injection chamber. The diffusion chamber receives the particles from the injection chamber. The diffusion chamber deaccelerates the particles and creates a particulate cloud. The coating chamber receives the particulate cloud. Housing encloses the

coating chamber which is isolated from the ambient atmosphere. The coating chamber has a cloud inlet and a cloud outlet and the cloud flows through the coating chamber from the inlet to the outlet. One or more deflectors, within the chamber, define a passage and two or more pockets adjoin the substrate or target objects. The deflectors deflect the carrier gas from the pockets to the substrate or target objects. The substrate or target objects are transported within the chamber along the passage. Coating material within the passage is concentrated around the substrate or target objects. The coating chamber includes electrodes and voltage biasing means. The biasing means acts upon the substrate or target objects, which are positioned within the passage. The particles are electro statically deposited upon the substrate or target objects within the passage.

Thermosetting Powder Coatings (TSP)

TSP is applied to substrate, and fused to a continuous film by baking, at temperatures in the range of 120-200°C. The binders for thermosetting powder coatings consist of a mixture of a primary resin and a cross-linker. According to binder resin types, thermosetting powder coatings can be classified as following

- Epoxy powder coating
- Polyester powder coating
- Acrylic powder coating
- Polyurethane powder coating

A global market breakdown by powder type[16] in 1996 (Figure 1.1) is Epoxy 18.4%, Polyester-epoxy hybrid (PET-EH) 43.5%, Polyester-TGIC (PET-T) 19.5%, Polyurethane (PU) 15.8%, Acrylics (PA) 2.0%, others 0.8%.

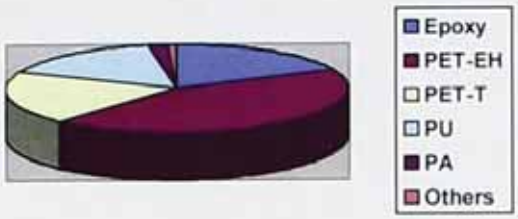

Figure 1.1 Proportion of different thermosetting powder coatings in the global market (%)

Early high epoxy resin content powder coatings lacked UV light stability, causing severe chalking to occur on exposure to sunlight and poor yellowing resistance. Epoxy powder coating applications were limited to interior use and non-decorative application. PET-EH powder coatings are now predominant as the resin of choice for powder coating formulation and manufacture. Acrylic resin was mainly successfully used in the Japanese market and there is now renewed interested in its use for automobile clear topcoats.

Ultraviolet (UV) Curing

UV curing is a chemical process, which uses UV sources to convert low molecular weight materials to higher molecular weight products, through polymerization and cross linking reactions [17].

Powder coatings and UV curable coatings are the two fastest growing coatings in the main commercial coatings market [18] (Table 1.1).

Table 1.1 Percent occupancy of the five main coating markets in Europe from 1990 to 2005

Types of coatings	1990	1995	2000	2005	Increase (%) (1990-2005)
UV curable coatings	2	4	5	7	250
Powder coatings	9	10	12	18	100
Water borne coatings	20	24	26	35	75
High solid coatings	19	24	27	27	42
Conventional solvent coatings	51	40	31	15	-70

Note: For figures in the table are stripped decimal fraction, add up results deviate to 100.

Powder coating combined with a UV radiation curing method gives a new type of powder coating-UV curable powder coating which is now in the early stage of commercialization [19]. Such a coating is fundamentally different from a traditional powder coating since UV light, not heat, is used to cure the coating. Heat is necessary to melt and make the UV curable powder flow to allow the film or coating to form and give the required cosmetic appearance. The amount of heat is much lower because the melting temperature is quite low at around 70°C, compared to the thermosetting cure schedules of around 150°C[20] . This study was to develop powder coatings for the finishing of heat sensitive and highly flexible substrates, such as leather. A thermosetting powder coating could not be used for a heat sensitive substrate due to the high fusion temperature required. The temperatures involved in an UV curing process are general not substantially above ambient and can be further reduced by filtering out IR radiation. So low cross-linking temperature, UV curable powder coatings have the most feasibility for the finishing of heat sensitive substrates.

In general, UV curable powder coatings offer the advantages [1,18,21] as following:

- Dry coating, no use of any type of solvent to assist spraying
- Fast and low temperature cure
- Small operating space
- Less energy demand
- High productivity
- No emission of volatile organic compounds (VOCs)
- Easy application
- Thick layers compared to standard liquid coatings
- Quick clean-up and overspray reclaim
- Minimal health risk by application of high molecular weight materials
- Good method for finishing heat-sensitive substrates
- Possible easily multi-color spray on the substrates

There are a few disadvantages [22] to UV curable powder coatings

- More strictly controlled manufacture process is required
- Storage limitation due to sensitivity to light
- Difficulty in finishing 3-D parts

In the world, many coating companies are actively developing UV curable powder coating products. Several UV curable powder coating products are now commercially available [21, 23 and 24], but most of them were developed to apply to metal substrates, and heat-sensitive substrates such as medium density fiber-board, paneling, wood, and certain plastics.

1.2 Application of UV Curable Powder Coatings on Heat Sensitive Substrates

Traditional heat curable powder coatings are generally not used in coating heat sensitive substrates, such as wood and plastic. Heat sensitive substrates demand lower cure temperatures, preferably below 120°C, to avoid significant substrate deformation and /or degradation. Unsuccessful attempts [25, 26] have been made to coat heat sensitive substrates with traditional powder coatings.

For instance, leather or leather composites are normally damaged by oxidation and chemical aging. Both oxidation and chemical damage occur faster at higher temperatures. If these heat sensitive substrates are heated to the high cure temperatures required for traditional powder coatings, shrinkage and out gassing of the volatiles during curing results in severe blisters, craters, pinholes, and other surface defects in the hardened film finish. Furthermore, overheating causes the leather to become degraded in terms of its physical and chemical properties. This is unacceptable for either film quality or product quality.

Low temperature UV curable powder coatings have recently been proposed for coating heat sensitive substrates [10, 25, and 26, 27-30]. UV powders still require exposure to a temperature which is above either the glass transition temperature (T_g) or melt temperature (T_m), to sufficiently melt and flow out the powders into a continuous, smooth, molten film over the substrate prior to radiation curing. However, the heat load on the substrate is significantly reduced, since UV powders are formulated to melt and flow out at much lower temperatures than traditional powder coatings, typically of the order of about 90°C.

Curing or hardening of UV powders is accomplished by exposing the molten film to light from a UV source, such as a mercury UV lamp, which rapidly cures the film. Since the cross-linking reactions are induced by UV radiation rather than heat, this

procedure allows the powder coatings to be cured more quickly and at much lower temperatures than traditional heat curable powder coatings.

Another significant advantage of UV curable powders is that the hot flow out step is divorced from the UV cure step. This enables the UV powders to completely outgas substrate volatiles during flow out and produce exceptionally smooth films prior to the initiation of any curing reactions. Accordingly, the film finishes created with UV powders are known to have extraordinary smoothness.

Whilst UV-curing may result in low temperature curing, it does not resolve other problems such as rigid coating and poor flow at low temperature. This is because current powder coatings are based on amorphous polymers or at least on amorphous polymers as the base resin of the system. There are two drawbacks for such powder coating systems. The first is that the film formed is inherently hard and not flexible, because a high T_g polymer (usually above 50°C) is required to avoid blocking and give a free flowing fine powder during and after storage at room temperature. The second drawback is their poor flow characteristics.

1.2.1 The Development of UV Curable Powder Coatings for Heat Sensitive Substrates

The first development in the powder coating field began early in the 1950s, when powdered thermoplastic polyethylene was successfully applied on a preheated metal surface; and the first thermosetting powder coatings appeared on the market in the late 1950s, developed by Shell Chemical, applied on underground natural gas and oil pipelines [31]. Use of powder coating has risen dramatically since changes in environmental regulations during the mid 1970s [32].

The first commercial application of UV curing technology was in the early 1960s in Germany when products based on unsaturated polyesters were introduced [33].

UV curable powder coatings combine the advantages of powder coating with UV curing technology; they make the application of powder on heat sensitive substrates possible [34]. In 1999, DuPont Powder Coatings installed the first commercial UV powder production line in Europe at Stilexo Industrial Ltd. UK, for manufacturing of MDF, television and furniture etc. In the mean time, DuPont powder coatings also developed a production line of UV-curable powder coatings, which passed the British FIRA Standard 6250 for general use for horizontal surfaces (excluding kitchen worktops). Nowadays, the Bayer Corporation, Nutro company, UCB and Govesan Industrial Ltd supply their UV-curable powder coatings to some motor car, TV set and MDF manufacturers in North America [35-38]. DSM Coating Resins Company has been working on the project of UV-curable powder coatings to apply to paper-like substrates [39] in the Netherlands.

1.2.2 The Finishing of Leather

1.2.2.1 The Development of Coatings for the Finishing of Leather

Nowadays, leather finishing techniques enable the development of completely solvent-free systems avoiding chemical reactants that are potentially toxic to human beings and to the environment [40]. During the past few years, there has been outstanding progress with the substitution of solvent-based polyurethane, polyacrylate and polybutadiene[41] coatings with waterborne systems.

Buechler[42] studied the finishing leather material by formulating acrylate and he was the first presented UV curable coating for leather at the American Leather Chemist Association. The use of UV radiation for preparing coatings for the large market of shoe upper leathers is of great interest. A clear topcoat for shoe leather can be prepared by UV radiation, and the resulting product has a good abrasion resistance as well as excellent flexibility. Uddin [43] studied the finishing of leather with solvent based UV curable urethane triacrylate in the presence of N-vinyl pyrrolidone, ethyl hexyl acrylate and tripropyl glycol diacrylate and Rock [44] invented an UV curable composition for coating onto leather. The composition comprises a prepolymer, of

which at least 50% by weight is butyl acrylate and up to 20% by weight is styrene, a second compound is one or more of urethane acrylate, epoxy acrylate etc.

1.2.2.2 The Feasibility of Using Powder Coatings for the Finishing of Leather

Powder coatings for application to heat sensitive substrates, such as plastics and medium density fiberboard (MDF), have been developed with limited success [39, 45]. The British School of Leather Technology has investigated the feasibility of using powder coating for leather finishing. Their finishing trials [1] on leather using thermosetting powder coatings have shown that a surface coating with an appearance no different to conventional pigmented finish leather can be achieved without loss of area or softness. Although the coating was incompletely cured, it still provided excellent wet and dry rub fastness, sufficient dry adhesion and adequate wet adhesion properties. However, the coating was not completely satisfactory due to the occurrence of surface cracking and poor flex–endurance. It was concluded that, although powder coating was feasible for leather application, further development of a low temperature powder coating (< 100°C) was needed.

The preferable stoving temperature of powder coatings for leather is 80°C or below. Leather can easily withstand such low temperature for a relatively long period of time (30 minutes or so) [1]. From the perspective of curing or cross-linking, a low stoving temperature of 80°C will inevitably require a curing system that is activated at low temperature but is stable at room temperature. This is difficult to achieve with conventional thermal curing, Thus ultraviolet (UV) radiation-curable powder coatings have been extensively studied and constantly associated with low temperature powder coatings. UV curing can be completed in a matter of seconds. For an UV-curable powder coating system, low temperature curing is possible because melting and cross linking of the coating film are performed separately. It is reasonable to believe that for leather finishing the best approach is to develop low temperature UV curable powder coatings. These is because such UV initiated cross-

linking systems [45-49], mainly based on acrylates, unsaturated polyesters, vinyl ethers and polyurethanes, are readily available.

1.3 Film Formation of UV Curable Powder Coating

UV curable powder is usually sprayed on the surface of a substrate by a corona charging gun or a tribo charging gun. Coating film thickness increases with increasing voltage and decreasing distance between the spray gun and the product being coated. Large particle size powders tend to give increased film thickness. One can apply thicker coatings by heating the object to be coated before applying the powder. However, film thickness is limited because the powder coating acts as an insulator and does not attract further particles. The insulating properties of the powder coating mean that defective coated parts generally cannot be recoated and must be stripped to be recoated [50]. Coating over other coatings, over plastics and over leathers frequently requires application of a conductive primer coating. After spraying of powder coatings, it still requires heat to melt the powder, enable it wet the substrate, flow out and coalesce. Due to the absence of solvent in powder coatings, it is more difficult to remove surface defects from the powder coatings than from conventional liquid-based coatings because the solvent assists the wetting properties and improves the film flow [53]. The coalescence is when powder particles sinter together or melt together into one solid unit; see Figure 1.2(a). The main factors that govern coalescence at a certain temperature are the melting point of the powder resin, the viscosity of the molten powder particles and the size of the powder particles [51]. The wetting and spreading of a powder melt on a substrate will occur when the spreading coefficient is positive [52].

$$S = \gamma_S - \gamma_L - \gamma_{SL} > 0 \qquad (1.1)$$

Where S is the spreading coefficient, γ_S is the surface tension of the substrate, γ_L is the surface tension of the powder melt and γ_{SL} is the interfacial tension between the powder melt and substrate.

The flow of a powder melt can be illustrated using equation (1.2) developed by Rhodes and Orchard [52]. Assuming surface tension (γ) and viscosity (η) of the powder melt are constant, the levelling velocity $\ln(a_0/a_t)$ is given by:

$$\ln\frac{a_0}{a_t} = k\frac{h^3\gamma}{\lambda^4\eta}\int_0^t dt \qquad (1.2)$$

where k is a constant = $(16\pi^4/3)$, h is the average film thickness, λ is the wavelength, a is the amplitude of the sine curve, see Figure 1.2(b) [53, 54]. Therefore, a good flow requires a thick film layer h, a high surface tension γ (driving force) for the powder melt, a low melt viscosity η (resisting force) and a small amplitude a_t, (meaning small powder particles). It is known that additives can decrease the surface tension of the base resin and they may be used to control the surface tension of powder system [53].

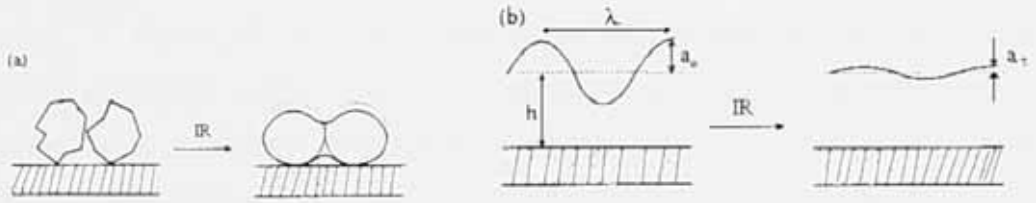

Figure 1.2 Schematic representation of powder coating film formation
(a) Melting and coalescence of powder coatings; (b) Powder coating levelling

The use of infrared (IR) radiation to raise the temperature of the sprayed powder has been found to be an advantageous method because it allows the coating to heat up in a very short period of time, whilst keeping the exposure of the substrate to heat to a minimum [55]. By heating of the powder with infrared radiation, the rough powder particles are melted, coalesce (fuse together), form a film (flow out) and level to a smooth continuous molten layer: subsequent exposure to UV radiation induces the curing reaction to form a desired protective coating film (Figure1.3) [56]. The most important factors [53] affecting the speed of melting and coalescence at a given

temperature are the melting point of powder coating resin, the viscosity of the molten powder and the size of the powder particles.

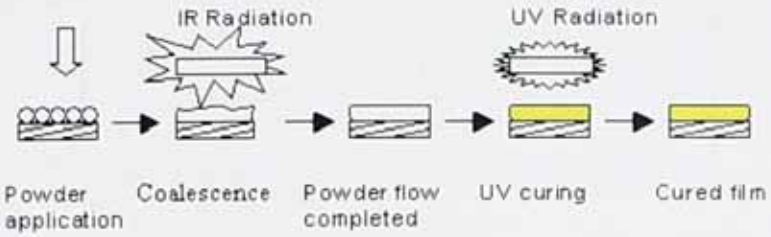

Figure 1.3 Film forming process for UV curable powder coatings

One approach that allows film formation at lower temperature while still retaining good storage stability is to introduce a crystalline component into the polymer system [45]. Figure 1.4 shows how polymer viscosities vary with temperature for a typical crystalline polymer resin, thermosetting amorphous polymer resin and thermoplastic amorphous polymer resin. At high temperature the crystalline resin will have low viscosity, compared to amorphous resin. The crystalline polymer will remain a solid up to the melting point, thus providing the storage stability; but when molten, its viscosity will decrease more rapidly than that of an amorphous polymer above T_g [57] (Figure 1.4). The thermosetting polymer shows that viscosity starts to increase as the temperature increases to about 160°C due to cross-linking whereas the thermoplastic polymer does not show viscosity increases at relatively high temperature. Thus, a powder coating formulation with crystalline resin should flow easily and aid film formation. The melt viscosity can be further reduced by additives or appropriate modification of polymer architecture [46].

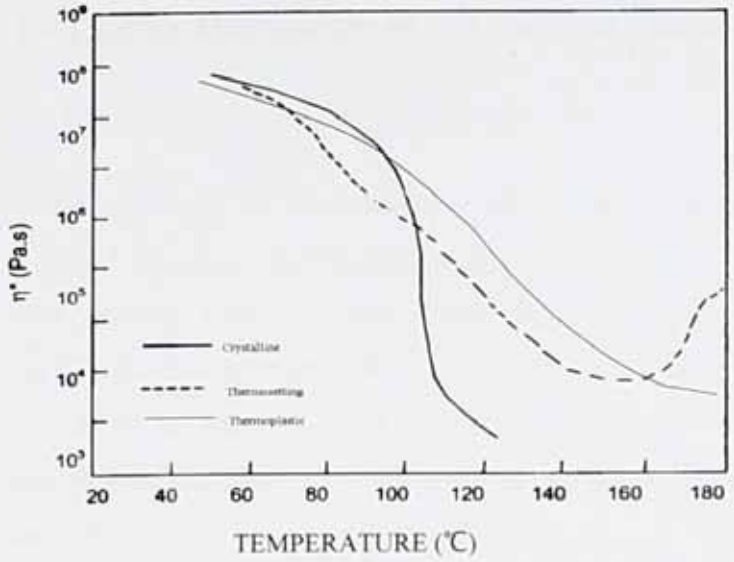

Figure 1.4 Typical dynamic viscosities as a function of temperature for thermosetting, thermoplastic and crystalline polymers[57]

During the film forming process with a rapid UV curing system, the double bonds in the binder molecules open and react as in polymerization, there is volume shrinkage resulting in internal stresses. The shrinkage will affect the adhesion between coating film and substrate, as well as the appearance of the coating film. Table 1.2 gives the volume shrinkage of several acrylates [58] on UV curing.

Table 1.2 Volume shrinkage of several acrylates

ACRYLATE	VOLUME SHRINKAGE (%)
Hydroxypropyl acrylate	13.2
Poly(ethylene glycol) diacrylate	12.0
Trimethylolpropane triacrylate	11.7
Pentaerythritol triacrylate	10.7
Urethane acrylate	8.7
Acrylated epoxide	5.4

1.4 Curing Mechanism of UV Curable Powder Coating Resin

1.4.1 Free radical UV Curing Mechanism

When heated by IR radiation etc., UV curable powders turn into liquid. The free radical UV curing mechanism is shown in Figure 1.5. Radiated by UV light, the photo initiator turns into free radicals, these then react rapidly with a double bond in the UV curable powder coating resin molecules, causing it open up and a new free radical to be formed. Thus monomers, oligomers or their mixture take part in polymerization, grafting or cross linking, resulting in the formation of polymer network [59, 60].

There are various termination reactions, such as recombination, chain transfer etc. and of course, if the source of UV radiation is turned off, the polymerization reaction will cease rapidly.

PHOTOINITIATION----absorption of UV light

$PI \xrightarrow{h\nu} R^{\bullet}$

$R^{\bullet} + M \longrightarrow RM^{\bullet}$

PROPAGATION----chain growth

$RM^{\bullet} + M \longrightarrow RM_2^{\bullet}$

$RM_2^{\bullet} + M \longrightarrow RM_3^{\bullet}$

.....

$RM_{(n-1)}^{\bullet} + M \longrightarrow RM_n^{\bullet}$

TERMINATION----end of chain growth

$R^{\bullet} + R^{\bullet} \longrightarrow R\text{-}R$

$RM_n^{\bullet} + RM_n^{\bullet} \longrightarrow RM_nM_nR$

$RM_n^{\bullet} + R'H \longrightarrow RM_nH + R'^{\bullet}$ (abstract hydrogen, chain transfer)

$RM_n^{\bullet} + O_2 \longrightarrow RM_nOO^{\bullet}$ (oxygen remove or inhibiting)

$RM_nOO^{\bullet} + R'H \longrightarrow RM_nOOH + R'^{\bullet}$

Figure 1.5 Free radical UV curing mechanisms

photo initiator (PI) ; free radical ($R^{\bullet}$) ; monomer or binder molecule containing functional group (M)

1.4.2 Cationic UV Curing Mechanism

A cationic UV curable powder coating resin is a solid bisphenol-A epoxy resin or a vinyl ether resin etc. In the coatings, a triarylsulfonium salt or a diaryliodonium salt is used as photocatalyst. The cationic UV curing mechanism is described below with the diaryliodonium salt as photo initiator [61].

PHOTOLYSIS OF CATIONIC SALT PHOTO INITIATOR

---- absorption of UV light results in both homolytic and heterolytic cleavage of a carbon-iodine bond of the diaryliodonium salt

$$Ar_2I^+X^- \xrightarrow{h\nu} \begin{bmatrix} ArI^+\bullet X^- + Ar\bullet \\ ArI + Ar^+X^- \end{bmatrix}$$

(where anion X^- can be a BF_4^-, PF_6^-, AsF_6^- and SbF_6^- etc.)

FORMATION OF LEWIS/BRONSTED ACID

$$\begin{bmatrix} ArI^+\bullet X^- + Ar\bullet \\ ArI + Ar^+X^- \end{bmatrix} \xrightarrow{RH} HX + Ar\text{-}R$$

INITIATION OF CATIONIC POLYMERIZATION

$$HX + M \longrightarrow HM^+X^- \quad (\text{where M is monomer})$$

PROPAGATION

$$HM^+X^- + nM \longrightarrow H(M)_{n-1}M^+X^-$$

TERMINATION

Cationic systems do not suffer from oxygen inhibition, but cure may be affected by various conditions, such as impurities, air humidity etc., Furthermore the photo-cationic initiation system is often heterogeneous [62]. Photo-cationic polymerization of bisphenol-A epoxy resin usually gives incompletely cured coatings.

There are at least two ways in termination process. The cation and anion may rearrange to form a polymer molecule with unsaturated end-groups, regenerating the original Lewis/Bronzed acid; alternatively, the cation and anion may react in the way that X^- combines with the cation and liberating the original photo initiator.

Both propagation and steps are dark reactions, and so proceed in the absence of light.

1.5 Polymer Crystallization

1.5.1 Crystallization

Crystallization is the process whereby an ordered structure is produced from a disordered phase. When a polymer has a highly stereo regular structure with little or no chain branching, or when it contains highly polar groups that give rise to very strong dipole—dipole interactions, it may exist in crystalline form [63]. Stereoregularity leads to a crystalline polymer. High chain regularity will allow the polymer to crystallize easily and produce a high crystallinity. Crystallinity can develop during the following processes: cooling of molten polymer, evaporation of solvent from polymer solutions, or heating of a polymer under vacuum or in an inert atmosphere (to prevent oxidation) at a specified temperature, a process called annealing. In some instances crystallization may be induced by stretching a polymer specimen at a temperature above its glass transition temperature, a process called drawing.

Crystallization is a process which takes place by two distinct steps, nucleation and growth. The growth rates of polymer crystals are highly dependent upon the crystallization temperature and molecular weight of the polymer [64]. The growth of a

crystal nucleus can take place in the form of rods, discs or spheres respectively to form different crystal morphologies, for examples

- Fringed Micelle Model

A bundle of regular segments from different polymer molecules come together to form a close packed crystalline array at localized points, and an individual polymer molecule passes through several crystalline as well as through a number of amorphous regions, as shown in Figure 1.6(a) . The individual crystalline regions thus formed are interconnected by amorphous regions.

- Folded-chain Lamellas Model

Single molecules folds themselves at intervals of about 10nm to form lamellae, as depicted in Figure 1.6(b). Even a single polymer chain may be partly in a crystalline lamella and partly in the amorphous state. Some chains even start in one lamella, cross the amorphous region and then join another lamella. So no polymer is completely crystalline. Normally, the degree of polymer crystallinity ranges from 0% (fully amorphous state) to about 90% (highly crystalline state) and is affected by molecular structure, temperature, molecular weight, stereochemistry and processing conditions.

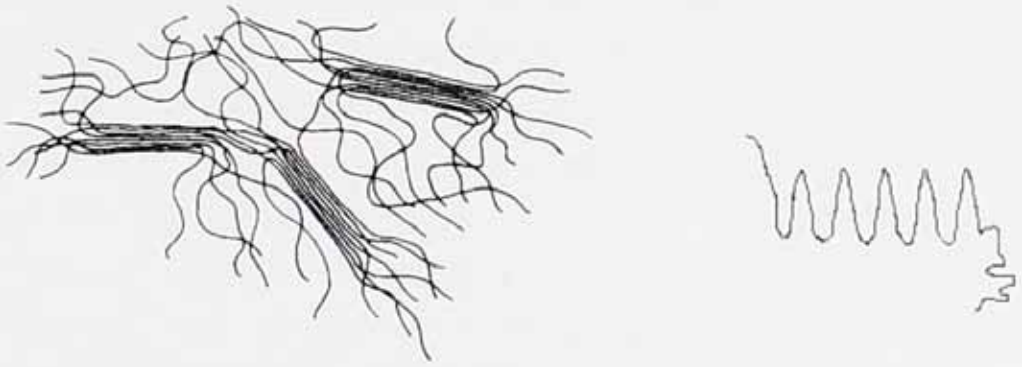

(a) (b)

Figure 1.6 Arrangements of molecules in crystalline polymers
(a) fringed micelle model; (b) folded chain lamella model

A variety of polymer crystalline morphologies have been identified, three of which are shown in Figure 1.7 [63]. Spherulites are aggregates of small hairlike strands, called fibrils, arranged as clusters in an essentially radial pattern. Drawing forces the spherulitic fibrils into the drawn fibrillar morphology. Epitaxial crystallinity, which usually arises during crystallization in stirred solutions or melts, is characterized by one crystalline growth on another, as in the so-called shish-kebab morphology that contains lamella growth on long fibrils.

(a) (b) (c)

Figure 1.7 Some crystalline morphologies:
(a) spherulitic (b) drawn fibrillar (c) epitaxial

For crystals grown from molten polymer, chain entanglements are of extreme importance and the crystals that form are more irregular than those obtained from dilute solution. Melt-crystallized polymers are never completely crystalline due to the enormous number of chain entanglements in the melt [64]. Chen [65] reported work on the effect of molecular weight on polymer crystallization. The crystallinity decreases as the molecular weight of polymer increases, due to the decreasing ability of polymer chains to arrange into crystallites. As previously noted, there is co-existence of crystalline and amorphous regions in most crystalline polymer. Stereoregular components form the crystalline regions where structural irregularity induces amorphous regions. Examples of sources of irregularity:

- Mixture of stereoregular segments with different tacticities
- Chain branching, which reduces local regularity within the structure

- Copolymerization, which limits the extent of possible crystallization
- Cross-linking in the molten state

1.5.2 Crystalline Melting Point Equation

Of fundamental importance to crystallization phenomena is the depression of melting point. The wide and variable melting temperature range of a polymer is attributable in large measure to variations in lamellar thickness. The following derivation is, however, completely general for any crystal subdivided into lamellae [64, 66]. The thermodynamic condition for solid and liquid phases to be in equilibrium at the melting point depends on their specific Gibbs functions (g) and we have:

$$g = u+pV— Ts \tag{1.3}$$

Where u is the internal energy; V the volume, and S the entropy at pressure P and temperature T. Consider an infinitely thick solid of cross-sectional area A and density ρ which melts at $T_m°$. Let $g = g_0$ at $T_m°$ for the crystal and its melt. Now suppose the crystal to be divided into lamellae thickness l and cross-section area A. Each lamella will have acquired $2A$ of new surface and $2A\sigma_e$ of surface free enthalpy where, for polymers, σ_e refers to the fold surface. Dividing by the mass $A\ \rho\ l$, one obtains $2\sigma\ /l\rho$ as the increase of g per lamella. This will depress the melting point to T_m. Recalling that

$$(\partial g/\partial T)_p = - S \tag{1.4}$$

and assuming that s may be regarded as constant near $T_m°$, one has as the new condition for melting

$$g_0 + s_L(T_m° - T_m) = g_0 + s_S(T_m° - T_m) + \frac{2\sigma_e}{l\rho} \tag{1.5}$$

with subscripts L and S referring to liquid and solid respectively. Substitution for the heat of fusion per unit volume, Δh, where

$$\Delta h = \rho T_m° (s_L - s_S) \tag{1.6}$$

and rearrangement gives

$$T_m = T_m° \left(1 - \frac{2\sigma_e}{l\Delta h}\right) \tag{1.7}$$

This equation is valid provided (i) the term $A\sigma_e$ is greater than equivalent terms relating to side surfaces, which have been neglected and (ii) that T_m is sufficiently close to T_m° for s_L and s_S to be regarded as constant.

1.5.3 Crystallization Kinetics

Analysis of the crystallization of a polymer is of profound importance in understanding structure/property relationships in polymers. If a polymer melt of mass W_0 is cooled below the crystallization temperature then spherulites will nucleate and grow over a period of time, t; if W_L is the mass of liquid; then the Avrami equation[64] bives the relation of W_L/W_0 to t can be expressed as

$$W_L/W_0 = \exp(-zt^n) \tag{1.8}$$

Where n is the Avrami exponent and z is a constant.

Measurement of the change in specimen volume is much easier than the mass of spherulitic material. If the initial and final specimen volumes are defined as V_0 and V_∞ respectively and the specimen volume at time t is given by V_t then it follows that

$$V_t = \frac{W_L}{\rho_L} + \frac{W_S}{\rho_S} = \frac{W_0}{\rho_S} + W_L\left(\frac{1}{\rho_L} - \frac{1}{\rho_S}\right) \tag{1.9}$$

and since

$$V_0 = \frac{W_0}{\rho_L} \quad \text{and} \quad V_\infty = \frac{W_0}{\rho_S}$$

Then equation (1.9) becomes

$$V_t = V_\infty + W_L\left(\frac{V_0}{W_0} - \frac{V_\infty}{W_0}\right) \tag{1.10}$$

Rearranging equation 1.10 and combining equations (1.8) and (1.10) gives

$$\frac{W_L}{W_0} = \frac{V_t - V_\infty}{V_0 - V_\infty} = \exp(-zt^n) \tag{1.11}$$

This equation then allows the crystallization process to be monitored by measuring the specimen volume changes with time. In practice the polymer sample is enclosed in a dilatometer and then the change in height of a liquid rather than direct measure

of specimen volume change is measured. In terms of heights monitored in the dilatometer, equation (1.11) can be expressed as

$$\left(\frac{V_t - V_\infty}{V_0 - V_\infty}\right) = \left(\frac{h_t - h_\infty}{h_0 - h_\infty}\right) = \exp(-zt^n) \qquad (1.12)$$

The Avrami exponent, n, can be determined from the slope of a plot of $\log\{\ln[(h_t - h_\infty)/(h_0 - h_\infty)]\}$ against $\log t$.

1.6 Binder Systems for UV Curable Powder Coating

Free radical curable coatings use acrylated epoxy resins and/or acrylated polyesters or unsaturated maleic polyesters etc. as binders. Cationic UV curable coatings use bisphenol-A epoxy resins etc. as binders [2].

UV curable powder technology requires different resins from standard powder coatings. However, the synthesis of a solid resin suitable for use and containing reactive double bonds, which can be UV cured, is not easy [67]. The synthesis of a solid resin, which can form cross linked films with flexibility and good adhesion to heat-sensitive substrates such as leather and paper, is ever more difficult.

1.6.1 Crystalline Binders

Currently the lowest stoving temperature is about 120°C for conventional powder coating system presently on the market. This temperature is a compromise between two factors, storage stability and film forming process-ability of amorphous polymer. A powder coating must be storable at 30-40°C without fusion, which requires the glass transition temperature (T_g) of the amorphous polymer to be 50°C or higher; when the powder is molten it must flow to form a homogeneous film, which requires a temperature at least 50°C above T_g. This rule is however only applicable for amorphous polymers [46].

Crystalline or semi-crystalline polymers may be incorporated with amorphous polymer in the formulation of UV-curable powder coatings [10, 68-72]. They are chiefly to improve the flow properties of the formulations. The presence of crystalline polymers sometimes leads to film hazing. To overcome the hazing and mottling problem, the level of crystalline resins is usually limited to below 10% (wt) of the resin system, with the consequence of poor flow which can only be alleviated by using higher temperature [73]. Alternatively, a re-crystallization or haze inhibitor may be employed to reduce or eliminate hazing [73]. Although the incorporation of crystalline polymers helps to improve the flow and storage stability, it does not help to solve the problem of low film flexibility, and may make it worse.

Li [74] studied polyurethanes with pendant acrylate groups, the synthesis processes were as follows: at first, isocyanates, such as 4,4´- methylene diphenylene diisocyanate (MDI), were reacted with polyester diols, for example polytetramethylene adipate (PTMA), in order to prepare prepolymers. Then the prepolymer was reacted with glycerine by using carefully controlled reaction conditions, During the reaction, the two primary hydroxyl groups of higher reactivity in the glycerine molecule will be consumed first, leaving most of the less reactive secondary hydroxyl group unreacted and as a pendant group of the polyurethane [75]. Finally, acrylic functionality was introduced to the polymer by the reaction of isocyanatoethyl methacrylate (IEM) with the secondary hydroxyl groups.

Li[74] and Couveret[76] published work on introducing acrylate groups in side positions on the backbone of oligomers or polymers. However, their work was neither in the context of powder coatings, nor related to crystalline oligomers/polymers, nor was it for controlling the crystallinity of oligomers/polymers.

Wenning[77] disclosed a UV-curable powder coating compositions based on polyurethane acrylate. The resin system is a polyurethane based on a polyester backbone and a terminal acrylate group. In the composition, the major binder resin

was amorphous and 60-90% by weight, with the crystalline resin(s), 10-40% by weight.

Hall disclosed a powder coating composition [78] comprising semi-crystalline polyurethane acrylate resins. In this system, the UV-curable functional groups were provided by monohydroxy acrylate monomers, such as hydroxyethyl acrylate. The resins prepared were end capped with acrylate groups.

The research work reported in this thesis concerns the affect of polymer structure modification on crystallinity and on the creation of novel UV curable powder coatings. As noted a polymer's structure, if it is regular and orderly, will allow it to easily pack into crystals. Intermolecular forces assist this process, e.g. polar ester groups in some polymers give strong crystals. During the curing process, the random movement of the polymer chains is restricted.

1.6.2 Polyacryates

Johansson and Falken[46] used mixtures of amorphous methacrylate-functional prepolymer and crystalline acrylate and methacrylate compounds as UV-curable powder coating binders. The introduction of a crystalline component in an amorphous resin mixture by blending was shown to markedly reduce the melt viscosity and thus enhance the flow properties of the UV-curable powder coating. The synthesis of the amorphous resin is shown in Figure 1.8 and the structures of the crystalline monomers are shown in Figure 1.9.

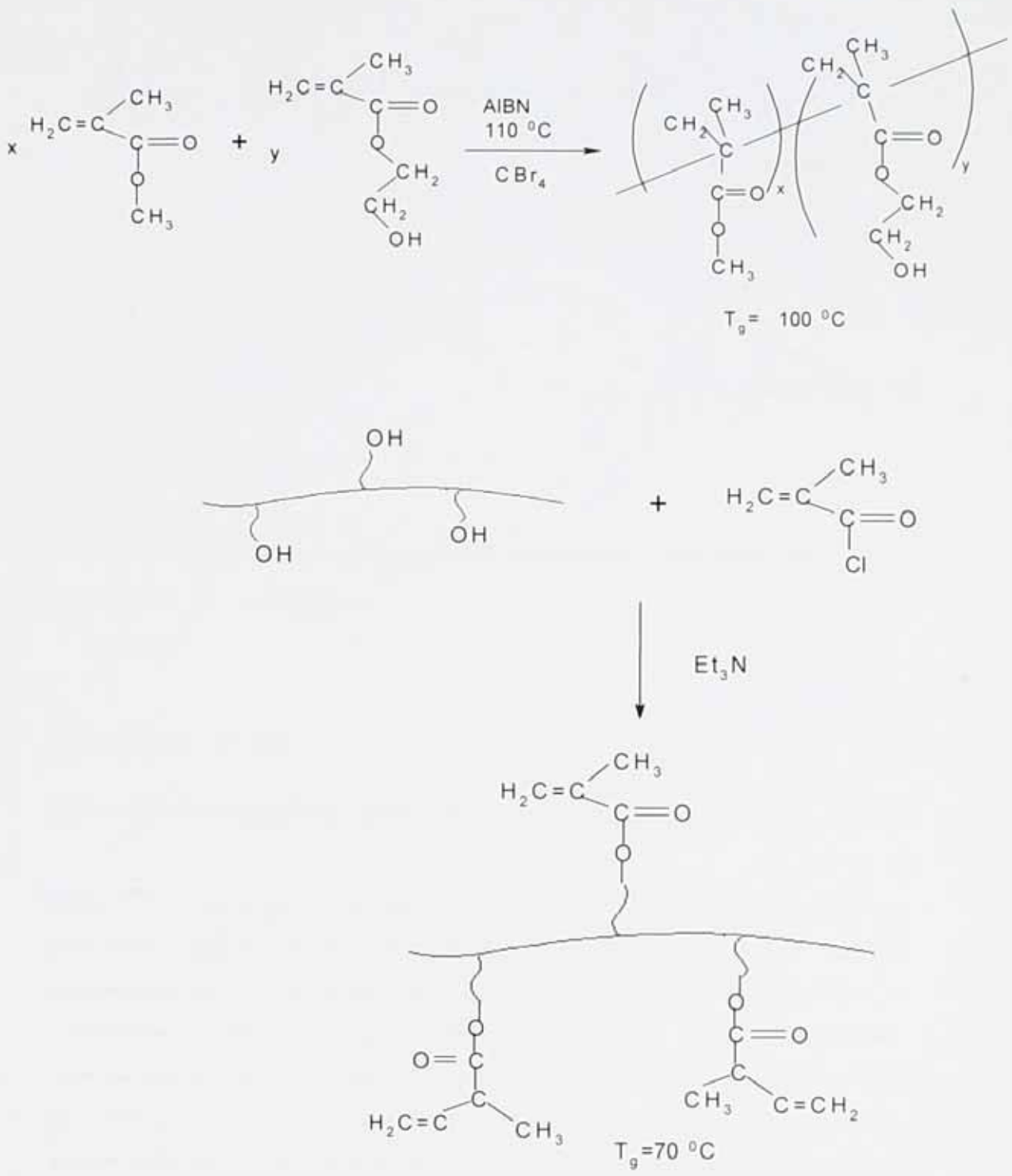

Figure 1.8 Synthesis of the amorphous polyacrylate resin

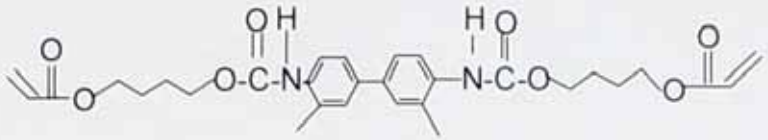

C1

mp=106^{0}C

C2

mp= 72-74^{0}C

Figure 1.9 Structures and melting points of the crystalline compounds with difunctional groups of acrylates

1.6.3 Polyester Acrylates

1.6.3.1 Acrylate-capped Polyester Binders

Moens [79] prepared crystalline polyester with methacrylate end groups which are used as UV curable powder coating binders. The polymer was made in a bulk condensation, two step polymerization process. This process involves reacting 1,4-cyclohexane dimethanol or other suitable diols with an excess of a suitable difunctional carboxylic acid, such as adipic acid, in the presence of a catalyst. Then, the molten polyester was cooled to 140°C, at which point glycidyl methacrylate in an amount sufficient to react with all of the carboxyl groups, plus a small excess, was added, along with a catalyst for acid-glycidyl reaction, the reaction schemes are shown Figure 1.10.

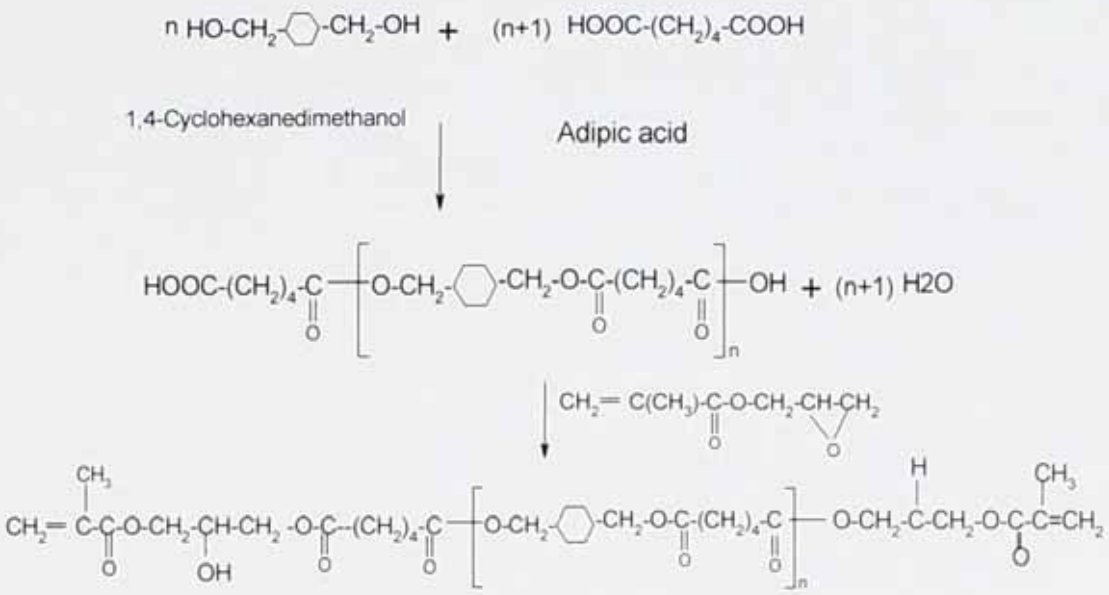

Figure 1.10 Synthesis of acrylate-capped Polyester resin

The final oligomeric product (number-average molecular mass of 5,600 and melting point of 130°C) is a methacrylate-capped crystalline polyester used as an UV curable powder binder.

1.6.3.2 Dendritic Polyester Based Acrylates

A series of resins based on dendritic polyester with different core structure and length of the crystalline grafts has been produced and studied. It has been shown that it is possible to graft crystalline end-groups by ring opening polymerization of ε-caprolactone(ε-CL) to hyperbranched polyester cores to produce a semi-crystalline starbranched hybrid structure with suitable melting temperatures[45, 80]. The grafting of ε-CL also allows the resin to be further functionalised to an UV curable structure (Figure 1.11). The resins had a melting point of approximately 60°C, above which the viscosity rapidly decreased to allow a film formation at around 80°C.

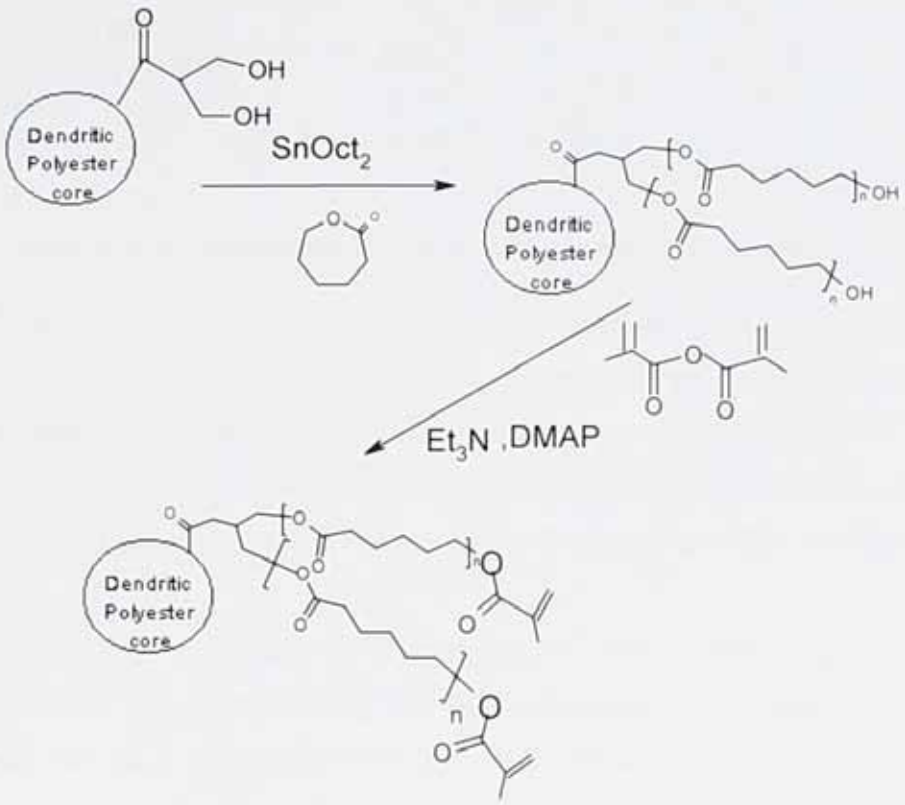

Figure 1.11 Schematic description of synthesis of semi-crystalline resins for UV curable powder coating

1.6.4 Unsaturated Polyesters

Fink [81] disclosed an UV curable powder system utilising a curing agent such as the combination of unsaturated polyester with a solid urethane acrylate as cross linking agent. The component raw materials have the following properties:

Unsaturated polyester	
Glass transition temperature	52°C
Melting range	75-90°C
Melt viscosity	6 Pa•s at 200°C
Acid number	25 mg KOH /g

Polyurethane acrylate	
Glass transition temperature	47°C
Melting range	65-85°C
Melt viscosity	40-60 Pa •s at 120°C

This UV curable powder coating can flow and level at a relatively low temperature.

Daly [68, 82] reported that an unsaturated polyester UV curable powder coating binder containing maleate or fumarate groups and a polyurethane co-reactant containing vinyl ether unsaturation have been developed and is commercially available. The curing mechanism is based on the free radical initiated 1:1-copolymerization of the electron-rich vinyl ether groups with the electron-poor maleate or fumarate groups.

Commercially available UV-curable unsaturated polyester powder coatings from Bayer Corporation [83] can be cured by UV light or heating. The coatings have low melting point and good adhesion to metals and MDF, but lack flexibility.

1.6.5 Polyurethane Acrylates

Wenning[84] discussed UV-curable powder coatings based on urethane acrylates in one of his papers. These are characterized by outstanding properties: they are easy to grind, have good storage stability and satisfy demands for curing at low temperatures. Moreover, their outdoor weathering and mechanical properties are the same as those of conventional liquid urethane acrylates based coatings.

1.7 Photo-initiators

1.7.1 Free Radical Photo-initiators

Free radical photo-initiators that have been considered for UV curable powder coating are given in Table 1.3[85]. The melting points of Irgacure® 819 and 2959 are relatively high.

Table 1.3 Photo-initiators considered for UV curable powder coatings

Class	Irgacure®	Form	Melting point (°C)	UV absorption peaks (nm)
Alpha-hydroxy Ketone (AHK)	184	White powder	44-49	240-250 320-335
Benzyldimethyl Ketal (BDMK)	651	Off-white Powder	63-66	330-340
Bisacylphosphine Oxide (BAPO) and blends	819	Light yellow Powder	131-135	360-365 405
BAPO and blends	1800	Light yellow Powder	48-55	325-330 390-405
BAPO and blends	1850	Light yellow Powder	>45	325-330 390-405
AHK	2959	Off-white powder	86.5-89.5	275-285 320-330

Valet and Rogez [86] studied the properties of three photo-initiators (Irgacure® 184, Irgacure® 1800 and Irgacure® 651) for UV curable powder coatings. All three initiators tested did provide fast cure and excellent film hardness. However, photo-initiator 651 was rejected as high yellowing after short term UV irradiation.

1.7.2 Cationic Photo-initiators

The general chemical structures of several cationic photo-initiators are shown in Table 1.4. Among them, triarylsulfonium and diaryliodonium salts are often used [87] in UV curable coatings. For UV curable powder coating formulations, they should be considered first.

Table 1.4 Cationic photo-initiators and their structures [61]

Name	Structures
Diazonium salts	$ArN_2^+ X^-$
Diaryliodonium salts	$Ar_2I^+ X^-$
Diarylbromonium salts	$Ar_2Br^+ X^-$
Triarylsulfonium salts	$Ar_3S^+ X^-$
Triarylselenonium salts	$Ar_3Se^+ X^-$
Dialkylphenacylsulfonium salts	$ArCOCH_2S^+R_2X^-$
Dialkyl-4-hydroxyphenyl-sulfonium salts	$HOArS^+R_2X^-$
Ferrocenium salts	$C_5H_5Fe^+ ArX^-$
Thiopyrylium salts	$Ar_3C_6H_2S^+ X^-$

Photo initiators bearing anions, X^- can be one of BF_4^-, PF_6^-, AsF_6^- and SbF_6^- etc.

1.8 Additives

Additives are important ingredients in the formulation of UV curable powder coatings. In general, additives perform the same functions in UV curable powder coatings as they do in conventional liquid coatings. Many of the same additives used in liquid coatings are also used in UV curable powder coatings. [88]

The ideal UV curable powder coating additive should have the following characteristics:

- solid, T_m or T_g >50°C
- 100% active
- specific in function
- chemically non-reactive with the binder resins and curatives
- effective at low levels.

1.8.1 Flow-control Additives

Flow-control additives are used for preventing craters and reducing orange peel in the UV curable powder coating formulations. Their functions are to reduce the surface tension of the melt of powder particles and to help coalescence at both the coating/substrate and the coating/air surface [88].

The most widely used class of flow-control additives is polyacrylates. Depending on the particular system of resin and curative, the use level is in the range of about 0.5 to 1.5% (w/w) active material based on the binder. Pigmented systems usually require a somewhat higher level than clear system.

In addition to the acrylate types, silicones are also used. They are more effective in their ability to reduce surface tension, and smaller amounts are needed than in the case of polyacrylates, typically 0.1 to 0.5% (w/w) based on binder.

Flow additives are used in the coating to increase flow properties e.g. 0.7 % (w/w) Byk 361 (Byk-Cera) for a clear coating or Resiflow PV5 (Worlee) for a white pigmented coating. For textured coatings Ceraflour 969 (Byk-Cera) 4% (w/w) can be used. [89]

1.8.2 Antifoaming Agents

After spraying, the melt viscosity of UV powder is relatively high. There can be a little air contained in the powder layer, which will cause foam to form with a resulting loss of product quality. Therefore, in most cases there is a need to add antifoaming agents to the powder formulation. These additives are usually low surface tension compounds, such as silicone. Normal silicone antifoaming agents are liquid. For the reason of good storage of powders, the amount of liquid silicone should be as little as possible. On the other hand, low surface tension agent, micro-crystalline wax also should be considered as an UV curable powder coatings antifoam agent.

1.8.3 Pigments

A standard pigment for white powder coatings, such as Kronos^{TM} 2160, TiO_2 (Kronos) can be used. For other colors, many pigments are available. Yellow

pigments can only be used with low color strength since these pigments generally absorb strongly in the near UV region. [89]

1.8.4 Additives for Improving Abrasion Resistance

One way to improve abrasion resistance includes the addition of silica acrylates, which are silica organosols in 1, 6-hexanediol diacrylate, and tripropylene glycol diacrylate, which improve surface properties. [90]

1.9 Aims and Scope of the Project

The aim of the project was to develop a new powder coating for highly flexible and heat-sensitive substrates, especially leathers. Therefore, the new powder coating must be applicable and curable at low temperatures, preferably below 120°C, and give highly flexible film.

To achieve low temperature curing, UV radiation curable chemistry was adopted in this research work. To achieve flexible film, it was proposed in this project to employ crystalline polyurethane polymers, rather than amorphous polymers commonly used in powder coatings. The concept was to start with semi-crystalline polyurethanes, therefore fulfilling the requirement of hard solid polymers for formulating powder coatings, but after curing the semi-crystalline polyurethanes will be turned into non-crystalline, low T_g polymers, therefore giving a flexible film. Semi-crystalline polymers also have the advantage of reducing melt viscosity, which would further facilitate the formulation of low temperature powder coatings.

This project would explore each or a combination of the following approaches in turning semi-crystalline polymers to non-crystalline ones:

- Random copolymerization of different crystalline moieties to give structural irregularity along the polymer chain

- Introducing branches to give structural irregularity along the polymer chain
- Introducing cross links in molten state to reduce crystallinity.

Any promising polyurethane binder system from the initial studies would then be further developed and applied to leather finishing, and the properties of the finishing would be investigated.

Chapter II Experimental Methodologies

2.1 Chemical Methods

2.1.1 Ceric Ammonium Nitrate Reagent to Test for the Methylhydroxy Group

For synthesis of functional monomers, the methylhydroxy group (-CH_2OH) needs to be determined by the Ceric Ammonium Nitrate Reagent. This analytical test method is an easy and common way to examine methylhydroxy groups and is used as a quality control method. In this study, the test was combined with UV-visible spectrum analysis to quantitatively analyze methylhydroxy groups in the solution or mixtures of prepared functional acrylate crude products.

Preparation of Ceric Ammonium Nitrate Reagent [91]:

1.3 ml of concentrated nitric acid was added to 40 ml of distilled water, and then 10.96 g of yellow ceric ammonium nitrate was dissolved in the dilute nitric acid solution. After the solid dissolved, dilute to 50 ml in a volumetric flask.

$$ROH + (NH_4)_2Ce(NO_3)_6 \longrightarrow (NH_4)_2\underset{\underset{OR}{|}}{Ce}(NO_3)_5 + HNO_3$$

Test Procedure:

To 1 ml of the ceric ammonium reagent was added 4 to 5 drops of a liquid unknown sample (or 0.1-0.2 g of a solid sample). These were mixed thoroughly and it was noted whether the yellow color of the reagent changed to red. Alcohol reacts with the reagent to form a red alkoxy cerium (IV) compound. If a red developed, the solution was observed carefully and the time for the mixture to become colorless was noted. If the red remained and no change was noted in 15 min, the test tube was allowed to stand for several hours or overnight, and it was noted if bubbles of carbon dioxide were liberated. Formation of a red alkoxy cerium (IV) compound was taken as a positive test.

2.1.2 Measurement of Cross-linking Degree of Powder Coating

The cross-linking degree of powder coating was measured according to the gel fraction in the cured powder coating film. This method is derived from the solvent cure test method [92, 93]. The percent cross-linking degree of powder coating was calculated by the following equation:

Percent cross-linking degree= $G_d=100[m_d / m_{iso}]$ (2.1)

Where m_{iso} is the isolated weight of the sample and m_d is the dry weight of the sample after extraction in solvent such as chloroform.

2.2 Instrumental Methods

2.2.1 Measurement of Viscosity

Viscosity (η) can be defined as follows:

η= viscosity = (f/A)/(dv/dx)= shear stress/shear rate (2.2)

where (f/A) is the force (dynes) per unit area (cm^2), (dv/dx) is the velocity gradient (s^{-1}) or shear rate, and η is the coefficient of absolute viscosity[94] . For the Brookfield Cone-Plate Viscometer [95]

SHEAR STRESS (dynes/cm^2): $f/A = M/ (2/3\pi r^3)$ (2.3)

SHEAR RATE (sec^{-1}): $dv/dx = \omega/\sin\theta$

Where M = torque input by instrument; r = cone radius (cm);

θ = cone angle (degrees); ω= angular velocity

Therefore viscosity is given by:

$\eta=3M\sin\theta/2\omega\pi r^3$ (2.4)

The model DV-III, Brookfield viscometer was used to measure viscosity. Selected suitable cone spindle, filled with about 0.5g sample into the sample cup, which can be removed from the bottom of the stationary plate, and its temperature was controlled via TC-500 bath. Set the measurement parameters and then the data of viscosity could be read on the screen or recorded.

2.2.2 Measurement of UV Curable Powder Coatings Finished Leather Flexibility

The SLP 14 test method [96] (measurement of flex resistance by flexometer method as given in Official Test Methods 1996) was used for testing flexibility of powder coating finished leather sample. The apparatus used was the Bally Flexometer. Leather samples 70×45mm were cut parallel or perpendicular to the back bone. Test procedure was as followings:

Set the machine counter to zero and start the machine (at 100 flexes /min.). The flexing action of the machine causes a running fold in the leather passing through an angle of 22.5°, and assesses the leather finish after a number of flexes.

2.2.3 Adhesion of Coating to Leather

The SLF 11 test method [96] (test for adhesion of finish to leather as given in Official Test Methods 1996) was used for this purpose. PVC strips (70×20×3mm) were cleaned with petroleum spirit adhered to powder coating finished leather with C/70 type adhesive (Caswell & Company Ltd., 6 Prince wood road, Northants, UK). Curing was for at least 16 hours and then adhesion strength was measured using the set up shown in Figure 2.1.

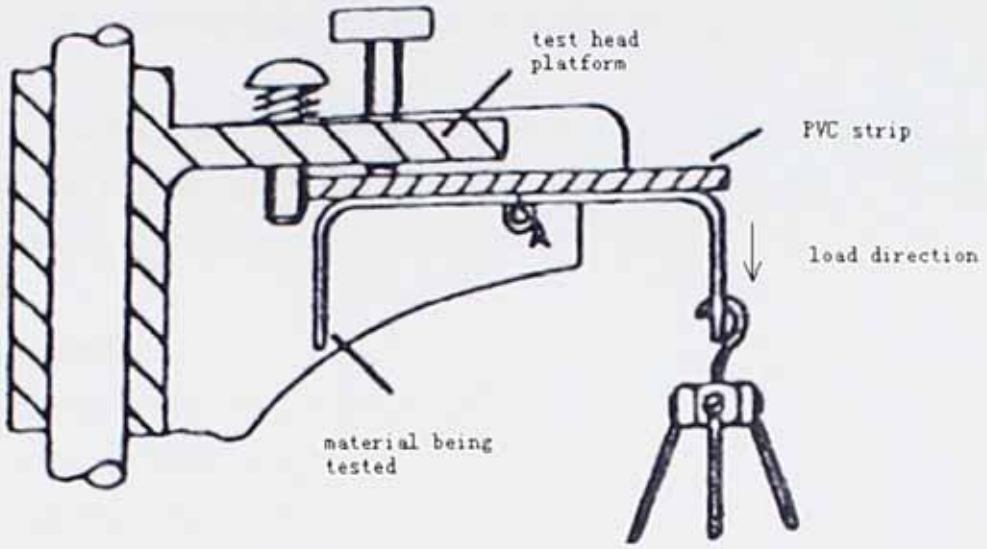

Figure 2.1 Schematic diagram of part of the set up used for measuring the adhesion of coatings to leather

2.2.4 Martindale Abrasion Test

The martindale abrasion tester method (as given in ASTM D4966-98) was used to test the abrasion resistance of samples of UV curable powder coating finished leather. During this test, sample pieces were clamped flat and rubbed under a constant load over a standard wool fabric abradant in a complex cyclical pattern using both wet and dry samples.

Dry test

A new 165mm circle of fabric abradant was placed on each test station and the coated leather placed finish side uppermost in contact with the abradant. The 2.5k_g disc weight was placed centrally on the abradant holder. The clamping ring was replaced and tightened uniformly.

Each test piece was placed face down on the abradant. The test piece holder was

positioned so that the spindle of weight could be pushed through the plate and located in the hole for it on the top of the holder. The spindle was free to rotate.

The machine ran for a fixed number of revolutions that had been pre-set on the counter. Each test piece holder was removed and the surface of the test piece was examined. The degree and type of damage was assessed and recorded.

Assessment

Using bright indirect lighting the tested sample was compared with the non-tested and the occurrence of any of the following noted.

(1) any abrasion; (2) pilling; (3) discoloration

Using the following rating scale

Rating	None	Very slight	Slight	Moderate	Severe	Almost complete	complete
Rank	7	6	5	4	3	2-1	0

Color change was assessed using the grey scale.

Assessment was repeated at defined stages until complete.

2.2.5 Wet and Dry-Rub Fastness

The SLF 5 test method [96] (test for color fastness to circular rubbing (wet and dry) of light leathers as given in Official Test Methods 1996) was used to assess the abrasion properties of UV-curable powder coating finished leather products. The experimental methods were as following

Dry rub test method

The powder coated finished leather sample was placed on the table and clamped; a dry felt pad was put in place with a 2.5 kg load. The leather was rubbed for the stated number of revolutions (512 and 1024 revolutions) in a new area with new pads. If

necessary, the leather was polished with a transparent polish prior to assessment. The felt pads were cut in half, one half reversed and placed on black card.

Wet rub test method

An appropriate number of felt pads were boiled in water to thoroughly wet them. They were then lightly squeezed (weight 2.9 - 3.2g) and placed at the bottom of the shaft. A 2.5 kg load was used and rubbed for the appropriate number of revolutions – 512 and 1024 revolutions in a new area with new pads.

Grey Scale for Assessing Change in surface

A Grey Scale was used for assessing change in the color or surface state

The scale consists of nine pairs of grey color blocks each representing a visual difference and contrast.

The fastness rating goes step-wise from:

Note 5 = no visual change (best rating) to

Note 1 = a large visual change (worst rating).

The Grey Scale has nine possible values:

5, 4-5, 4, 3-4, 3, 2-3, 2, 1-2, 1

2.2.6 Measurement of Thickness of Powder Coating Finished Leather Samples

The thickness of powder coating finished leather samples after hot plating treatment was measured using a standard leather thickness gauge (made by Thomas Mercer Ltd., England, Model 110) at room temperature (test method IUP 4) [97].

2.2.7 Digital Photography of Powder Coating Finished Leather Surfaces

A digital camera, model E600, Eclipse, produce by Nikon Ltd., was used to record images of the powder coating finished leather samples. The digital images were used to evaluate the quality of the hot plating treatments.

2.3 Powder Coating Application Equipment

2.3.1 Hot Plating Method

Powder coated leather samples were compressed in a hot plating machine in order to improve adhesion and film formation. A manual hydraulic press (Turner No. 623, "O"—Press, from Turner Machinery, Leeds, UK) was used for this purpose. The powder coated leather samples were subjected to hot plate pressure under different conditions, including various elevated temperatures, compressing under various pressures and for different time, and with and without different kinds of releasing agents.

2.3.2 Electrostatic Spray Gun Application and UV Cross-linking Process

2.3.2.1 Infrared (IR) Oven and Ultraviolet (UV) Curing Equipment

The Infrared oven emits radiation in the IR wavelength band and the powder and substrate absorb the radiated energy. This approach allows a relatively rapid temperature rise, which causes the powder to melt and flow [98]. The equipment used is shown in Figure 2.2, to the left part of the conveyor section, on the top of the delivery belt, is the IR oven. It is used for melting, flowing and leveling powder coatings; to the right part of the conveyor section, on the top of the delivery belt, is the UV section.

UNIVERSITY OF NORTHAMPTON
LIBRARY

Figure 2.2 UV/IR Equipment

In the UV curing section the UV lamp system is the main part, which consists of five basic components: the power supply, lamp head, bulb, reflector and cooling mechanism [99].

The UV curing process for powder coatings involves transforming a molten powder coating into a solid film by using UV light. In UV curable powder coatings, the binder resins are pre-polymers or oligomers, which are induced to start a cross-linking reaction by the photo-initiator, which absorbs UV light and generates free radicals [100].

2.3.2.2 Electrostatic Spray System

The powder coating application equipment comprised pumps, hoses and guns.
The powder coating application process involved a powder delivery system, an electrostatic spray gun system, a spray booth, and a powder recovery system [98].

Figure 2.3 Electrostatic spray gun system used

The delivery system consisted of a storage container, and a pumping device that transported a mixture of powder and air into hoses. The ITW GEMA spray gun system is supplied with a 100,000 volt potential to give the ability to coat powder coating on parts, e.g. leather substrate. There are straightforward procedures to guide on the operation menu and of the spray gun, the patented digital valve control automatically and precisely adjusts all air required for powder coating

2.3.3 Electro Magnetic Brush (EMB) for Powder Coating Application Method

UV curable powder coatings based on the commercially available powder coating resins from the UCB Co. Ltd (Anderlrechtstraat 33, B-1620 Drogenbos, Belgium) were coated onto leather using the novel EMB powder coating application process, which was developed by the DSM Coating Resins Netherlands B.V. (Slachthuisweg 30, 3151 XN Hoek Van Holland).

2.4 Instrumental Analysis methods

2.4.1 Thin Layer Chromatography

Thin layer chromatography (TLC) is one of the simplest, fastest, easiest and least expensive of several chromatographic techniques [101]. TLC is used for determining the purity of products and also for preliminary identification or to monitor reaction process. TLC is useful for determining the best solvent system for preparative separations of mixtures.

Commercially available poly (ethylene terephthalate) plastic sheets pre-coated with silica gel 60 (layer thickness 0.2mm and 0.25mm) were used. The size of plate for TLC analysis about 8×2.5cm, which permits two samples to be spotted onto the baseline (a line marked about 1 cm from one end of the plate). A small quantity of the sample (liquid or solution) was introduced onto a TLC plate before developing it by using a micro-pipette. The TLC plates used in section 3.2.3.1 had the following specifications: layer thickness 0.2mm, pre-coated with silica gel 60 without fluorescent indicator type (produced by E. Merck Darmstadt Company, the plate type is Art. 5748). The mobile liquid system was selected as ethyl acetate/petroleum ether (b.p 40-60 °C) in the ratio of 10.0 to 1.0 (v/v). The TLC plate, Art. –Nr. 805025 type (made by Machery-Nagel Gmbh) was used in section 3.2.3.2. The mobile liquid system: ethyl acetate/petroleum ether (b.p 40-60 °C) at ratio of 10 to 1.0 (v/v) was used to develop the Art. –Nr.805025 TLC plate, the ranges of R_f were too wide, so a mobile liquid system: Butyl acetate/petroleum ether (b.p 40-60 °C) at a ratio of 10 to 1.0 (v/v) was utilized.

Performing the TLC Analysis

Glass development tanks (TLC Chromatank Shandon®, 11.5×11.5 ×5.5 cm) with a lid for TLC were used in experiments. Samples were spotted onto the TLC plates by using micro-pipettes and the TLC spotted plate was put into the glass developing tank, and left in the tank and the developing solvent allowed contacting the lower

edge (about 0.5cm) of the TLC strip, the plate was developed to the top marked line and then stopped. The TLC plate was then removed from the tank and the solvent vapor allowed evaporating in the fume cupboard.

Visualizing the developed plate

After development, if the spots were not easily seen, visualizing agents for TLC plates were used to assist the identification of the location of the displaced sample. By far the most useful means of analysis uses a combination of observation under UV light and staining with iodine vapor.

Ultraviolet (UV) Light Visualization Method

The TLC strip was placed under a UV light with the room light turned off or eliminated as much as possible. For the TLC strips used in these experiments the background color under UV light was dark blue, and sample spots appeared white. Sample spots visible under UV light were traced with pencil. Sometimes an iodine visualization method was used when sample spots were too faint to be visible under UV light.

Iodine Visualization Method

The TLC strip was placed in the dried TLC glass development tank containing a few iodine crystals and covered with the glass lid. The sample which had been spotted onto the strip absorbed some of the iodine vapors and was visible as dark brown spots. The absorption of iodine required about two minutes. The spots were marked with a pencil when the strips were taken out of the tank. Iodine de-adsorption gradually occur in the air.

In TLC analysis, comparing how far the substance moves compared to the solvent front can be used to identify samples. This is called the retention factor (R_f)

$$R_f = \frac{\text{distance from origin to spot center}}{\text{distance from origin to solvent front}} \qquad (2.5)$$

If two compounds have the same R_f valve, they are likely the same compound.

Flash chromatography

Flash chromatography is a rapid chromatographic technique for preparative separations with moderate resolution; it is basically an air pressure driven hybrid of medium pressure and short column chromatography [102, 103]. This technique was used to purify the prepared functional acrylate monomer product in this study. A glass column packed with silica gel 60 was used in the experiment.

2.4.2 Ultraviolet-visible (UV-VIS) Spectroscopy

The ultraviolet (UV) region of the electromagnetic spectrum comprises radiation with wavelengths from just below 10^{-7} m up to 3.5×10^{-7}m. UV spectroscopy is usually extended into the visible region, so the technique is more correctly called ultraviolet-visible (UV-VIS) spectroscopy. A Spectronic 501 type instrument made by Milton Roy UK Ltd. (Oaklands Business Park, Workingham, Berks, UK) was used for quantitative analysis of prepared fuctional acrylate monomer in this study.

The most common theory, which is applied to UV-VIS spectroscopy, is the Beer-Lambert Law [104]. The absorbance (A) of a sample at a particular wavelength is proportional to the concentration (c) of the sample (in moles per liter) and the path length (l) of the light through the sample (in centimeters). When the solution is sufficiently dilute, A is defined as the logarithm of the ratio of the intensity of the incident light (I_0) to the intensity of transmitted light (I).

Hence

$$A=-\log(\frac{I}{I_0})=\varepsilon cl \qquad (2.6)$$

ε is called molar absorption coefficient, in units of mol^{-1} cm^{-1}.

So calibration curve of absorbance (A) versus concentration (c) can be utilized for quantitative analysis of hydroxymethyl groups in synthesized monomer.

2.4.3 Differential Scanning Calorimetry (DSC)

Differential scanning calorimetry (DSC) is a valuable technique in detecting phase transition and determining quantitively the transition temperature (T), the enthalpy change (ΔH) and so the order of the transition. A differential scanning calorimeter consists of sample and inert reference holders, to which the difference in power inputs to maintain them at the same heating rate is recorded and plotted against the temperature.

A modular type DSC instrument the DSC822^e (Mettler-Toledo Ltd., 64 Boston Road, Beaumont Leys, Leicester, UK) was used. The computer to control DSC module was set up with the Mettler Toledo professional STAR^e Software for analysis of DSC results.

Determination of crystallinity of polymer

The crystallinity, C, of the semi-crystalline polymers was calculated as follows:

$$C = \frac{\Delta H}{\Delta H_{100\%}} \cdot 100\% \qquad (2.7)$$

Where

ΔH is the measured heat of fusion [J/g] from the DSC

$\Delta H_{100\%}$ is the heat of fusion of the corresponding 100% crystalline polymer [J/g] given by literature.

Determination of glass transition temperature of polymer

The software allows one to draw a frame around the feature of interest which is then followed by clicking onto 'DSC/glass transition temperature', which causes the glass transition temperature to be calculated automatically in STAR^e midpoint. The STAR^e midpoint is defined as the intersection point of the bisector of angle with the

measuring curve. This bisector of angle goes through the intersection point of the baselines before and after transition [105], this operation is shown in Figure 2.4.

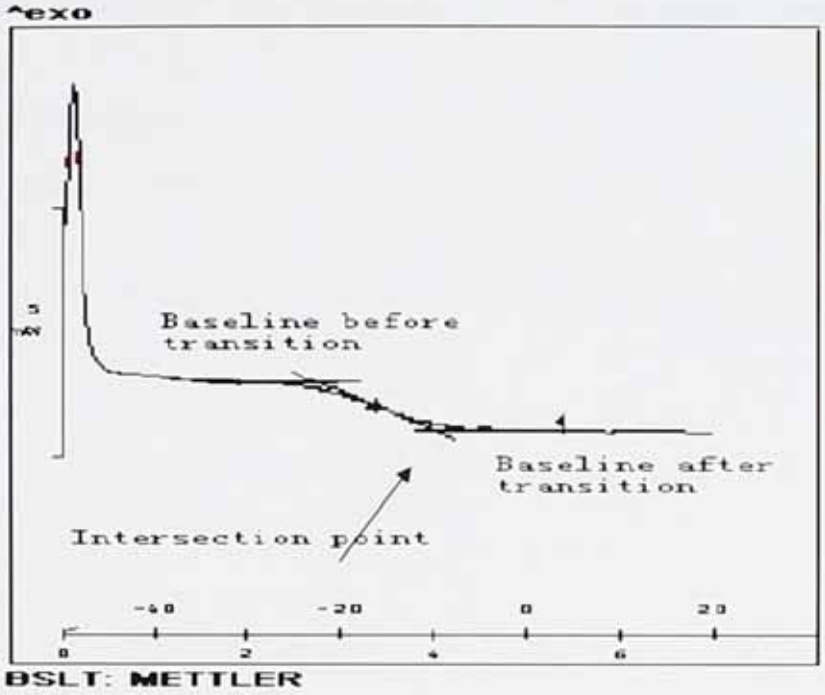

Figure 2.4 Scheme for calculating the glass transition temperature

DSC samples were analyzed in 40μ standard aluminum pans. Samples were analyzed under following conditions: the DSC data was collected from -50 to 150°C or 0 to 150°C at a heating rate of 5 or 10°C/min under a nitrogen purge. The DSC thermograms were normalized to an equivalent sample weight for comparison. Degrees of crystallization, melting points and glass transition temperatures were measured using the standard DSC software provided by the Mettler Company. When calculating degree of crystallinity, the theoretical heat of fusion for samples was taken as 181.8 J/g [106].

Amounts of samples used were 9.2 mg (sample 428A), 11.3 mg (sample 428B), 10.7 mg (sample 428C), 7.6 mg (sample 428D) and 11.2 mg (sample 428E). Samples

were analyzed in 40μ standard aluminum pans. The data was collected from -50 to 150°C at a heating rate of 10.00°C/min under a nitrogen purge. Analysis of samples 512A, 512B, 512C and 512D was at a different temperature scan rate of 2.5°C, 5°C, 10°C and 20°C respectively. For other samples DSC data was collected from -50 to 150°C or 0 to 150°C at a heating rate of 5 or 10°C/min under a nitrogen purge

2.4.4 Scanning Electronic Microscope (SEM)

The scanning electron microscope (SEM) does not actually view a true image of the specimen; it produces an electronic map of the specimen that is displayed on a cathode ray tube (CRT) [107]. A scheme for a generic SEM is shown in Figure 2.5.

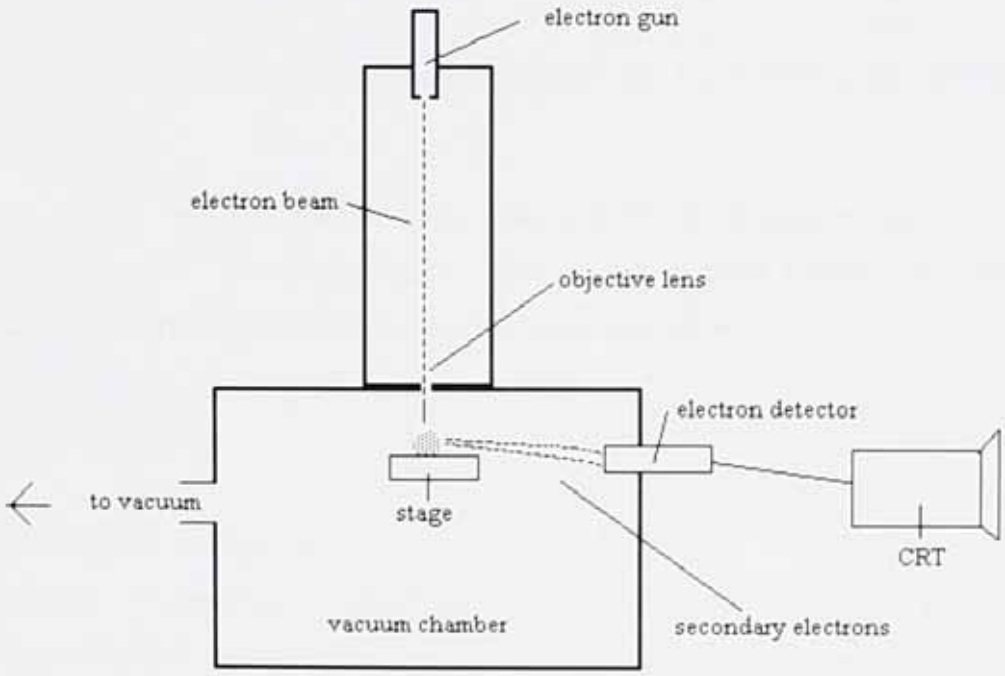

Figure 2.5 A scheme for SEM structure

Electrons from a filament in an electron gun are beamed at the specimen in a vacuum chamber. The beam forms a line that continuously sweeps across the specimen at high speed. This beam irradiates the specimen which in turn produces a signal in the form of either x-ray fluorescence, secondary or backscattered electrons.

The SEM has a secondary electron detector. The signal produced by the secondary electrons is detected and sent to a CRT image. The scan rate for the electron beam can be increased so that a virtual 3-D image of the specimen can be viewed. The image can also be captured by standard photography.

A Hitachi, S-3000N SEM instrument was utilized to visualize microscopic features of the surface of cross linked coating film[108] and the cross section structure of coated leather samples.

2.4.5 Fourier Transforming Infrared Attenuated Total Reflection (FTIR-ATR) Spectroscopy

The infrared region of the spectrum extends from the long-wavelength end of the visible region at 1μm out to the microwave region at about 1000μm. It is common practice to specify infrared frequencies in wave number units:

$$\nu\,(cm^{-1}) = 1/\lambda \qquad (2.8)$$

where λ is the wavelength

Thus the infrared region extends from 10 000cm^{-1} down to 10cm^{-1}. The spectral range from 4000 to 400 cm^{-1} has received the greatest attention because the vibration frequencies of most molecules lie in this region [109]. So FTIR was used to determine the prepared monomers' structures. FTIR-ATR is a surface sensitive absorption spectroscopy method that can be used to detect small amounts of material close to an interface. In the ATR geometry, IR radiation is totally reflected at the interface between a crystal element and a sample (solid, coating layer or polymer). Each internal reflection results in the production of an evanescent field that extends a few

microns into the sample and any IR absorbing species that approaches the surface will absorb radiation and attenuate the main beam, giving rise to an absorption spectrum. FTIR-ATR can provide valuable information related to the chemical structure of polymer materials and organic compounds. A Shimadzu UK Ltd. (Featherstone Road, Milton Keynes, UK) produced; FTIR-8400S was utilized to analyze prepared functional monomers and polymer resins.

The ATR accessory for the FTIR instrument is suitable for monitoring single layers of organic, polymer films or powders, to give extra information about the structures, orientations and dynamics of polymer materials and surface modified particles and was used in this project.

In chapter III, the sample of prepared polyurethane was directly loaded under the lens of the ATR, which was attached to the FTIR instrument and controlled by a computer with Shimadzu IR Solution software.

The sample of surface modified silica particles, which had been treated with acryloyl chloride (AC), was directly loaded under the lens of the ATR, which was attached to the FTIR instrument controlled by a computer with Shimadzu IR Solution software. The surface modified silica particles, treated with 3-(trimethoxysily)propyl methacrylate (TPMA) and fumed silica raw material were analyzed using FTIR since the ATR lens wasn't available at the time. The sample preparation procedure for FTIR analysis was as follows: One drop of a 1.0% solution of sample in dried acetone was added onto a sodium chloride disc. After evaporating the acetone in the fume cupboard, the sodium chloride disc was loaded in the FTIR sample clamp and then analyzed.

2.4.6 Measurement of Tensile Properties

The SLP 6 test method [96] (test for measurement of tensile strength and percentage elongation as given in Official Test Methods 1996) was used to determine the tensile

strength and elongation. The mechanical properties of polymer binder resins and powder coated cross-linked films were measured in tension using a Stable Micro System (SMS) tensile tester.

Tensile strength was calculated as:

$$\text{Tensile Strength} = \frac{\max imum\ breaking\ load}{cross\ sectional\ area} \qquad (2.9)$$

(Units Pascals (N m^{-2}), cross sectional area = mean width x mean thickness)

Percentage elongation at break was calculated as:

$$\text{Percentage elongation} = \frac{final\ \ free\ length - initial\ \ free\ length}{initial\ \ free\ length} \times 100 \qquad (2.10)$$

The tensile test specimen was tested at a test speed of 100 mm/min tensile and temperature of 20°C. The tensile test data were used to determine the relationship between: nominal stress σ (force per unit unstrained cross-section area) and extension ratio λ (extended length/initial length) [110].

$$\sigma = G(\lambda - \lambda^{-2}) \qquad (2.11)$$

A plot of σ against $(\lambda - \lambda^{-2})$ should give a straight line with slope G (modulus factor) [111].

2.4.7 Dynamic Mechanical Thermal Analysis (DMTA)

The prepared polymer binder is a viscoelastic material; it is subjected to a sinusoidally varying strain:

$$\varepsilon = \varepsilon_0 \sin(\omega t) \qquad (2.12)$$

where ε_0 is the amplitude and ω is the frequency in radians per second, and t is the time in second. The stress resulting from the strain will not be in phase due to the viscoelastic binder. Then the resulting stress will be:

$$\sigma = \sigma_0 \sin(\omega t + \delta) \tag{2.13}$$

where δ is the shift between stress and strain. The assumption made that the stress varies sinusoidally is valid as long as the material is linearly viscoelastic. By using classic trigonometry the equation (2) can be rewritten:

$$\sigma = \sigma_0 \sin(\omega t) + \sigma_0 \cos(\omega t) \sin(\delta) \tag{2.14}$$

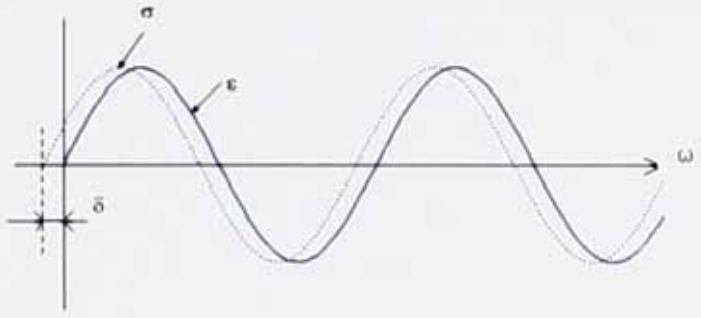

Figure 2.6 Illustration of dynamic stress and strain

The stress can be expressed in two terms, the first one describes in a phase stress and the second one describes a curve shifted 90 degree out of phase. The stress has been divided into an *elastic* term and a *viscous* term. So an elastic modulus and a viscous modulus can be defined as:

Elastic modulus (storage modulus): $E' = \sigma_0/\varepsilon_0 \cos(\delta)$ (2.15)

Viscous modulus (loss modulus): $E'' = \sigma_0/\varepsilon_0 \sin(\delta)$ (2.16)

It is appropriate to view material damping performance in relation to its stiffness a good expression for damping performance is the loss tangent:

$$\tan(\delta) = E''/E' \tag{2.17}$$

E', E'' and tan(δ) were used to characterize material dynamic properties.

A Gearing Scientific Company (1 Ashwell Street, Herts, UK) Dynamic Mechanical Thermal Analyzer was utilized to analyze the viscoelastic properties of powder coating films before and after cross-linking. It was also used to study the effect of surface modified nano-scale silica on the powder coating system. Measurement of the storage modulus and loss tangent of samples in single cantilever bending mode, tension mode or shear mode were used to detect interfacial failure or internal molecular motions. The glass transition temperature (T_g) was taken as the temperature of the maximum of the loss tangent curve [112]. DMTA samples were measured in powder clamp sheets. The specimens were analyzed under the following conditions: frequency 1.00Hz, temperature range from -80°C to 100°C at ramp rate 5°C/min, with a rectangular specimen in a single cantilever bend mode.

Chapter III Synthesis of Novel Binders and Study of the Effect of Curing on Crystallinity

3.1 Introduction

Various structural polymer materials, which are applicable as surface coatings, can be obtained via step polymerization. It is well known that polyurethane or acrylated polyurethane with its good flexibility and adhesion to leather surfaces is one of the most suitable binders for the finishing of leather. In order to prepare novel powder coating binders suitable for the finishing of leather, the synthesis of semi-crystalline polyurethane with or without pendant functional groups has been studied in order to understand how to control crystallinity. The idea was to have a storable powder of relatively high crystallinity which could be transformed to a clear-coat film of low/zero crystallinity.

In the first part of the research work described in this chapter, different molecular weight polycaprolactone diols have been employed and their effects on the crystalline properties of polyurethane prepared have been studied. Diols with pendant carboxylic groups or hydroxyl groups for thermal curing have been introduced into the polyurethane molecular architecture in order to prepare functional polyurethanes and the properties of these polymers were investigated.

In the second part of the research work described in this chapter, the aim was to develop a novel UV-curable polyurethane powder coating binder system with a molecular architecture involving the introduction of UV-curable side-chain functional groups and branches, to interrupt structural regularity, onto the polymer backbone. Since there was no commercially available functional monomer dihydroxymethyl butylacrylate (DHBA) the synthesis of DHBA was studied during this research.

3.2 Experimental

3.2.1 Chemicals

The following chemicals were used as received from the Sigma-Aldrich Co. Ltd (The Old Brickyard, New Road, Gillingham, Dorset, UK).

Acryloyl chloride (AC) (96%); Triethylamine (TEA) (99.5%);
Trimethylolpropane (TMP) (97%); Toluene (99.5%);
Acetone(99.5); Ethyl acetate (99.5%);
Chloroform (CF) (99%); Ethanol (99.5%);
Iodine (99.99%); Methanol (99.8%);
Ceric ammonium nitrate; Butyl acetate (99.5%);
p- Toluene sulphonic acid; Anhydrous calcium sulphate (99%);
Diethylene glycol (DEG) (99%); Glycerine (98%);
Molecular sieves (4Å); Glycerol (99%);
Ethyl acetoacetate (EAA); Petroleum ether (b.p. 40-60°C and 80-100°C);
Anhydrous potassium carbonate; Anhydrous magnesium sulphate;
Tetrohydrofuran (THF, dried with anhydrous calcium chloride);
Anhydrous calcium chloride (fused granule 8-24mesh);
Sodium hydroxyl solution (0.5N and 2.0N);
Hydrochloride solution (0.5N and 2.0N).
Polycaprolactone diols (molecular weight M_n=530, 1250 or 2000);
2-butyl-2-ethyl-1,3-propanediol (BEP) (99%);
2,2-Bis(hydroxymethyl) butyric acid (BHB) (98%);
Hexamethylene 1,6-diisocyanate (HDI) (98%);

Photo initiators, e.g. Alpha-hydroxy Ketone (Irgacure ®184) were supplied by Ciba Company, Switzerland)

3.2.2 Preparation of Semi-crystalline Polyurethane Binders

3.2.2.1 Polyurethane Prepared from Different Molecular Weight Polycaprolactone Diols

Different molecular weight crystalline polycaprolactone (PCL) diol oligomers, e.g., PCL diol Mn=2000 (PCL-2000), PCL diol Mn=1250 (PCL-1250), and PCL diol Mn=530 (PCL-530) were selected to react with hexamethylene diisocyanate (HDI) to prepare semi-crystalline polyurethane binders. The scheme of the reaction used to prepare polyurethane is shown in Figure 3.1.

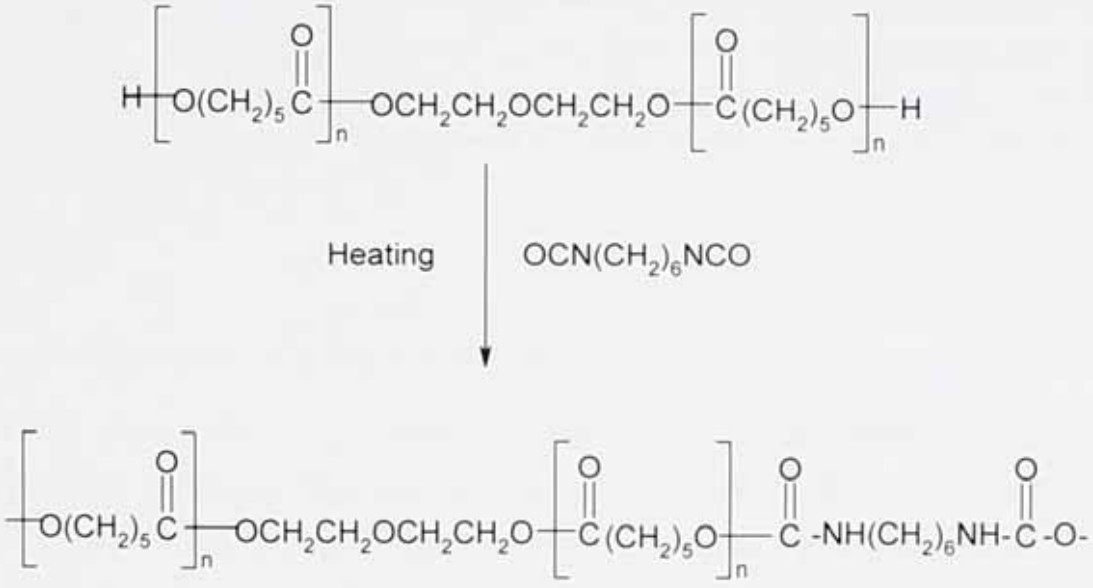

Figure 3.1 Scheme of representation for the preparation of semi-crystalline polyurethane

Random copolymerization of HDI with a mixture of different molecular weight PCL diols was also carried out. The experimental design and reaction conditions are listed in Table 3.1. The total mass of reactants used for each experiment was between 0.80 to 2.30g. The reaction was carried out in sealed test tubes with a nitrogen blanket at 70-76 °C in oil bath. The test tube was agitated from time to time by shaking.

Table 3.1 Synthesis experiment for semi-crystalline polyurethanes

Exp. No.	Component (molar ratio)				Reaction condition
	HDI	PCL-530	PCL-1250	PCL-2000	
pu-1	1.00	---	1.00	---	at 75-76 °C for 7.5h
Pu-2	2.00	---	1.00	---	at 75-76 °C for 7.5h
Pu-3d	3.80	3.20	---	1.00	at 74-76 °C for 13.0h
Pu-3a	3.05	2.00	---	1.00	at 74-76 °C for 10.5h
Pu-3b	2.09	1.00	---	1.00	at 74-76 °C for 5.0h
Pu-3c	4.25	1.00	---	2.04	at 74-76 °C for 4.0h
Pu-4a	3.33	2.05	1.00	---	at 70-73 °C for 12.5h
Pu-4b	2.22	1.00	1.02	---	at 70-73 °C for 12.5h
Pu-4c	3.00	1.00	2.00	---	at 70-73 °C for 12.5h

3.2.2.2 Polyurethane Prepared from Diols Containing Alkyl Side-chain

In this part of work, a diol monomer with the side chain, 2-butyl-2-ethyl-1,3-propandiol (BEP), was introduced into polyurethane molecule structure (Figure 3.2) as a source of irregularity to reduce crystallinity and heat of fusion of the semi-crystalline polyurethane binders.

The experiments and reaction conditions are listed in Table 3.2. The mass of reactant for each experiment in total is between 0.15 to 0.85g. The reaction was carried out in sealed test tubes with a nitrogen blanket at about 73-95 °C in an oil bath. The test tube was agitated by shaking from time to time.

Table 3.2 Synthesis experiments to produce semi-crystalline polyurethanes from PCL/BEP/HDI

Exp. No.	Component (molar ratio)			BEP/(PCL+ BEP)	Reaction condition
	BEP	PCL- 1250	HDI	(%)	
pu-5a	1.00	6.66	8.19	13.1	73-76 °C for 15.5h
pu-5b	1.00	3.00	4.36	25.0	73-76 °C for 11.5h
pu-5c	1.23	1.00	2.81	55.2	73-76 °C for 3h; 76-83 °C for 4.6h; 85-95 °C for 1.2h
pu-5d	1.61	1.00	3.54	61.7	73-76 °C for 3h; 76-83 °C for 4.6h; 85-95 °C for 1.2h
pu-5e	3.90	1.00	6.46	79.6	73-76 °C for 3h; 76-83 °C for 4.6h; 85-95 °C for 1.2h

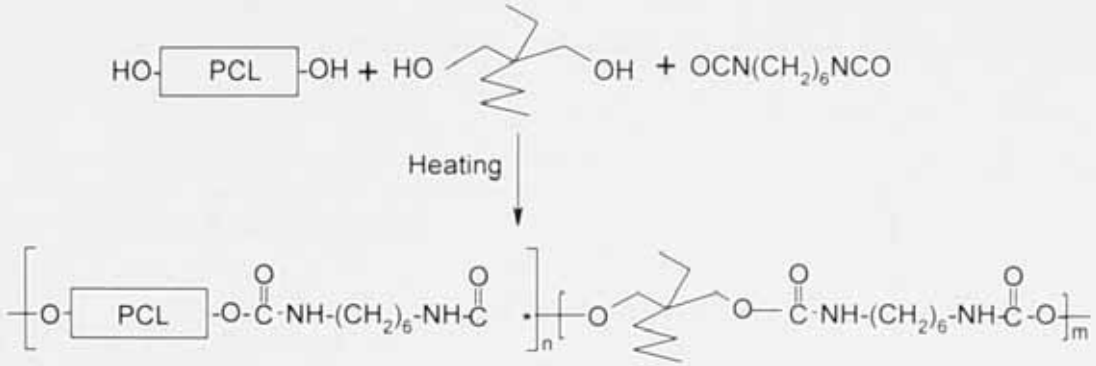

Figure 3.2 Scheme of reaction for the preparation of branched polyurethane by a second diol monomer

3.2.2.3 Synthesis and Characterization of Polyurethanes with Pendant Functional Carboxylic Groups

Semi-crystalline polyurethane resin was prepared by reacting the HDI with a diol mixture comprising diethylene glycol (DEG) and 2,2-bis(hydroxymethyl)butyric acid (BHB). The molar ratio of reactants was HDI: DEG: BHB = 1.00:0.708:0.283. The bulk polymerization was carried out in a dried flask under nitrogen at 66±1°C, for 20 minutes. The preparation process can also be performed in a solvent (such as tetrahydrofuran).

The semi-crystalline polyurethane resin was then formulated with a cross-linker (such as HDI, about 3% by weight), and samples were thermally cured at 100°C in an oven for 2 hours. The DSC curves obtained with this material are shown in Appendix C3.1; the data were collected from 0 to 150°C at a heating rate of 10°C/min under a nitrogen purge.

3.2.2.4 Synthesis and Characterization of Polyurethane with Pendant Functional Hydroxyl Groups

According to the polyurethane synthesis conditions put forward by Li [74], the polyurethane containing pendant functional groups was synthesized in a reaction as shown in Figure 3.3.

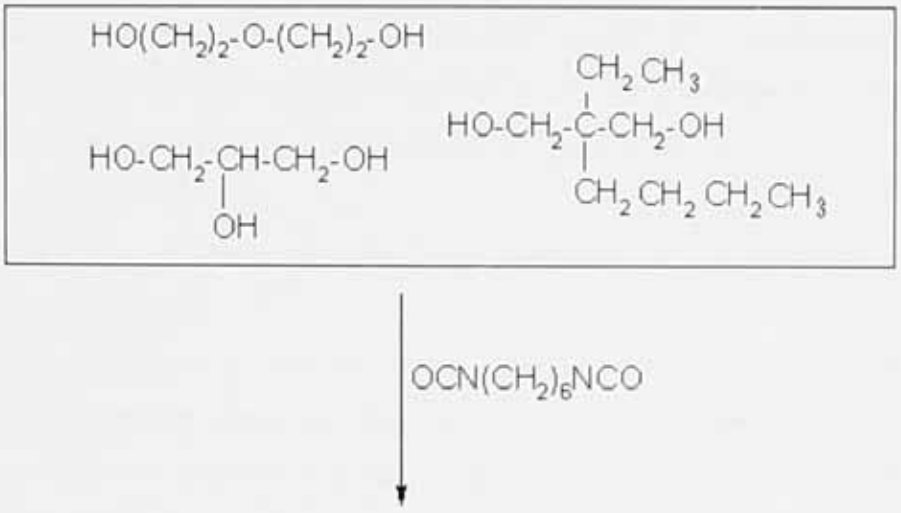

Fig. 3.3 Scheme of reaction for preparation of functional polyurethane [74]

10.0 ml of acetone was added along with 10.0 ml toluene (both dried with molecular sieves, and filtered) to a 50 ml flask, fitted with a condenser cooled with tap water. The solvents were mixed for 10 minutes using a magnetic stirrer bar at a speed about 400 RPM, after which was then added 7.43g （0.044 mol） HDI, and then a mixture

of 2.55g (0.024 mol) diethylene glycol (DEG), 1.19g (0.074 mol), 2-butyl-2-ethyl-1,3-propandiol (BEP) and 0.80g (0.0087 mol) glycerine (GLY). Nitrogen was slowly purged into the flask during the reaction. The solution was stirred vigorously (900 RPM) and the reaction took place at 45±1°C. After 4 hours a solid had appeared on the wall of the flask, with a total reaction time of 9 hours. There was only 7.0 ml of polyurethane in solution, and the other polyurethane was in the solid state.

Part of the solid polyurethane sample was put onto a watch glass, and dried in a fume cupboard at room temperature for 5 days; this sample was marked as PU-6.

Cured polyurethane sample

1.25g of polyurethane sample PU-6 was placed in a Petri dish, and melted by exposure to Infrared Radiation, and afterwards 0.0875g HDI was added as cross-linker. The cross-linker was mixed uniformly with the melted polyurethane, and the Petri dish was covered with a watch glass. The polyurethane was cured in an oven at 100°C for 10 hours. The cured sample was marked PU-7.

Samples for tensile testing and DMTA analyzing

Polyurethane resin PU-6 and cross-linked polyurethane sample PU-7 were put onto silicone release paper, and then covered with another piece of the same paper, and then put between steel hotplates (samples had just been heated in an oven at 100°C for 1 hour), pressed between hotplates using a hydraulic laboratory press (produced by Apex construction Ltd., Type A1), at a pressure of 6MPa for 10 minutes. Sample films prepared in this way were gradually cooled to room temperature prior to tensile testing and DMTA analysis.

3.2.3 Preparation and characterization of Semi-crystalline UV-curable Polyurethane Binders

Synthesis and Characterization of Polyurethane Acrylate Binders

Polyurethanes prepared from hexamethylene diisocyanate (HDI) and diethylene glycol (DEG) are semi-crystalline oligomers or polymers, with melting points below 125°C. The polyurethanes were selected as polymer backbone, dihydroxyl functional monomer with branched acrylate group, such as 2,2-dihydroxymethylbutyl acrylate (DHBA), CH_2=CHCOOCH_2C(CH_2OH)$_2$CH_2CH_3, was introduced into the polymer backbone and dihydroxyl functional monomer with branched alkyl groups was also formulated into the preparation of the polymer binders for the purpose of controlling crystallinity. No commercial DHBA was available, the synthesis and characterization of DHBA was studied.

3.2.3.1 Synthesis of 2, 2'-Dihydroxymethyl butylacrylate by Method I

The monomer DHBA was synthesised by the reaction of trimethylolpropane with acryloyl chloride (Figure 3.4), according to the synthesis methods described in the references [76, 113-116]. The optimal synthetic condition for DHBA functional monomer was investigated.

Figure 3.4 Reaction scheme for synthesis of DHBA

The purification of the DHBA has been studied by thin layer chromatography (TLC) flash chromatography combined with ceric ammonium nitrate reagent to determine hydroxymethyl groups and UV-visible spectroscopy to monitor product concentration.

Optimization of Chromatographic methods

For the non-polar solvents, e.g. petroleum ether and toluene, the spots had moved very little from their original places after the TLC plates were developed; for the polar solvents, e.g. ethyl acetate, acetone, chloroform and methanol, the mixture of samples on the TLC plates could be separated, but the front component on the developed TLC plate was too broad. Thus a combination of polar solvent with non-polar solvent as a mobile eluent for crude product was studied. At this stage it was found that ethyl acetate/petroleum ether can be used as the eluent system [102] to easily separate the isomers of epimeric alcohols, so a mobile phase was developed to utilize this information to achieve the separation of prepared crude products. In the DHBA crude product, there are by-products, e.g. biacrylate (BIA) and triacrylate (TRA), and un-reacted TMP etc.

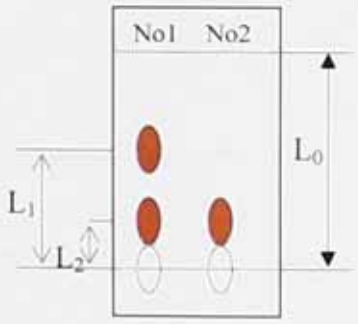

Figure 3.5 A developed TLC plate comparing samples of monomer crude product with TMP; Sample No. 1 is DHBA crude product; sample No.2 is the alcohol mixture of TMP

In the crude product, the solubility of TMP, DHBA, BIA and TRA in toluene are different, with the solubility increasing from TMP to TRA; in water the order is reversed. For example, when 1.5 ml of crude product was extracted with 5 ml

toluene, there were only DHBA and TMP spots on TLC plate after development (Figure 3.5); the original picture of the TLC plate is shown in Appendix C3.2 (the iodine visualization method was used to observe the developed TLC plate).

Following TLC it was found that: $R_{fDHBA}=L_1/L_0=28.5mm/73.0mm=0.39$; and $R_{fTMP}=L_2/L_0=15.0mm/73.0mm=0.21$, so $\Delta R_f= R_{fDHBA}- R_{fTMP}= 0.18$. When the crude product was extracted with toluene, the TEA, BIA and TRA were removed and further purification was then achieved by using flash chromatography.

The conditions used in the flash chromatography were as follows:

Column diameter:	21 mm
Silica gel depth:	280 mm
Volume of eluant:	280 ml
Sample (loading):	900 mg
Fraction size:	10 ml
Flow rate:	6 ml/min.

Fractions containing the product DHBA were combined (110ml to 140ml). About 0.37g of purified DHBA was obtained after removing the solvent by rotary evaporator, where the bath water was maintained at 34-38°C and the pressure gradually reduced to about 300 mmHg. The yield of DHBA based on TMP is 12.1%.

Monitoring the Synthethis Process Using UV-visible Spectrophotometry with Ceric Ammonium Reagent

Aqueous ethanol water solutions were used as a standard solution in order to provide a calibration curve. Hydroxymethyl groups reacted with the ceric ammonium reagent will produce a colored complex which can be measured by using a UV-Visible spectrophotometer. Measurements were made within 5 minutes to avoid the effect of

air, especially oxygen on the reaction. The calibration curve obtained is shown in Figure 3.6.

1.5 ml of prepared crude product was extracted with 15 ml toluene, the toluene solution became light yellow, but no change in the volume of product was observed. Following this 7 ml distilled water was added to the sample and stirred well. Solid

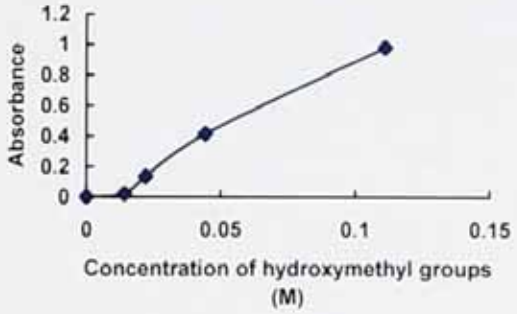

Figure 3.6 Calibration curve for hydroxymethyl groups

was suspended in the aqueous solution, which was filtered out, dried and labeled PLs; other product was separated from water by distillation under reduced pressure at 35-40°C, this was labeled PLc. 0.0051g of PLs was reacted with 1.5929g ceric ammonium reagent and the absorbance measured as A=0.414, thus the concentration of hydroxymethyl group in PLs according to the calibration curve in Figure 3.6 was about 0.0448M, giving an estimated 43.6% hydroxymethyl groups in PLs.

3.2.3.2 Synthesis of 2, 2'-Dihydroxymethyl butylacrylate by Method II

In method I, DHBA crude product was purified by the flash chromatography method and only about 0.37 gram of product was obtained each time, representing a yield of 12.1% based on TMP.

This section describes the preparation of a relatively large quantity of DHBA, by Method II [76, 115 and 116]. The synthetic scheme is shown in Figure 3.7. The process has three steps: the first step is the synthesis of 5-ethyl -5-hydroxymethyl -2,2-dimethyl-1,3-dioxolane (EHDD); the second step is the synthesis of 5-acryloyloxymethyl-5-ethyl-2,2-dimethyl-1,3-dioxolane (AEDD) and the third step is hydrolysis of AEDD to remove protective groups and obtain the DHBA product.

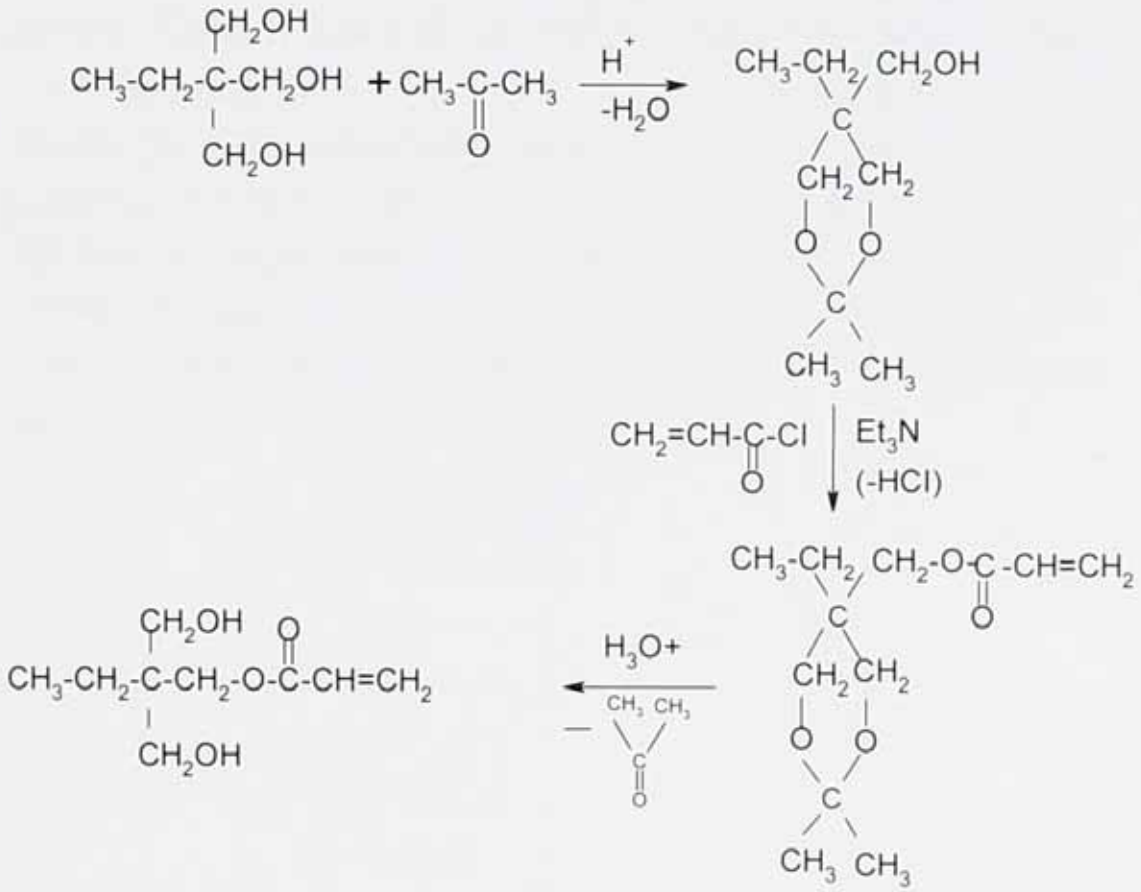

Figure 3.7 Scheme of preparation of DHBA

After several trials, an improved synthesis procedure was used as described in the following. A paraffin oil bath was placed over a magnetic stirring hot-plate with a stirring speed control system and a heating temperature control system, and a 3 litre round bottom 3-necked flask containing a magnetic stirring bar, fitted with a thermometer and reflux condenser was set up. 2.0 mol TMP was added followed by

20 mol (1350ml) acetone with 3.1g *p*-toluene sulphonic acid. The stirring speed was controlled at 700 RPM for 3 minutes; The TMP was completely dissolved in acetone at 18°C, and then 4.0g anti-bumping granules were added, and then 1000ml toluene (which had been dried over 4Å molecular sieves) was added, and then 60g anhydrous calcium sulphate was added, and reacted for 4.0 hours at 62-64°C (gas phase temperature). After filtration, the solution was transferred into a flask, which was connected with a distillation device to remove acetone, water and partially toluene at temperature between 62 and 109°C (gas phase temperature) over 3 hours. About 590 ml EHDD-toluene solution was obtained and the sample was marked as 040129A. The EHDD solution was neutralised with 0.5N NaOH solution to pH=7.0, then washed with 80 ml×2 distilled water and separated. In this way the residual TMP in the crude product solution was washed out. The product solution was dried with 43.2g molecular sieves for 12 hours and then filtered off the molecular sieves, distilled to remove solvent (gas phase temperature from 64 to 180°C); this gave 240.2g EHDD product, yield was 69.0%.

Figure 3.8 TLC method used for monitoring the synthesis and purification processes used during preparation of monomer

During synthesis and purification, the purity of intermediate products and DHBA were monitored by the TLC method.

Figure 3.8 shows one sample, 040129A (the original picture of the TLC plate is shown in Appendix C3.3), which had been developed on the TLC plate in the presence of *p*- toluene sulphonic acid. $R_{f\,EHDD}$ = 39.5mm/76.5mm= 0.52; and $R_{f\,TMP}$ = 8.0mm/76.5mm= 0.11. The developed area ratio of EHDD to TMP was about 11:1.

3.2.3.3 UV Curable Powder Coating Binder (System I)

A semi-crystalline polyurethane acrylate resin was prepared by reaction of a hexamethylene diisocyanate (HDI) with a diol mixture comprising diethylene glycol (DEG), Dihydroxymethyl butylacrylate (DHBA), and 2-Butyl-2-Ethyl-1, 3-propandiol (BEP). In this system, the molar ratio of diisocyanates to diols was 2.0: 3.0, therefore, only low molecular weight polyurethane end-capped with hydroxyl group would be produced. The ratio of monomer DHBA to BEP varied but the total content of monomers DHBA and BEP in the diols was kept at 40% by mole. The polymerization was carried out in a dried flask under nitrogen at 55±1°C for 10 hours in bulk. The detailed information about the reactants in the binder example system I is given in Table 3.3. It was found that the preparation of this binder example system could also be done by a solvent (such as chloroform) method as well.

The photo-initiator Irgacure® 184 (Ciba Company, Switzerland) was then added to the semi-crystalline or crystalline polyurethane acrylate resin and samples were heated by infrared radiation to an elevated temperature below 100°C at which flowing and leveling occurred and then cured with UV radiation (the UV intensity was 0.8-1.5 J/cm^2) for about 20 seconds.

Table 3.3 Reactants information of polyurethane binder system I

Exp. No.		1	2	3	4	5
DHBA	(g)	0.1983	0.1415	0.1031	0.0542	0
	(mol)	0.001055	0.0007526	0.0005484	0.0002883	0
BEP	(g)	0	0.04200	0.08370	0.1242	0.1671
	(mol)	0	0.0002620	0.0005221	0.0007748	0.001042
DEG	(g)	0.1689	0.1698	0.1642	0.1800	0.1645
	(mol)	0.001592	0.001600	0.001548	0.001697	0.001550
HDI	(g)	0.3007	0.2987	0.2971	0.2963	0.2996
	(mol)	0.001788	0.001776	0.001766	0.001762	0.001781
HDI/DEG/ DHBA/BEP (Molar ratio)		1:0.89:0.59:0	1:0.9:0.42 :0.15	1:0.88:0.31 :0.3	1:0.96:0.16 :0.44	1:0.87:0:0.59
T_g (°C, cured sample)*		-5.70	-18.6	-0.80	----	-24.2

* T_g values were determined by DSC

3.2.3.4 UV Curable Powder Coating Binder (System II)

In this case the monomer selections for the polyurethane acrylate resins were the same as those in binder example system I. However in this resin system, the polyurethanes were prepared with a molar ratio of diisocyanates to diols of 1.1:1.0, thus polyurethane would have a higher molecular weight than system I. The detailed information about the reactants in the binder example system II is given in Table 3.4. The polymerization was carried out in chloroform as a solvent by refluxing at 60-61°C for 10 hours. The solvent was removed at 80°C under reduced pressure after the polymerization was completed. The content of monomer DHBA was varied, while the mole fraction of DHBA and BEP in the total diols was kept constant at 0.40.

Table 3.4 Reactants information of polyurethane binder system II

Exp. No.		I	II	III	IV	V
DHBA	(g)	0.6598	0.4363	0.3451	0.177	0
	(mol)	0.005592	0.002321	0.001836	0.0009414	0
BEP	(g)	0	0.1367	0.2775	0.3629	0.5258
	(mol)	0	0.0008528	0.001731	0.002264	0.003281
DEG	(g)	0.5092	0.5266	0.5358	0.543	0.5134
	(mol)	0.004796	0.004962	0.005049	0.005117	0.004838
HDI	(g)	1.9372	1.5101	1.5853	1.5337	1.5348
	(mol)	0.01152	0.008978	0.009425	0.009118	0.009125
HDI/DEG/DHBA/ BEP (Molar ratio)		1.00:0.42: 0.49:0	1.00:0.55: 0.26:0.095	1.00:0.54: 0.19:0.18	1.00:0.56: 0.10:0.25	1.00:0.53: 0:0.36
DHBA content in pendant functional monomers DHBA/(DHBA+BEP) (%)		100	73.2	51.4	28.6	0
T_g (°C, cured sample)*		18.2	6.48	0.80	1.25	-15.7

* T_g values were determined by DSC

The semi-crystalline polymer was then formulated, heated and cured under the same conditions as described for binder system I.

3.2.3.5 UV Curable Powder Coating Binder (System III)

In this system, the monomer selections for the polyurethane acrylate resins were different from those in systems I and II: there was no monomer BEP added into the diol blend. The molar ratio of diisocyanates to diols was 2.0: 3.0. Otherwise the polymerization, formulation with photo-initiator, and heating and curing, were the same as described for system I.

Table 3.5 Reactants data for binder system III

Exp. No.		1	2	3	4	5
DHBA	(g)	0	0.101	0.1949	0.2227	0.3991
	(mol)	0	0.0005856	0.001037	0.001185	0.002123
DEG	(g)	0.2985	0.2292	0.1674	0.0828	0.0566
	(mol)	0.002813	0.002160	0.001578	0.0007804	0.0005335
HDI	(g)	0.3095	0.3084	0.2946	0.2438	0.2966
	(mol)	0.001840	0.001834	0.001751	0.001449	0.001763
HDI/DEG/DHBA (Molar ratio)		1.00:1.50:0	1.00:1.18:0.32	1.00:0.90:0.59	1.00:0.54:0.82	1.00:0.30:1.20

3.2.3.6 UV Curable Powder Coating Binder (System IV)

In this case the monomer selections for the polyurethane acrylate resins are the same as those for system III

In this system, the polyurethane acrylate resins were prepared without adding monomer BEP. The mole fraction of monomer DHBA in the diols was varied. The molar ratio of diisocyanates to diols was 1.1: 1.0, and they were reacted in a refluxing chloroform solvent at 60-61°C for 9.0 hours, and then the solvent was removed. Otherwise the polymerization, formulation with photo-initiator, heating and curing, were the same as described for system II.

Table 3.6 Information about the Reactants of binder system IV

Exp. No.		1	2	3	4	5
DHBA	(g)	0	0.1110	0.2010	0.2995	0.4564
	(mol)	0	0.0005904	0.001069	0.001593	0.002428
DEG	(g)	0.3015	0.2434	0.1727	0.1146	0.0681
	(mol)	0.002844	0.002296	0.001629	0.001081	0.0006425
HDI	(g)	0.5340	0.5436	0.4909	0.50060	0.5615
	(mol)	0.003175	0.003178	0.002919	0.003008	0.003338
HDI/DEG/DHBA (Molar ratio)		1.00:0.896:0	1.00:0.722:0.186	1.00:0.5558:0.366	1.00:0.359:0.530	1.00:0.192:0.727
DHBA content in diols DHBA/(DHBA+DEG) (%)		0	20.5	39.6	59.6	79.1

3.3 Results and Discussion

3.3.1 Characterization of Prepared Semi-crystalline Polyurethane without Functional Pendant Groups

Effect of reactants ratio on prepared polyurethane properties

In Figures 3.9 to 3.11, the results for melting temperatures, determined as onset and peak temperatures from DSC curves, for prepared polyurethane samples are shown. In Figure 3.9, the reactants are HDI and PCL-1250. When the molar ratio of HDI to PCL-1250 was 0 (i.e. it was just the PCL-1250), onset and peak temperatures were the highest. When the molar ratio of HDI to PCL-1250 was 1, the onset and peak temperatures of the prepared polyurethane were the lowest, (the original DSC traces are shown in Appendix C3.4).

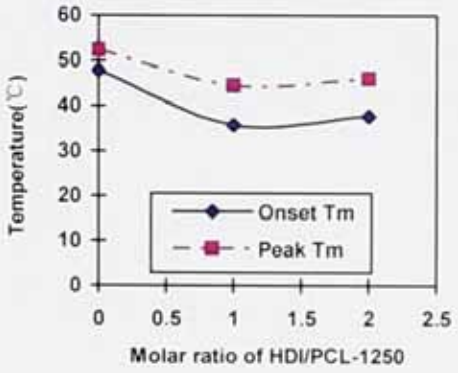

Figure 3.9 Reactant ratio effect on melting point of prepared polyurethane

Effect of copolymerization of different molecular weight diols effects on prepared polyurethane properties

In Figure 3.10, the reactants are HDI, PCL-1250 and PCL-530. As the content of PCL-1250 in total PCL diols (PCL-1250 and PCL-530) increased, the onset and peak temperatures were obviously increased (the original DSC traces are shown in Appendix C3.5)

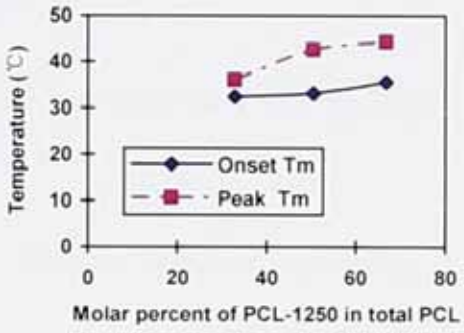

Figure 3.10 DSC onsets and peaks of prepared polyurethane

In Figure 3.11, the reactants are HDI, PCL-2000 and PCL-530. As the percentage of PCL-2000 in total PCL diols (PCL-2000 and PCL-530) increased, there was no obvious change of onset and peak temperatures, the original DSC curves are shown in Appendix C3.6.

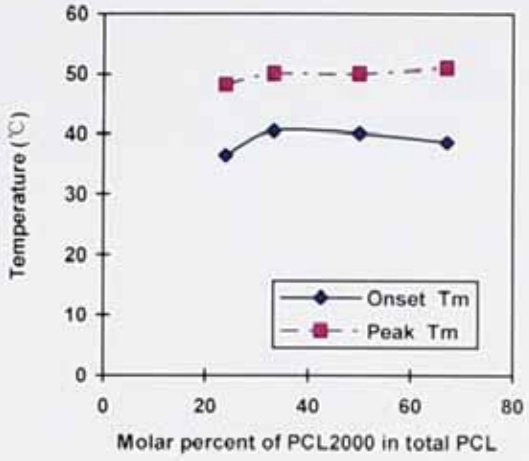

Figure 3.11 DSC onsets and peaks temperatures of PCL copolymers

Effect of Alkyl Side-chain Diols on Prepared Polyurethane Properties

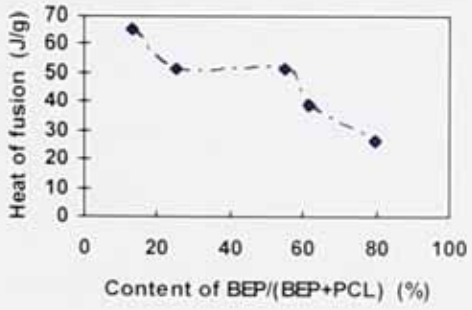

Figure 3.12 Heat of fusion vs content of PEP/(BEP+PCL) (%)

It can be seen in Figure 3.12 that, as the content of BEP in total diols increased from 13.1% to 79.6%, the heat of fusion of semi-crystalline polyurethane prepared decreased from about 65J/g to 26J/g. From Figure 3.13, it can be seen that the effect of the content of BEP on the onset melting temperature and peak melting temperature of polyurethane was not significant.

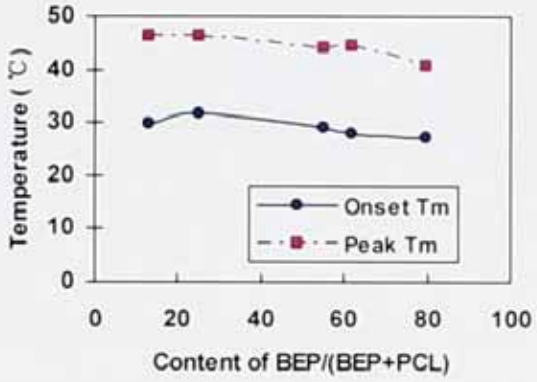

Figure 3.13 Melting temperature vs content of BEP/(BEP+PCL) (%)

3.3.2 Characterization of Prepared Semi-crystalline Polyurethane with Functional Pendant Carboxylic Groups

Selection of Dihydroxyl Monomer with Side Chain Carboxylic Group

During the preparation of functional polyurethane resins by the reaction of isocyanates with alcohols, which contain sterically hindered carboxylic acid groups, the reaction of isocyanates with hydroxy groups is faster than the reaction of isocyanates with the carboxylic acid groups, although isocyanates can react with any active hydrogen compound [75].

There are two commercially available dihydroxyl carboxylic acid monomers where the carboxylic acid group is sterically hindered, one is 2, 2-dimethylolpropionic acid (DMPA) and the other is 2, 2-Bis (Hydroxymethyl) butyric acid (BHB). Their structures are shown in Figure 3.14 and Figure 3.15 respectively.

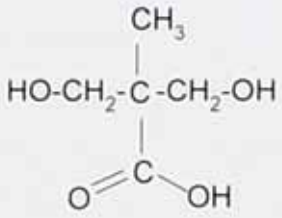

Figure 3.14 Scheme of DMPA structure .

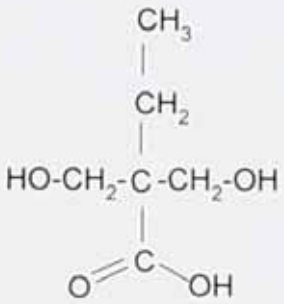

Figure 3.15 Scheme of BHB structure .

BHB (£19.30 per 100g) is more expensive than DMPA (£14.00 per 100g) [117], however the steric hindrance effect is more significant for BHB than DMPA (the ethyl group in BHB is bigger than the methyl group in DMPA); BHB should be a more suitable monomer for this study. A further potential benefit of selecting BHB is that a larger side ethyl group may have greater effect on melting point and reduce crystallinity. Any unwanted reaction of carboxylic acid groups with isocyanates will result in polyurethane cross-linking rather than leaving a pendant carboxylic acid group on the polyurethane chain. If the degree of cross-linking increases to a high enough level, it will cause a decrease in, or elimination, of the formation of crystalline regions in the prepared polyurethane system. Therefore BHB was selected as the functional monomer rather than DMPA in this study, to ensure less carboxylic acid groups to react with isocyanates during the preparation of semi-crystalline polyurethane and keep more functional cross-linkable groups for curing at a later stage when the powder coatings are cured. On the other hand, there is one more methylene group in the BHB molecule than the DMPA molecule, and so it is possible to offer greater flexibility (lower T_g) to the final coating film. Tsuyoshi [118] studied the effect of the length of alkyl side chain on the polymer properties, in

particular the crystallinities, and it was found that crystallinities decreased with increasing length of alkyl side chain in the comonomer.

The application of 2,2-Bis(hydroxymethyl)butyric Acid (BHB) to Reduce Crystallinity of Polyurethane

DSC results are listed in Table 3.7 for a sample prepared with BHB, and the detailed preparation information is shown in section 3.2.2.3. Before curing the semi-crystalline polyurethane resin, had a crystalillnity of 20.6% and onset melting point of 50.6°C; after curing, it showed no crystallinity and was completely amorphous. The glass transition temperature (T_g) of the cured resin was about 25.2°C. Polyurethane having no side groups (Table 3.6 Exp. No.1 and results in Figures 3.31 to 3.32) had a crystalillnity of 45.0% and onset melting point of 104 °C. The data indicates that functional monomer BHB greatly affects the crystalline property of polyurethane resin. BHB can decrease crystallinity of polyurethane; especially crystallinity of the prepared polyurethane from BHB can be further decreased or eliminated via cross-linking.

Table 3.7 DSC results for the polyurethane sample with pendant carboxylic acid groups before and after cross-linking

Resin	DSC results		
	T_m / °C (Onset)	T_g / °C (Midpoint)	Crystallinity / %
Before curing	50.6	---	20.6
After curing	---	25.2	0

3.3.3 Characterization of Prepared Semi-crystalline Polyurethane with Functional Pendant Hydroxyl Groups

Characterization of Polyurethane Resin by FTIR-ATR

The formation of polyurethanes was confirmed by FTIR. An example is given here by PU-6. The structure of polyurethane resin PU-6 was characterized by FTIR-ATR and the results are shown in Figure 3.16.

Figure 3.16 FTIR- ATR spectroscopy of polyurethane sample PU-6

It can be seen that there is a N-H absorption band at 3321cm^{-1}, and a carbonyl (C=O) stretching vibration at 1685cm^{-1}, showing that urethane groups had formed as expected. The asymmetrical stretching vibration $\nu_{as\ (CH2)}$ at 2935cm^{-1} and symmetrical stretching vibration $\nu_{s\ (CH2)}$ at 2858cm^{-1} can be seen as well as the N-H

bending vibration $\delta_{(N-H)}$ at 1535cm^{-1} and the C-N stretching vibration $\nu_{(C-N)}$ at 1257cm^{-1}. The absorption peaks at 1126 and 1057cm^{-1} are $\nu_{as\,(C-O-C)}$ and $\nu_{s\,(C-O-C)}$.

DSC Results of Polyurethane Resin

The polyurethane resin PU-6 and its cross-linked form, PU-7, have been thermally analyzed using DSC. The DSC traces are shown in Figure 3.17, and the corresponding results are listed in Table 3.8. The results show that the glass transition temperature of PU-6 is at -6.0 °C. For PU-6 there are two crystalline peaks, and the total crystallinity is 14.8%, with the first onset melting point being 38.2 °C and the second onset melting point 60.1 °C. But after cross-linking, there is no melting peak evident on the DSC curve: the cross-linked sample just shows a glass transition at 8.6 °C.

Table 3.8 DSC results of prepared polyurethane resin

Exp. No.		PU-6	PU-7
HDI/DEG/GLY/BEP (Molar ratio)		1.00: 0.545: 0.196: 0.168	
Cross-linker		-----	HDI (7.0%w.t in resin)
DSC	Crys. (%)	14.8	0
	T_m (°C, Onset)	38.2; 60.1	----
	T_m (°C, peak)	46.1; 71.0	----
	T_g (°C, Midpoint)	-6.0	8.6

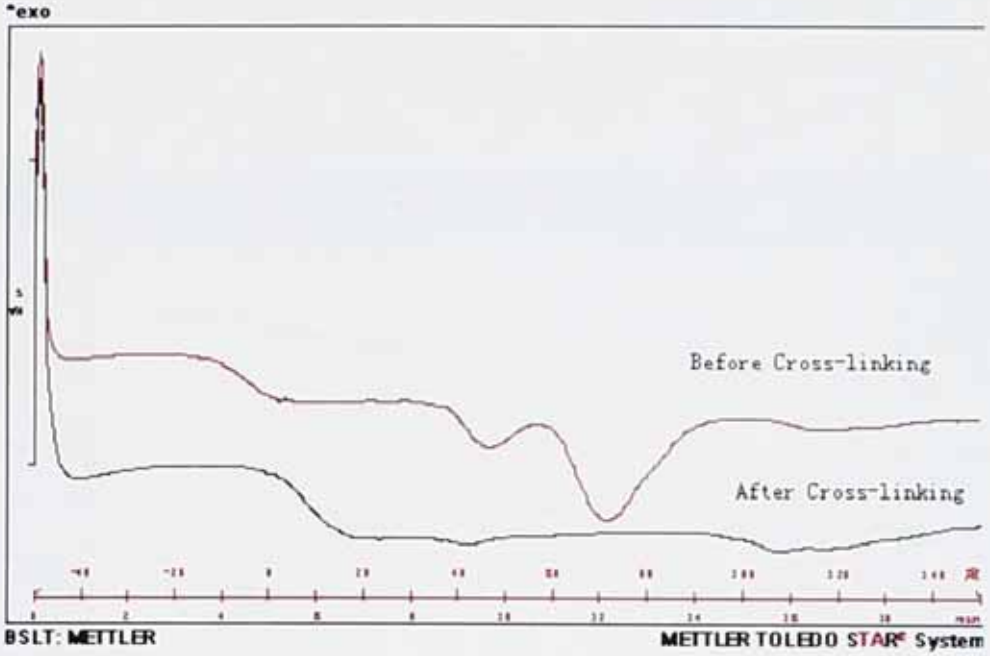

Figure 3.17 DSC curves of polyurethane samples PU-6 and PU-7

DMTA Analysis

The polyurethane resin PU-6 was analyzed using DMTA; samples were measured in the powder clamp. The analysis conditions are described in section 2.4.7. Figure 3.18 is the DMTA curves of polyurethane resin PU-6. One curve is the storage modulus and the other is the measured mechanical loss tangent (Tan Delta). Tan Delta is the ratio of loss modulus to storage modulus. When Tan Delta is at its peak value, the corresponding temperature represents the glass transition temperature (T_g). Figure 3.18 indicates the T_g of PU-6 is 14.1°C, and the second transition is about 40°C. The higher T_g value (14.1°C) determined by DMTA rather than by DSC (-6.0°C) is because of the difference in the principles of these analytical techniques.

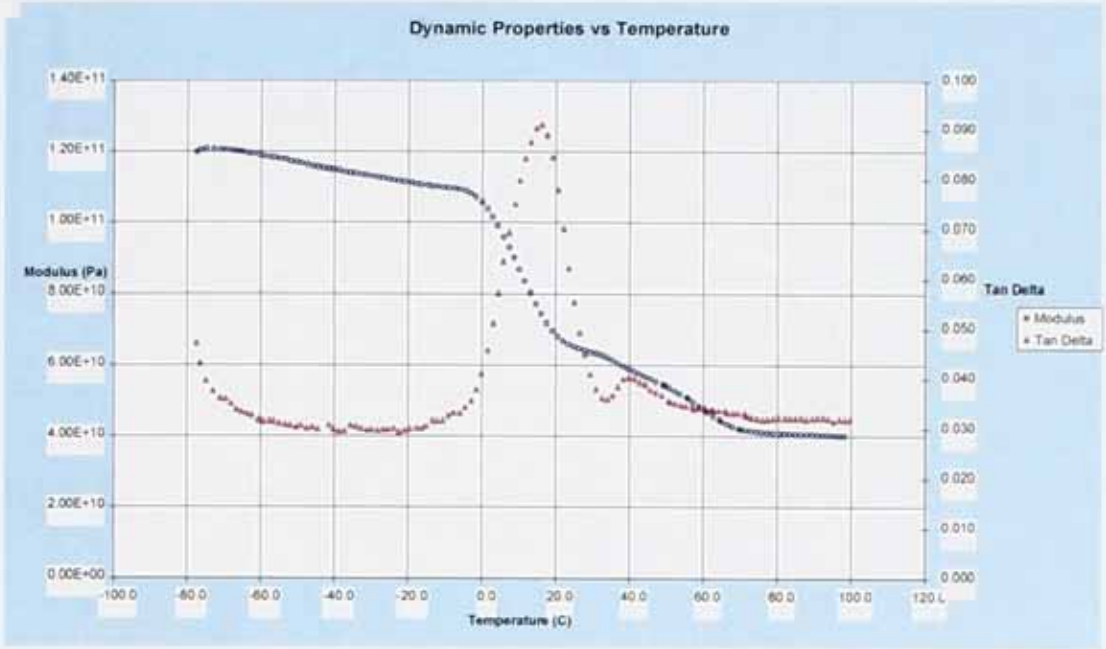

Figure 3.18 DMTA curves of polyurethane resin PU-6

Tensile Test Results

Load-extension curves for PU-6 from tensile test are shown in Appendix C3.7, two replicate samples were tested. The stress-strain curve derived is shown in Figure 3.19. The data was taken as an average. The Figure shows that up to a strain of 6%, the variation of stress with strain is linear and if the gradient of this part of straight line is taken as the modulus, then the Young's modulus is about 45.1MPa. The average elongation at break was 16.5%, stress at break (tensile strength) was 5MPa, and the calculated standard deviations were ≤ 1.10.

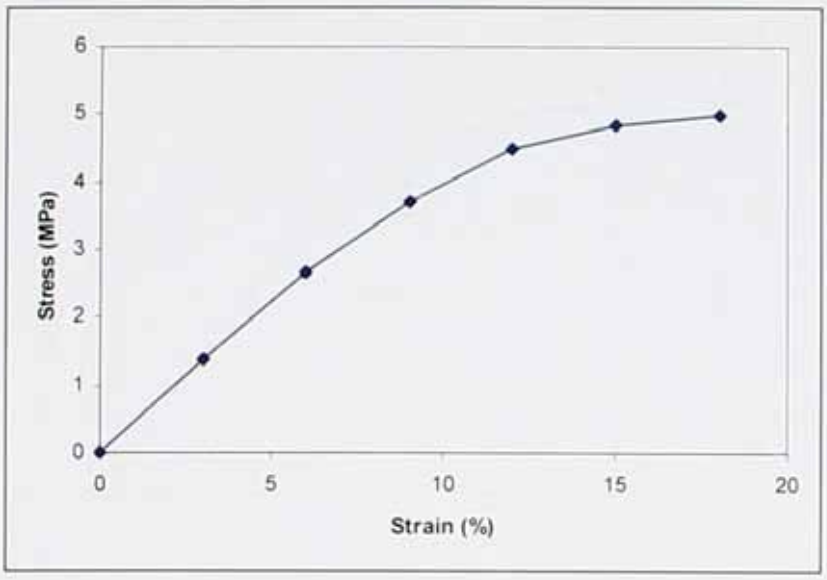

Figure 3.19 A typical tensile test result for polyurethane resin PU-6

Load-extension curves for polyurethane after cross-linking, sample PU-7 are shown in Appendix C3.8. Two replicate samples were tested. The stress-strain curve derived is shown in Figure 3.20, the data being an average taken. If the slope of the initial trend line represents the modulus then this is about 138MPa. As far as breaking is concerned the average elongation at break was about 32.8% and the tensile strength was 18 MPa (the calculated standard deviations were ≤ 0.165).

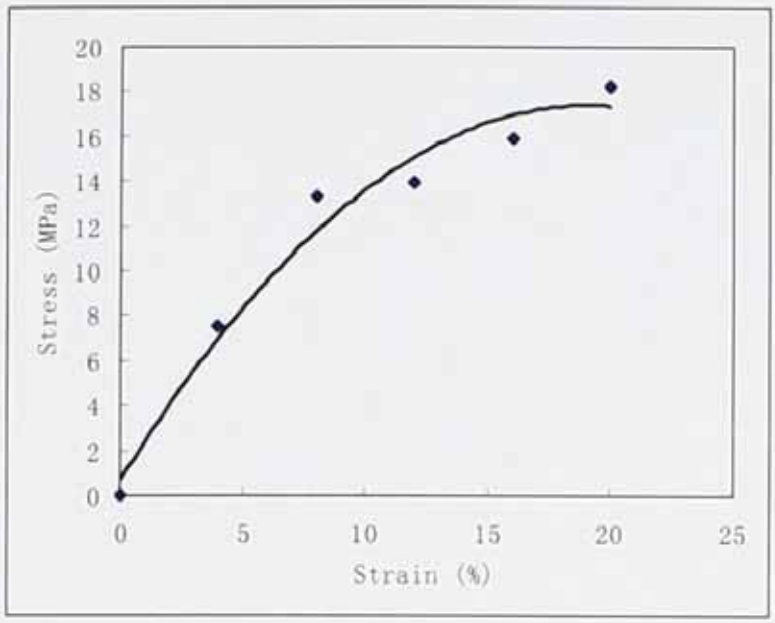

Figure 3.20 Tensile test results for cross-lined polyurethane sample PU-7

3.3.4 Characterization of Prepared Semi-crystalline Polyurethane with Functional Pendant Acrylate Groups

Characterization of Monomer DHBA and Intermediate Products

The monomer DHBA used to prepare polyurethane acrylate binder resins was characterized by FTIR and chromatography. During the preparation of monomer DHBA, the intermediates, e.g. EHDD and AEDD had been synthesized and purified. Figure 3.21 (for the original picture of TLC plate, see Appendix C3.9) shows the purified samples, EHDD, AEDD and DHBA, on a developed TLC plate ($R_{fDHBA}=L_3/L_0=12.3mm/79.3mm=0.16$, $R_{fAEDD}=L_2/L_0=33.0mm/79.3mm=0.42$ and $R_{fEHDD}= 27.5mm/79.3mm= 0.35$).

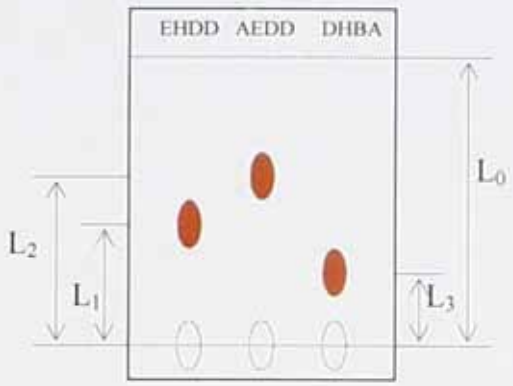

Figure 3.21 Developed TLC plate for monomer DHBA and intermediate products

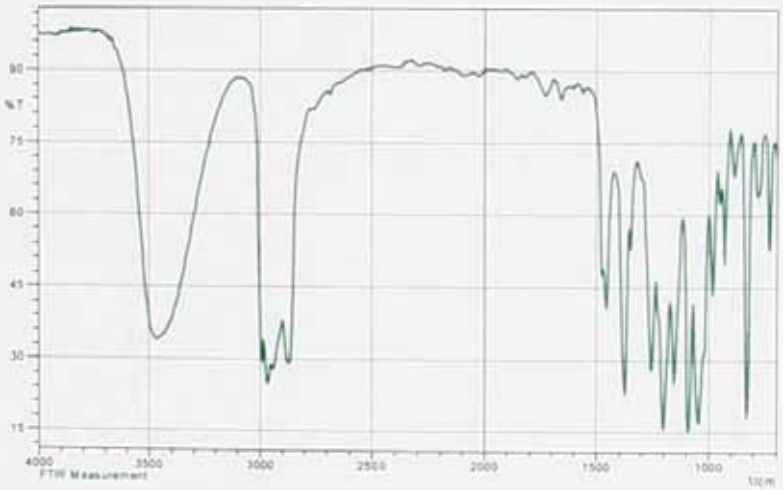

Figure 3.22 FTIR spectrum of EHDD

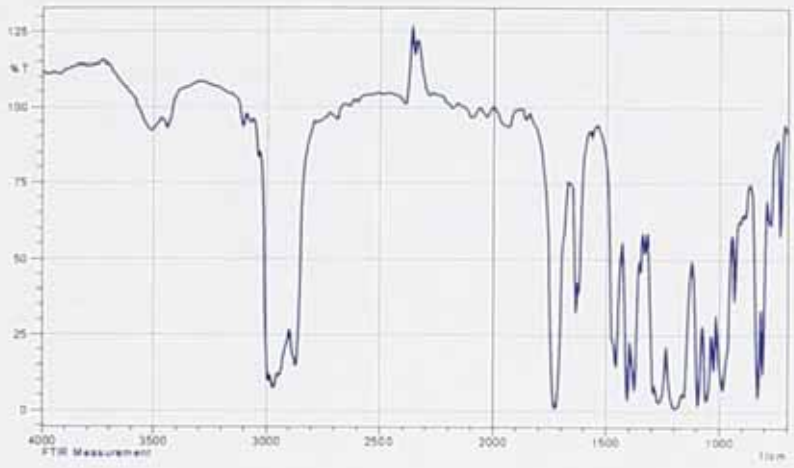

Figure 3.23 FTIR spectrum of AEDD

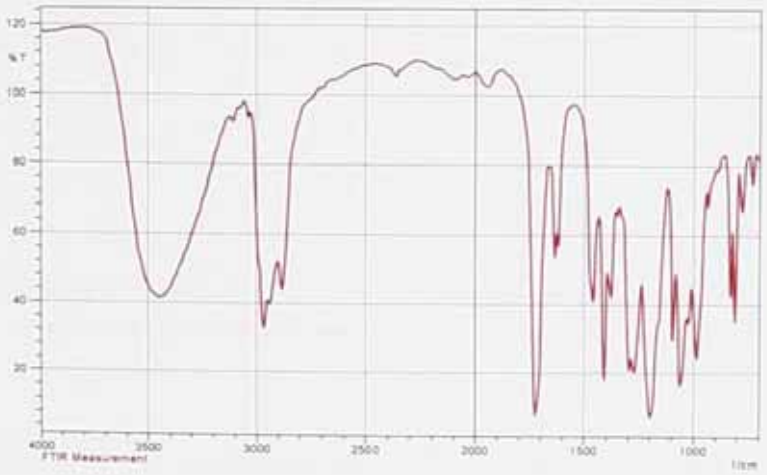

Figure 3.24 FTIR spectrum of DHBA

Table 3.9 Assignment of IR absorption bands (wave numbers) to bond vibrations of EHDD, AEDD and DHBA molecules

	Absorption band (cm^{-1})							
EHDD	3480	2980 2940 2930 2880	----	----	1450 1400 1380	----	1098 830	1060
AEDD	----	2980 2940 2930 2880	1730	1640	1450 1400 1380	1150-1200 (w&s)	1098 830	1060
DHBA	3460	2940 2930 2880	1730	1640	1450 1400 1380	1150-1200 (w&s)	----	1060
Response group	ν_{O-H}	ν_s ; ν_{as} -CH3 -CH2-	$\nu_{C=O}$	$\nu_{C=C}$	δ_{C-H}	ν_{as} C-O-C (in ester molecules)	ν_{C-O} (in the ring)	ν_{as} C-O-C

Note: ν—stretching vibration; δ—bending vibration;
ν_s – symmetrical stretching vibration; ν_{as} – asymmetrical stretching vibration;
w&s—wide and strong peak.

The analysis of intermediates EHDD and AEDD, and monomer product DHBA using FTIR was carried out and the spectra are shown in Figures 3.22, 3.23 and 3.24. The assignments of IR absorption band to structural features of EHDD, AEDD and DHBA are listed in Table 3.9. The stretching vibration of O-H groups about 3460-

3480cm^{-1} confirms the presence of hydroxyl groups in the DHBA and EHDD molecules. There is no hydroxyl group absorption in the FTIR spectrum for AEDD; The stretching vibration of C-O groups in the ring skeleton at the location 830 cm^{-1} and 1098 cm^{-1} shows the C-O groups in EHDD and AEDD molecules, there are no 830 cm^{-1} and 1098 cm^{-1} absorptions in the FTIR spectrum for DHBA; the carbonyl (C=O) absorption is present at 1730cm^{-1} and absorption of C=C groups is present at 1640cm^{-1} in DHBA and AEDD. The FTIR analysis results confirm the structures of the prepared DHBA and the intermediate products EHDD and AEDD.

Studies on improving the yield of EHDD

During the synthetic procedure, some problems were found:

Problem 1. Reactant ketones were azeotropic with toluene

The water produced needed to be removed with toluene from the reacting system by a Dean-Stark trap. It was found that reactant ketones, such as acetone and ethyl acetoacetate (EAA), were azeotropic with toluene during the reaction.

At 760 mmHg, the boiling temperature of acetone is 56.2°C, water is 100.0°C and toluene is 110.6°C [119]. The azeotropic temperatures of the mixture of acetone and toluene are between 60 and 86°C. Most of unreacted acetone is distilled out of the reacting system before the water produced is removed sufficiently from the reacting system during reaction.

The reactant acetone was replaced by EAA which has a higher boiling temperature (181°C, at 760 mmHg), But EAA is still azeotropic with toluene, and the azeotropic temperature is 100-108°C when the ratio of EAA/toluene (V/V) is 3:1. The unreacted EAA is still distilled out from the reacting system during the removal of water from the system. Therefore acetone was used as reactant for the benefit of a low boiling temperature, and easy removal during the purification stage (required after the reaction to avoid or reduce side reactions).

Problem 2. Reactant TMP is insoluble in toluene at room temperature

The solubility of TMP in toluene at 19°C is about 0.053g/ml. If TMP was dissolved in acetone in the presence of *p*- toluene sulphonic acid at first, and then this was followed by adding toluene, there were still two phases in the flask at room temperature; one phase could be obtained at elevated temperature, but as the concentration of acetone decreased, a TMP layer was deposited on the bottom of the flask. The temperature needed to be controlled below 130°C; otherwise the solution color turned from light to dark brown and some side reactions occurred.

On the other hand, that insolubility of TMP in toluene could be used to purify EHDD by recrystallization of TMP from EHDD toluene solution. It was found that a small quantity of remnant acetone, about 0.6% acetone in the solution, will affect the crystalline process, making it difficult for the TMP to form crystals from solution.

In 1991 Denis [76] reported that a yield of EHDD of about 80% was obtained, but there was no detailed information. Imre [120] reported that the yield of dioxolanes fundamentally depended on the structure of the reactants and yield decreased with increasing molecular weight of the reactants. The molecular weight of TMP is somewhat greater than that of 1, 2-propanediol, which was noted in the above references. Also it was noted that when there is one more hydroxymethyl group in the TMP molecule, it will affect the yield of EHDD. Shubham [121] reported an improved preparation method for the reaction of 1,2-propanediol with acetone by adding a molecular sieve; he obtained a net yield of 35%.

In this work the yield of EHDD was about 15.4% at first. In the case of the presence of anhydrous calcium sulphate and extracting EHDD by toluene from the deposited TMP phase, and recrystallising TMP from toluene solution, a yield of EHDD of 20.0% was obtained at a reaction temperature of 62-64°C. When the raw material ratio used was acetone: TMP = 10:1 (in mole), the yield of EHDD increased to 39.7%. After several trials, an improved synthetic procedure for EHDD was found,

as described previously in details in section 3.2.3.2, and the yield is 69% by the improved procedure.

During preparation of EHDD, there are some side reactions, such as the EHDD open ring polymerization and the esterification of TMP with acetone, so it was felt that with the use of a conventional synthesis method to prepare EHDD, it is very difficult to get the net yield of EHDD to such a high level as 80% as described by Denis [76].

The following UV curable powder coating binder resins were made from reactants, which contain monomer DHBA.

UV Curable Powder Coating Binder System I

The effect of DHBA content on the degree of crystallinity and the melting points, before and after UV-curing, is shown in Figure 3.25 and Figure 3.26 respectively (original DSC analysis curves are shown in Appendix C3.10 and C3.11 respectively). The crystallinities and melting points of the prepared resins all increased with the content of DHBA for polymer which had not been UV-cured. However, after UV curing, the cross-linked polymer became non-crystalline for a particular range of DHBA content, and the T_g of the cross-linked polymers were in the range -5 to -25°C. This indicates that DHBA is less effective than BEP in reducing crystallinities and melting points. The molecular structure difference between DHBA and BEP is that DHBA has an acrylate side chain and BEP has an alkyl side chain, the alkyl side chain is less polar than that of acrylate, the alkyl side chain is more effective in causing irregularity along the polyurethane chain. In cross-linking, the random movement of the polyurethane chain is restricted, so UV-curing results in decreasing crystallinity of polyurethane, at the same time as the content of BEP increases, the irregularity along the polyurethane chain increases, there is a window where there is no crystallinity, as may be seen in Figure 3.25 and Figure 3.26.

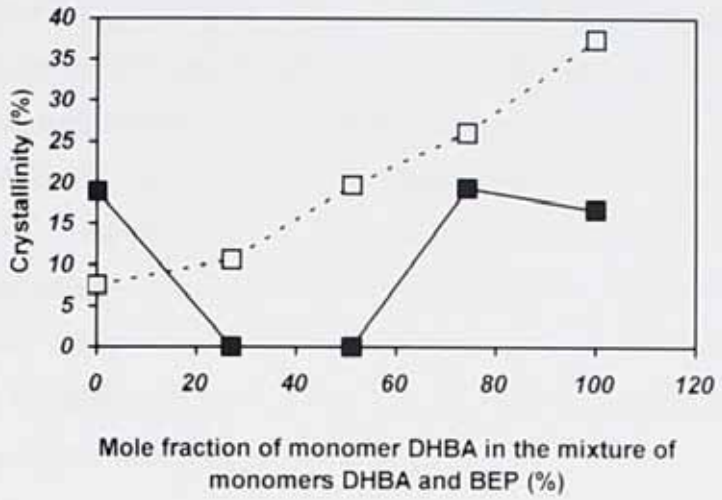

Figure 3.25 Effect of the content of monomer DHBA on the crystallinity of PU acrylate resins (system I), before (□) and after (■) UV-curing. The total mole fraction of monomers DHBA and BEP in the diols is kept constant at 40%.

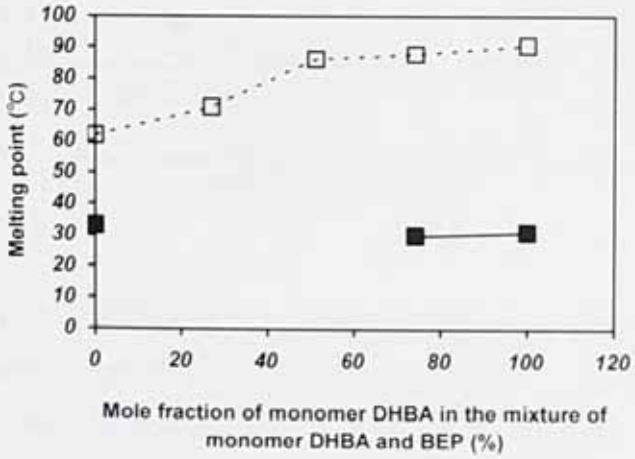

Figure 3.26 Effect of the content of monomer DHBA on the melting point of PU acrylate resins (system I), before (□) and after (■) UV-curing. The total mole fraction of monomers DHBA and BEP in the diols is kept constant at 40%.

UV Curable Powder Coating Binder System II

The effect of the content of monomer DHBA on the crystallinities and melting points is shown in Figure 3.27 and Figure 3.28 and the original DSC curves are shown in Appendix C3.12 and C3.13 respectively. It is clear from Figures 3.27 and 3.28 that the crystallinities and melting points increase and then level off as the content of monomer DHBA in the mixture of monomer DHAB and BEP increases for polymer not subjected to UV curing. After UV curing, the degrees of crystallinity and the melting points decrease as the content of monomer DHBA increases; and when the content of DHBA is above about 50% (or the mole fraction of DHBA in the total amount of diols is higher than about 20%), the polymer is non-crystalline. The T_g of the crosslinked polymer was in the range 18 to -20°C.

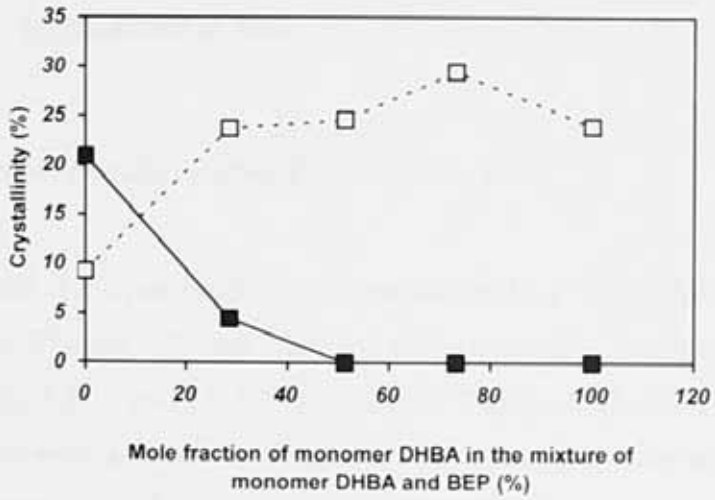

Figure 3.27 Effect of the content of monomer DHBA on the crystallinity of PU acrylate resin (system II), before (□) and after (■) UV-curing. The total mole fraction of monomers DHAB and BEP in the diols was kept constant at 40%.

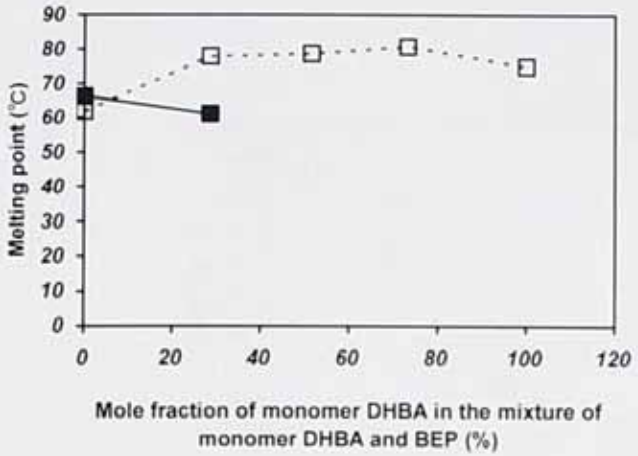

Figure 3.28 Effect of the content of monomer DHBA on the melting point of PU acrylate resin (System II), before (□) and after (■) UV-curing. The total mole fraction of monomers DHBA and BEP in the diols was kept constant at 40%.

UV Curable Powder Coating Binder System III

The effect of the monomer DHBA content on the crystallinity and melting points are shown in Figures 3.29 and 3.30, and the original DSC analysis curves are shown in Appendix C3.14 and C3.15 respectively. The crystallinity (Figure 3.29) decreases with increasing content of DHBA both for uncured polymer and after UV curing, but it decreases more sharply after UV-curing when the monomer DHBA content varies from 0% to about 40%. For the uncured polymer the melting point, however, increases with increasing content of DHBA. In the case of UV-cured polymer, the melting point shows a slight increase with increased content of DHBA, until monomer DHBA content reaches about 40%. The melting point then decreases abruptly until eventually the polymer becomes non-crystalline when the monomer DHBA content reaches about 80% (see Figure 3.30).

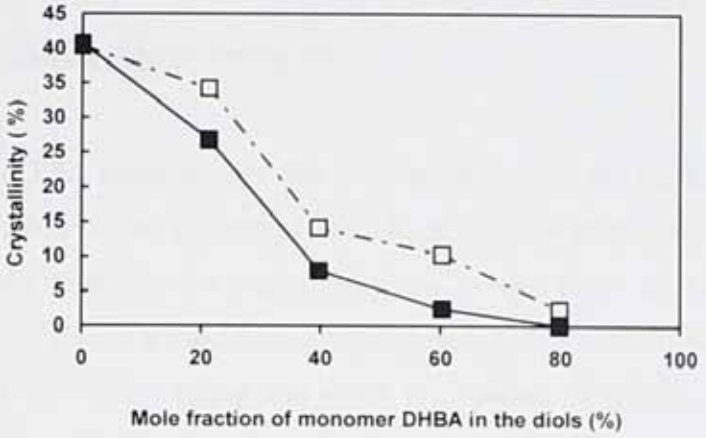

Figure 3.29 Effect of the content of monomer DHBA on the degree of crystallinity of PU acrylate resins (System III), before (□) and after (■) UV-curing.

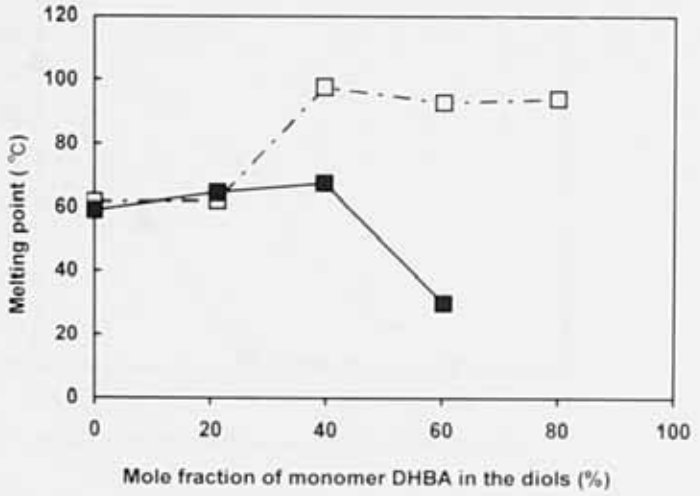

Figure 3.30 Effect of the content of DHBA on the melting points of PU acrylate resins (System III), before (□) and after (■) UV-curing.

From Figures 3.31 and 3.32, it can be seen that both crystallinities and melting points decrease with the increase of the content of DHBA, both for uncured polymer and after UV-curing. After UV curing, the crystallinity and melting point are lower than that of before UV curing (the original DSC curves are shown in Appendix C3.16 and C3.17 respectively). It is worthy noting that when the content of DHBA is higher than about 40%, the polymer becomes non-crystalline after UV-curing.

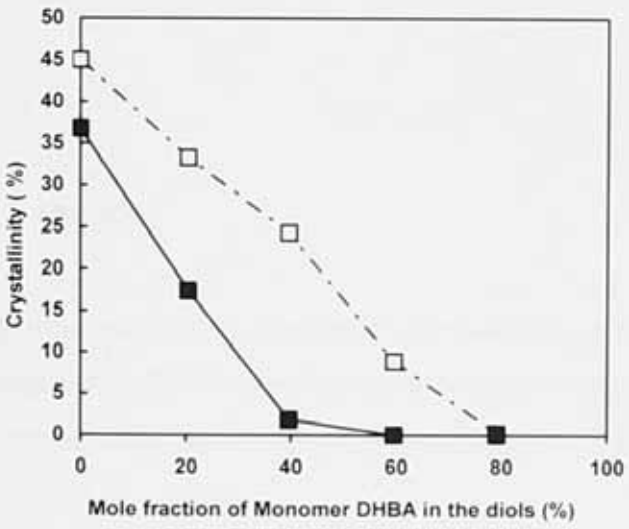

Figure 3.31 The effect of the content of DHBA on the degree of crystallinity of PU acrylate resins (System IV), before (□) and after (■) UV-curing.

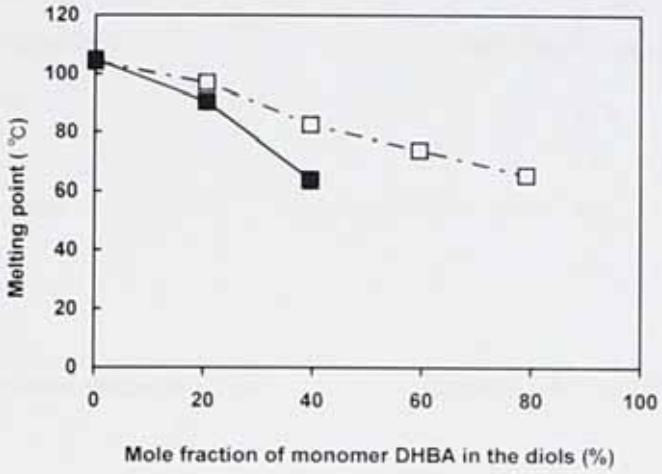

Figure 3.32 The effect of the content of monomer DHBA on the melting points of PU acrylate resins (System IV), before (□) and after (■) UV-curing.

Structure-property Correlation

The two dihydroxyl monomers, 2, 2-dihydroxymethylbutyl acrylate (DHBA) and 2-butyl-2-ethyl-1,3-propandiol (BEP), are playing an important role on the properties of prepared binder resins. Their structures are shown in Figure 3.33 and Figure 3.34 respectively.

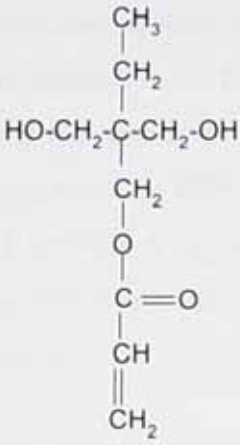

Figure 3.33 Structural formula of DHBA

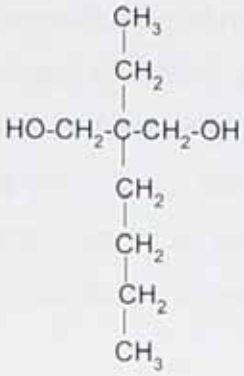

Figure 3.34 Structural formula of BEP

A series of UV curable powder coating binder resins based on polyurethanes with pendant groups have been synthesized. Figures 3.25, 3.27, 3.29 and 3.31 show that for polyurethane prepared with UV curable dihydroxyl acrylate monomer DHBA, crystallinities decreased after cross-linking by UV. The cross-linkage of pendant acrylate groups in the polyurethanes caused the irregular rank of polyurethane chain rather than orientating rank of polyurethane chain.

There was no BEP added when system III and system IV binder resins were synthesized. Crystallinities of prepared resins are obviously decreased when the content of DHBA is increased (Figure 3.29 and 3.31), this is mainly caused by the replacement of diethylene glycol (DEG) with DHBA. HDI reacts with DEG to give semi-crystalline polyurethane with higher crystallinity (about 40-45%). The higher the content of DHBA introduced the more disorder of the prepared polyurethane molecular structure. This results in decreasing crystallinity of the prepared polyurethane binder resin.

During the preparation of system I and II binder resins, in addition to the dihydroxyl monomer DHBA (with pendant acrylate group), the dihydroxyl monomer BEP (with pendant alkyl groups) was also introduced to polyurethane molecular architectures. The variation of molar ratio of DHBA to BEP resulted in a variation of crystallinites

of prepared polyurethane resins, when total content of DHBA and BEP in the total diols was kept at 40%. For system I and II resins, crystallinities of resins increased with increasing mole fraction of DHBA in the mixture of DHBA and BEP, that means if the content of BEP decreased it would result in decreasing crystallinity of preparing resin. So BEP is more effective in reducing crystallinity. The mole fraction of BEP or DHBA in the mixture of the two monomers can be an important factor guiding the preparation of binders with suitable crystallinity for powder coating application.

Figures 3.26, 3.28 and 3.30 show that the increased content of DHBA resulted in increased melting points of prepared resins (System I, II and III). However, Figure 3.32 shows that the increased content of DHBA resulted in decreased melting points of prepared resins (System IV).

The melting point is a key factor for optimizing semi-crystalline resin for powder coatings. The melting point of binder resin should be high for the prepared powder coating to show good storage property. If the effect of functional monomer content on melting points of prepared binder resins is small, this will be beneficial for preparing semi-crystalline resin with relatively higher melting point. Balancing the ratio of the functional dihydroxyl monomers DHBA and BEP, gives a way to adjust crystalline and amorphous phases in prepared resins for use as powder coating binders.

The above research data shows that semi-crystalline polyurethane resin prepared from HDI/DEG/DHBA/BEP is more suitable for use as a powder coating binder, and the optimal reactant molar ratios are: diisocyanates to diols is 2:3 or 1.1:1; DHBA to (DHBA+BEP) ranges are from 0.35 to 0.65 and (DHBA+BEP) to total diols ranges are from 0.35 to 0.65.

Chapter IV Application of Novel Powder Coating Binders for Leather Finishing

4.1 Introduction

The synthesis of UV curable polyurethane acrylate (PUA) binder resins has been discussed in the previous chapter. This Chapter is concerned with the study of representative new UV curable PUA powder coating resins and the application for the finishing of leather. For example, PUA resin PUA-1, is a UV curable powder coating resin with higher crystallinity, and was used to study the influence of different photo-initiator content and the effect on powder coating properties; PUA resin PUA-2, is a UV curable powder coating resin with relatively low viscosity; and PUA resin PUA-3 is a UV curable powder coating resin with better general properties and was adopted to optimize developed powder coating formulations.

The results for evaluation of some commercially available UV curable powder coatings for the finishing of leather will also be discussed.

A hot plating process was studied to examine hot-plating as a method to assist powder coating flow-out and decrease powder coatings stoving temperature required for flow-out in leather finishing.

The Sol-gel process which is used for the preparation of silica gels [98] is a wet chemical method, involving the hydrolysis and condensation of metal alkoxides and inorganic salts. The hardness and abrasive properties of silica gels and powders are of interest in their use as reinforcing agents in materials [99]. Nowadays, high performance coating systems are always a compromise between elasticity on one hand and good abrasion resistance on the other hand. Organic-inorganic hybrid materials offer the opportunity to combine the desirable properties of organic polymers (toughness, elasticity) with those of inorganic solids (hardness, chemical resistance) [100]. Fumed silica is produced by burning silicon tetrachloride in an oxygen-hydrogen flame [98].

The Company INEOS Silica [99] has designed different types of silica to apply in coatings. Their products GASIL UV55C and UV70C are formulated in coatings as matting/flattening agents and GASIL GM2 is used in coatings as an anti-caking, free-flow agent whereas UV70C can improve coating surface abrasion resistance properties.

Nanopowder and nanoparticle dispersions have been increasingly used in coatings applications. Nanoscale particles greatly increase the abrasion resistance of traditional coatings [100]. Tronche [98] reported their work on using acrylated nano-sized silica particles to improve the surface abrasion resistance of a UV-curable coating, without a detrimental effect on adhesion or transparency. Frank [99] studied methacryl grafting onto silica. In this Chapter an investigation of surface modification of nano-scale silica particles and the use of such particles as fillers to improve powder coating properties will be discussed.

The new powder coatings formulated with or without nano-scale silica particles have been studied as well.

4.2 Experimental

4.2.1 Chemicals

The following chemicals were mainly ordered from the Sigma-Aldrich Co. Ltd (The Old Brickyard, New Road, Gillingham, Dorset, UK).

Acetone (99.5%); Acryloyl chloride (AC) (96%);
Chloroform (CF) (99%); Diethylene glycol (99%);
Dihydroxymethyl butylacrylate; hexamethylene diisocyanate (98%);
Fumed silica: size 7 nanometer, surface area 380m^2/g;
Hydroquinone (99%); Maleic anhydride (95%);
Molecular sieves (4Å); Toluene (98%);
Triethyl amine (99.5); 3-(Trimethoxysilyl)propyl methacrylate (TPMA)(98%);
2-butyl-2-ethyl-1, 3-propanediol (BEP) (99%);

powder coatings (their softening points are between 90-115°C, and melting viscosities are above $1\times10^5 mP_a \cdot S$, the powders were supplied by Hoechest Company, UK); chromium tanned cow leather samples were used for test; silicone paper and liquid wax were selected as hot-plating release agents.

4.2.2 Preparation of UV Curable Powder Coating Binder Samples

4.2.2.1 Synthetic Process for UV Curable Powder Coating PUA Resin PUA-1

The polyurethane was prepared with a molar ratio of diisocyanates to diols of 1.1:1.0 and DHBA to BEP of 5:4; the mole fraction of monomers DHBA and BEP in the total diols was 29.7%. The detailed information on the reactants for powder coating resin sample PUA-1 is given in Table 4.1. The polymerization was carried out in chloroform as a solvent by refluxing at 60-61°C for 10 hours. The solvent was removed at 80°C under reduced pressure after the polymerization was completed.

Table 4.1 Reactants composition for powder coating resin sample PUA-1

Reactant	unit	Quantity
DHBA	g	3.06
	mol	0.01628
BEP	g	2.14
	mol	0.01335
DEG	g	7.35
	mol	0.06926
HDI	g	18.34
	mol	0.1089
Hydroquinone	g	0.0145
Chloroform	ml	300
HDI/DEG/DHBA/BEP (molar ratio)		1.00 : 0.64 : 0.15 : 0.12

* The hydroquinone was used as inhibitor during the removed solvent stage.

4.2.2.2 Preparation of PUA-2

Preparation of UV curable powder coating resin PUA-2 is summarized in Table 4.2 for convenience.

Table 4.2 Preparation of powder coating resin PUA-2

Materials	HDI	DEG	DHBA	BEP
Weight (g)	3.7188	2.1092	2.6365	0.0339
Quantity (mol)	0.02211	0.01988	0.01402	0.0002115
Molar ratio	1.00 :	0.899 :	0.634 :	0.00957
Experimental procedure	Reacted in a bath of oil at 55 °C for about 25minutes, the viscosity of the system increased rapidly, during stirring, there were lots of bubbles on the liquid surface. Stirring speed was decreased from 490 RPM to 200RPM. After 1 hour, the system was stirred with difficulty. After reaction for 7 hours the reaction was stopped by taking the flask out of bath oil and cooling it at room temperature, the resin gradually turned from liquid to solid.			

Measurement of the Viscosity of PUA-2

The viscosity of sample PUA-2 was measured with a Brookfield cone/plate viscometer, attached to a TC-500 temperature control bath system at 90±0.5°C, spindle 52# was used. The sample weight was 0.5967gram. The detailed test theory is described in chapter II, section 2.2.1. Viscosity was measured at different cone rotation speeds and after different times.

4.2.2.3 Synthesis of UV Curable Powder Coating PUA Resin PUA-3

PUA resin components and preparation conditions are listed in Table 4.3.

Table 4.3 PUA resin PUA-3: components and preparation conditions

Sample		PUA resin PUA-3
DHBA	g	16.80
	mol	0.08936
BEP	g	11.98
	mol	0.07474
DEG	g	25.23
	mol	0.2377
HDI	g	73.14
	mol	0.4348
Hydroquinone (g)		0.0062
HDI/DEG/DHBA/BEP(molar ratio)		1.00:0.57:0.21:0.17
Reaction condition		Reacted in 307g chloroform, heating with bath oil at 60°C for 10 hours, and then removed out solvent under reduced pressure at temperature no more than 81°C

4.2.2.4 Preparation of PUA-4

Polyurethane acrylate (PUA) resin PUA-4 was prepared as follows:
To a 3L flask, was added 25.2g diethylene glycol (DEG), 16.8g dihydroxymethyl butylacrylate (DHBA), 2-butyl-2-ethyl-1,3-propanediol (BEP) 11.6g and 240ml chloroform (CF). The flask was fitted with thermometer and condenser, and was cooled with tap water. Then 73.1g hexamethylene diisocyanate (HDI) was added and the chemicals mixed by magnetic stirrer bar at 400-650RPM. The system reacted for 10 hours in an oil bath at 60°C, and then 0.0041g hydroquinone was added to the product solution and mixed well. Afterwards the system was cooled to room temperature, and the flask fitted with distillation devices, and the oil bath temperature controlled to 80 to 90°C, CF was then removed from the prepared PUA product, and the product was marked as PUA resin PUA-4.

4.2.2.5 Surface Modification of Nano-scale Silica Particles

4.2.2.5.1 Modification of the Surfaces of Fumed Silica Particles with Acryloyl Chloride (Method I)

Preparation of Surface Modified Silica Particles

2.67g of fumed silica (Sigma-Aldrich Co. Ltd), having a size of 7 nanometer and a surface area 380m^2/g, was added to a 3-necked 250 ml flask as well as 100 ml of molecular sieves dried toluene as well as 0.27 g acryloyl chloride (AC). The flask was fitted with condenser and dropping-funnel, and the system was cooled in an ice/water bath and the reaction system was stirred vigorously. After 2 hours, 0.47 g triethylamine (TEA) was added drop-wise over 10 minutes, and then the reaction was allowed to proceed at room temperature (between 23-29°C) for 20 hours. After filtering and washing the product with toluene, the dried surface modified silica produced was marked as **Sil-1.**

Characterization of the surfaces of Silica Raw Material and Surface Modified Silica by Attenuated Total Reflection-Fourier Transform Infrared Spectroscopy (ATR-FTIR)

Nano-scale fumed silica raw material was characterized with FTIR and the prepared surface modified nano-scale silica particles with AC were characterized by using surface sensitive in-situ-ATR-FTIR spectroscopy and the results are shown in Figure 4.1 and Figure 4.2 respectively. Figure 4.1 shows the H-O absorption at 3420cm^{-1} that means there are hydroxyl groups on the silica surface that can be used for coupling reactions in modifying surface properties of the silica and improving application range of the silica. The stretching vibration ν_s and ν_{as} of Si-O-Si are seen at 1650 cm^{-1} and 1110 cm^{-1} in Figure 4.1. In Figure 4.2 it can be seen that the carbonyl (C=O) absorption at 1685 cm^{-1}, the asymmetrical stretching vibration $\nu_{as\,(COO^-)}$ at 1550cm^{-1} and the stretching vibration $\nu_{(=CH2)}$ at 2975cm^{-1} : these show that acrylate is present on the silica surface. After the surface modification of silica, the absorption of H-O groups at 3420cm^{-1} was obviously eliminated, there is absorption at 3300-3400cm^{-1} , this caused by the residual triethylamine salt. The FTIR results suggest that the AC was successfully bonded onto the silica surface.

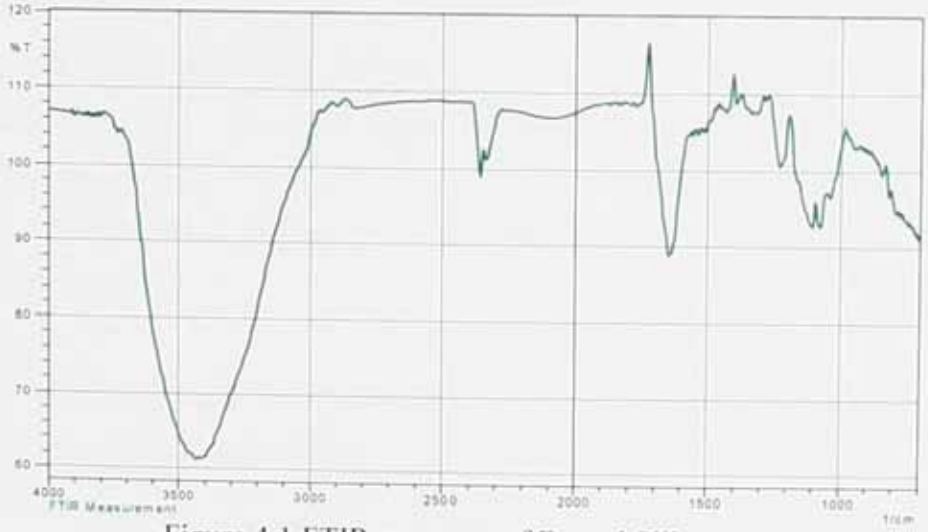

Figure 4.1 FTIR spectrum of Fumed Silica raw material

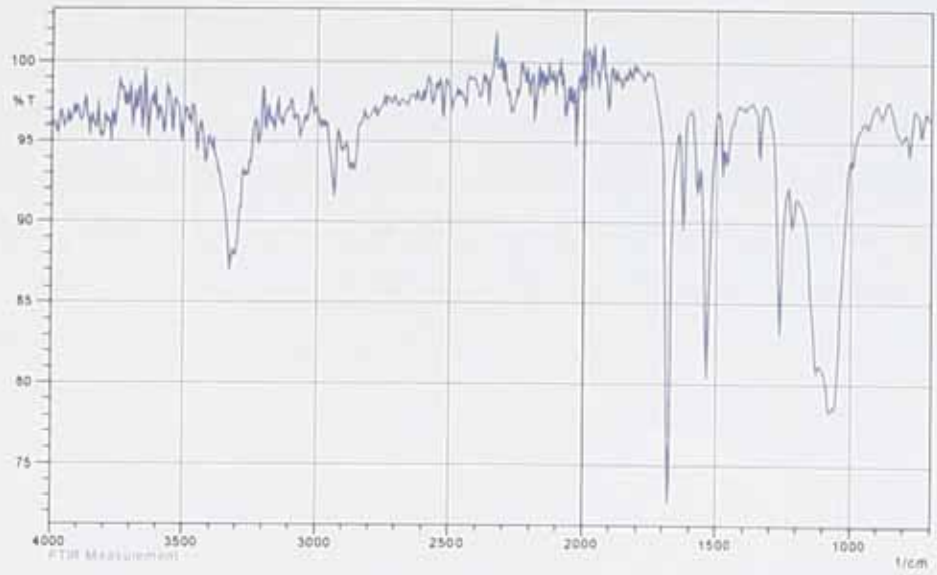

Figure 4.2 ATR-FTIR spectrum of sample Sil-1

4.2.2.5.2 Surface Modification of Nano-scale Silica Particles ---- Method II

Surface Modification of Nano-scale Silica Particles with 3-(Trimethoxysilyl)propyl methacrylate (TPMA)

Preparation of Surface Modified Silica Particles

The grafting of 3-(Trimethoxysilyl)propyl methacrylate (TPMA) onto silica was carried out according to the method by Frank[99]. First, 5.91g TPMA and then 0.18g maleic anhydride, diluted in 1.2 ml water (formed maleic acid), were added to 11.8g nano-sized silica, intensively stirred in 500ml of boiling acetone. This maleic acid is used as a catalyst. The mixture was refluxed for 2 hours under air then left overnight. The methacrylatel-grafted silica was dried under vacuum and this product was marked as **Sil-2**

Characterization of Surface Modified Silica Sil-2 Structure by Fourier Transform Infrared Spectroscopy (FTIR)

The FTIR spectrum for Sil-2 is shown in Figure 4.3. Compared with uncoated silica (Figure 4.1), the hydroxyl group absorption at 3420 cm^{-1}, was diminished after surface modification, and the presence of a 1670 cm^{-1} peak in Figure 4.3 indicates the absorption of carbonyl (C=O). The information supports the view that TPMA was grafted onto the surface of the fumed silica. The absorption seen in both Figure 4.1 and 4.3 at 2380 cm^{-1} are due to the absorption of carbon dioxide in the air. The stretching vibration ν_s and ν_{as} of Si-O-Si at 1650 cm^{-1} and 1110 cm^{-1} can be seen in both Figures.

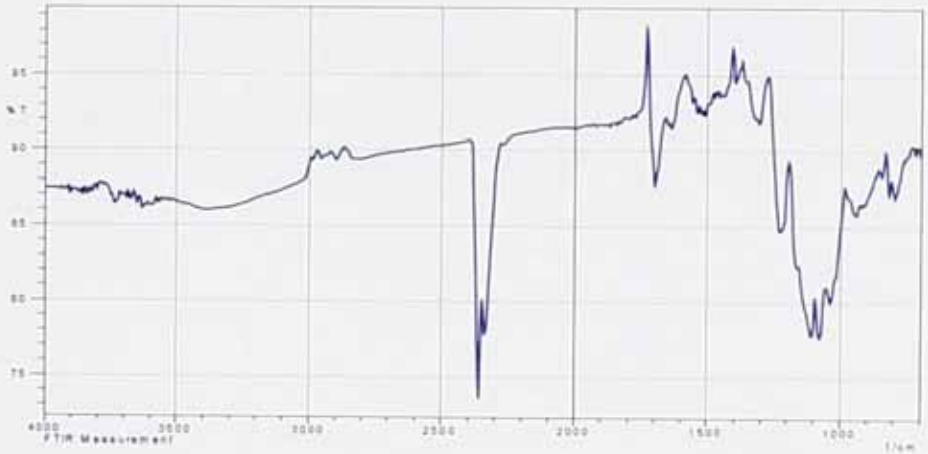

Figure 4.3 FTIR spectrum of sample Sil-2

4.3 Results and Discussion on Investigation of Parameters for Leather Application

4.3.1 Effect of the Synthesis Processes on the Properties of Binder Resins

4.3.1.1 Effect of Solvent on the Properties of Binder Resins

The preparation of powder coating binder resins has been discussed in previous chapters. Both bulk and solvent processes have been used as synthetic methods and

the following results compare the effects of the two processes on final binder resin properties. The reactants selected were HDI and DEG, without adding side chain diol monomers. The detailed information is shown in Table 4.4. Sample 512B was prepared by the bulk method, with no added solvent; sample 512E was prepared by solvent method.

Table 4.4 comparing the effect of different synthetic processes on binder resin properties

Synthesis method		Bulk (without solvent)	Solvent
Exp. No.		512B	512E
DEG	g	1.5984	1.6003
	mol	0.01506	0.01508
HDI	g	2.7849	2.8011
	mol	0.01656	0.01665
Chloroform (g)		----	34.0
HDI/DEG (Molar ratio)		1.1 : 1.0	1.1:1.0
Reaction condition		55 °C, 10h	60 °C, 10h
DSC measuring method		From 0 to 150°C at 5.0°C/min	
DSC	Crystallinity (%)	59.55	47.13
	T_m (°C) Onset	110.4	103.0
	T_m (°C) peak	123.3	112.0

The DSC analysis shows that both crystallinity and melting point of the product produced from the solution method are lower than that produced from the bulk method. The remnant solvent (although very little, measured by weight change) in the product by the solution method is the main cause of the difference, because the solvent acted as a plasticiser in the product, and which resulted in the semi-crystalline product melting at lower temperature range. The original DSC curves are shown in Appendix C4.1 and C4.2. DSC data was collected from 0 to 150°C at a heating rate of 5°C/min.

4.3.1.2 Effect of Temperature Scan Rate on DSC Results

Information about samples used for this DSC analysis is listed in Table 4.5. For samples from 512A to 512D, their reactant composition and preparation process were the same as that of 512B (see Table 4.4); there are differences in the DSC scan rate as shown in Table 4.5. The DSC curves are shown in Figure 4.4.

Table 4.5 Temperature scan rate effect on DSC results

Exp. No.		512A	512B	512C	512D
Sample mass (mg)		13.1	10.7	12.2	7.3
DSC measuring rate (°C/min)		2.5	5.0	10	20
DSC	Crys. (%)	58.66	59.55	59.37	58.80
	T_m (°C) Onset	114.5	110.4	110.8	116.8
	T_m (°C) peak	122.5	123.3	121.8	122.9

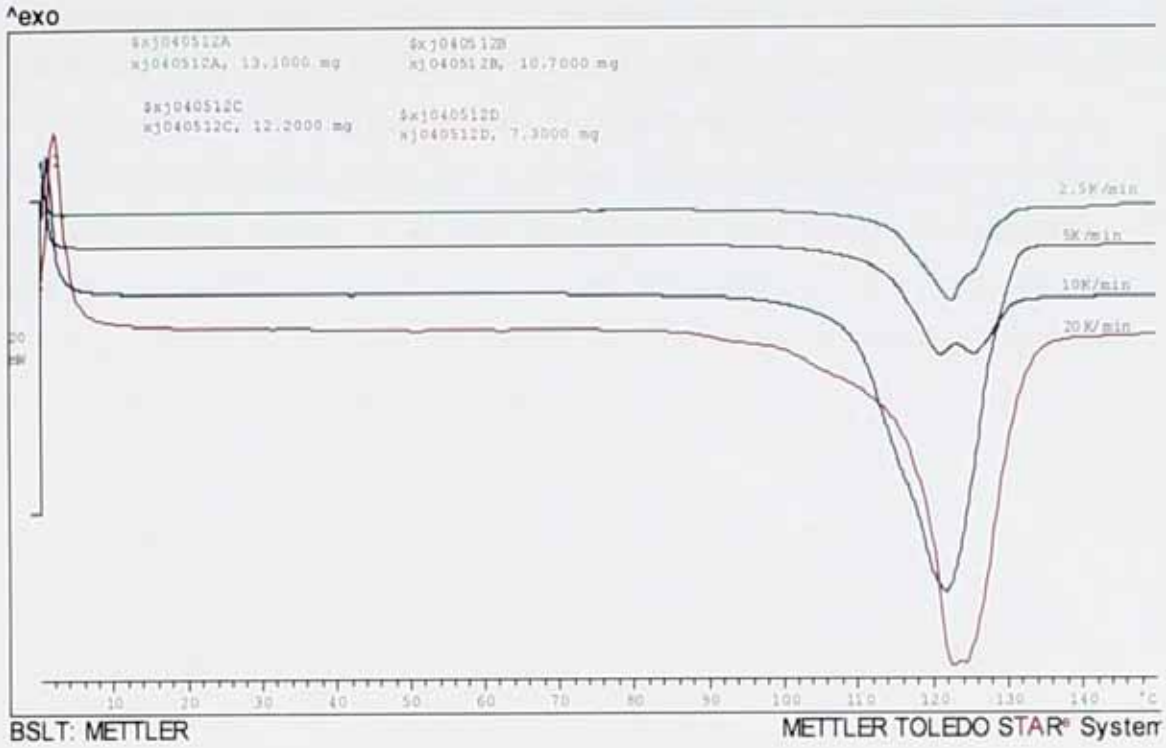

Figure 4.4 DSC curves at different temperature scan rates

Samples analyzed at different temperature scan rates, showed no obvious differences in crystallinity or peak melting points; For onset melting points, temperature scan rates of 5 and 10°C/min gave the same result; but at 2.5 and 20°C/min, are 4 to 6°C higher. But regarding the DSC peak shape, when analyzing at the rate of 10°C/min, the peak shape is more uniform than that analyzed at the rate of 2.5, 5 and 20°C/min.

4.3.2 Hot Plating Process Application to the Finishing of Leather

Hot plating is often used as a method to smooth the surface of finish for metal products [122-124], wood based composite materials [125] and coatings on composite materials [126]. In a conventional leather finishing process, hot plating is often applied to the surface of finished leather to even out the finish [127]. Because poor flow, especially at low temperature, is a common problem for powder coating and leads to finish defects, it was thought useful to investigate the value of a hot plating process

to powder coating sprayed leather. If hot plating is applicable to powder coating, it will help to achieve the goal of low temperature powder coating, because the coating will not solely rely on high temperature to achieve adequate flow. This part of the research work was done during the first stage of the project using a commercially available powder coating to evaluate the feasibility even though the subsequent powder coating film was brittle since the powder coating was not formulated for finishing a flexible material such as leather. Nevertheless it is felt that the findings of this investigation are of value to the main study.

4.3.2.1 Effect of Hot Plating on Powder Coating Finished Leather

Powder coating finished leather samples, with or without undergoing hot plating, were studied.

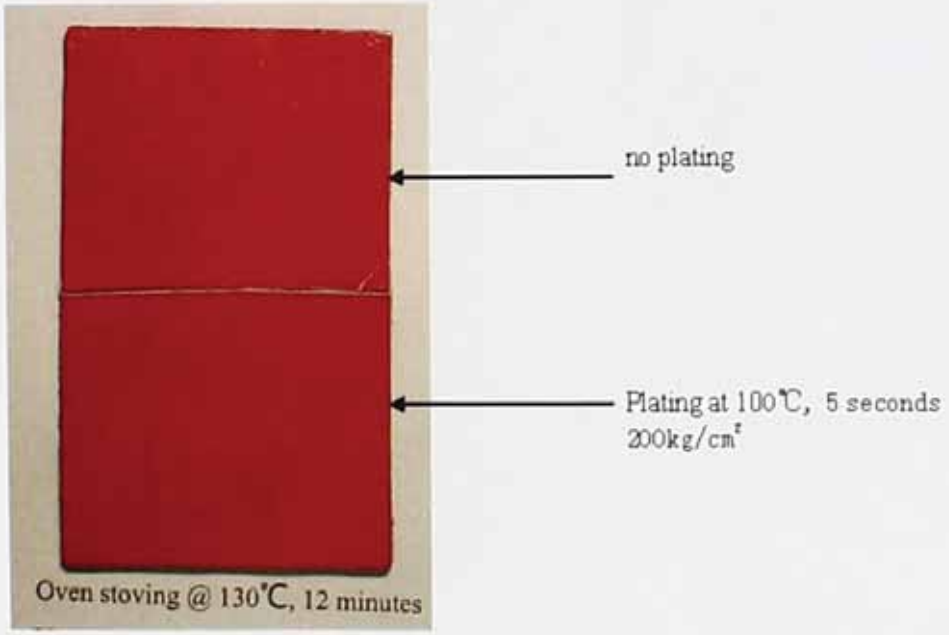

Figure 4.5 Effect of plating on the powder coating finished leather sample

The powder coating was sprayed onto a piece of bovine crust leather by an electrostatic spray method, and then the sample was stoved in an oven at 130°C for 12 minutes, after which the finished sample was cut into two pieces, one half sample was left without plating, and is shown in Figure 4.5 (upper part). The other half sample was plated under a pressure of 200 kg/cm^2 at 100°C for 5 seconds, and the resulting appearance is shown in the lower part of Figure 4.5. Comparing the two half pieces, the sample treated by a plating process , showed an obvious improvement in appearance and uniformity, but the thickness of the plated leather was decreased to 1.44mm from 1.80mm before hot-plating.

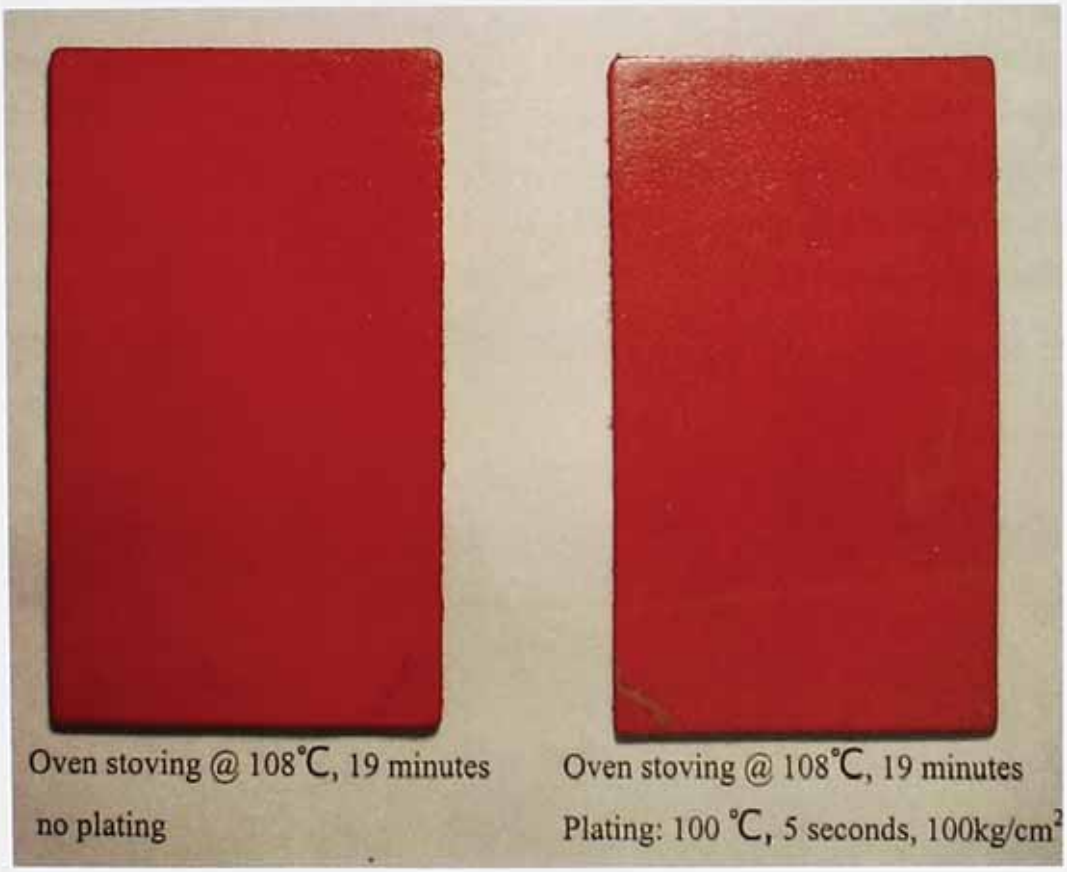

Figure 4.6 Effect of plating on the powder coating finished leather sample

In Figure 4.6, the powder coating was sprayed on two pieces of bovine crust leather by an electrostatic spray method, and then the samples were stoved in an oven at

108°C for 19 minutes, after which one sample was left without plating, shown on the left side of Figure 4.6, and the other sample was plated with 100K_g/cm^2 pressure at 100°C for 5 seconds, giving the sample shown on the right side of Figure 4.6. Comparing the two samples, the gloss and smoothness of the plated sample is slightly higher than that without plating due to the applied pressure plating process.

4.3.2.2 Time Effects of Hot Plating on Powder Coating Finished Leather

During these tests, the samples were stoved at a temperature of 90-96°C for 15 minutes. The plating temperature was 100°C, silicone paper was used as the release agent for the hot-plate, and the applied pressure was 100 K_g/cm^2. The results are shown in Figure 4.7. As the plating time increased from 5 seconds to 20 seconds, the thickness of powder coating finished leather sample decreased from 1.66mm to1.55mm to 1.38mm, i.e. the hot plated leather became thinner as the plating time increased. However, as the plating time increased, the appearance of the coating film was not visibly improved. So hot-plating time is not a key factor, which affects quality of powder coating for the finishing of leather.

Figure 4.7 Hot plating time effect on powder coating finished leather

4.3.2.3 Temperature Effects of Hot Plating on Powder Coating Finished Leather

The sample had not been stoved in oven first. The plating pressure was 200K_g/cm^2, hot plating time was 15 seconds, silicone paper was used as the release agent for the hot-plate. When the hot plating temperature was 86°C, the powder coating films were nearly completely peeled off the crust leather surfaces (Figure 4.8). However, if the plating temperature was 100°C while the other conditions were the same, good powder coating films were obtained (Figure 4.9). This illustrates are the benefit of the hot plating process to lower the powder coating fusion temperature (as low as 100°C).

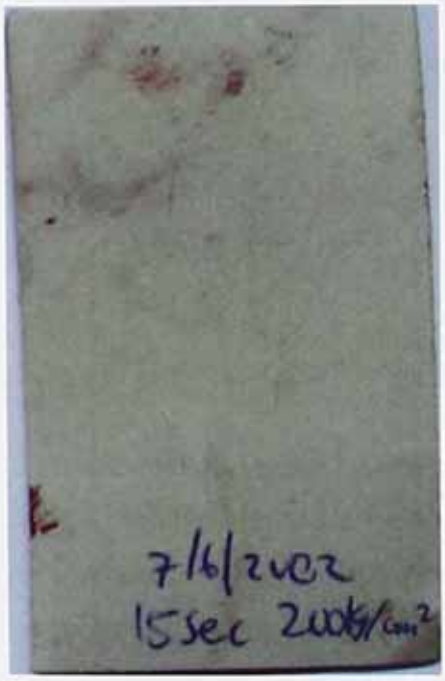

Figure 4.8 Red powder coating finished leather without pre-fusion, hot plating at 86°C

Figure 4.9 Red powder coating finished leather without pre-fusion, hot plating at 100°C

4.3.2.4 Release Agents Effect of Hot Plating on Powder Coating Finished Leather

The effect of several different release agents on the plated powder coating film surface have been studied. The test conditions were a plating pressure of $200K_g/cm^2$, a hot plating time of 5 seconds and a hot plating temperature of 100°C. The results of using Silicone paper as the release agent are shown in Figure 4.10; the result of using liquid wax as release agent is shown in Figure 4.11. The results clearly show that silicone paper is more suitable as a release agent for the hot plating process.

Figure 4.10 Silicone paper as the hot plating release agent

Figure 4.11 Wax as the hot plating release agent

Flow-out of powder coatings requires heat from IR radiation or an oven to assist the process, rather than solvents or diluents as in liquid coatings. For having good storage property, the glass transition temperature (T_g) of powder coating binders, based on amorphous polymers, is normally between 47-55°C, and the flow out temperature should be about 70°C above T_g, that means the lowest flow out and fusion temperature for powder coatings is in the range 120-130°C. Heat sensitive substrates, such as leather can not withstand a temperature above 120°C for a long period, such as 30 minutes [1]. Although the commercially available powder coatings used in this study had a relatively high fusion temperature, their flow out can be assisted by hot plating process at a temperature as low as 100°C. Semi-crystalline

UV curable polyurethane acrylate (PUA) binder resins developed for the finishing of leather in this study, have melt viscosity lower than traditional thermally curable powder coating binder resins based on amorphous polymers. If their flow is further assisted by a hot plating process, there will be no flow-out problem for the new PUA resins at low temperature.

After a hot plating treatment, the appearance of powder coating finished leather is improved, for example the gloss of the powder coating film is enhanced. The powder coating fusion temperature can be as low as 100°C when using the hot plating process.

4.3.3 Filler Effects on the Properties of UV Curable Powder Coatings

4.3.3.1 Effect of Nano-scale Silica Particles on the Crystalline Properties of Cross-linked Powder Coating Films

The UV powder formulations for leather finishing are shown in Table 4.6. The DSC curves of the cross-linked powder coating films are shown in Figure 4.12.

Table 4.6 UV powder coating formulations for leather application

Experiment No.	428B	428A	428C	428D	428E
Component	Parts (by weight)				
PUA resin PUA-4	98.0	98.0	98.0	98.0	98.0
Photo-initiator	2.0	2.0	2.0	2.0	2.0
Sil-2	0	1.0	3.0	6.0	10.0

Note: photo-initiator was Irgacure 184

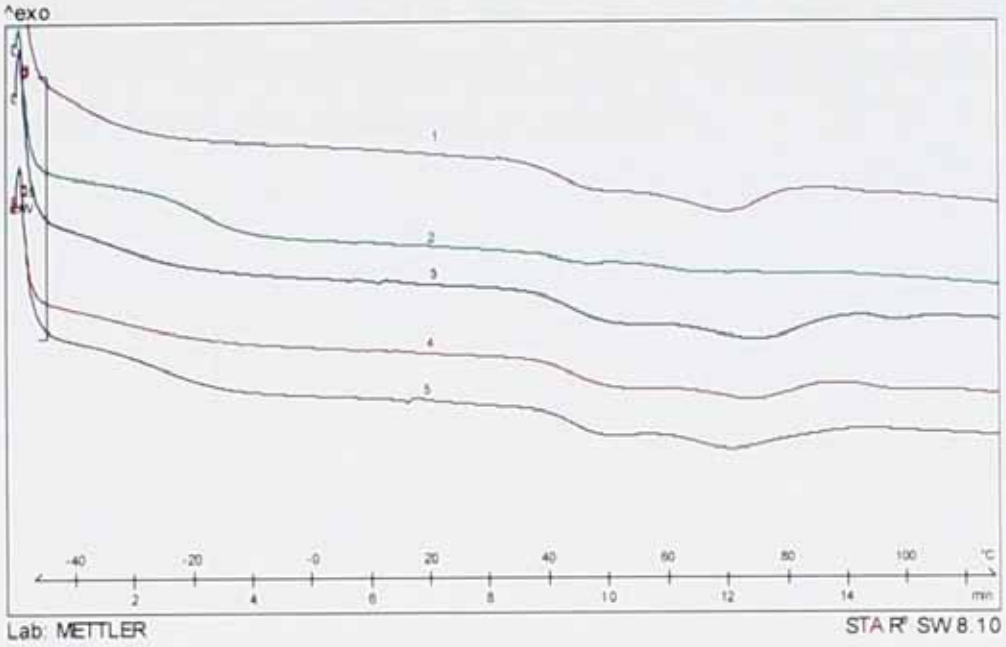

Figure 4.12 DSC curves of coatings containing different content of surface modified nano-scale silica. DSC trace No. 1, 2, 3, 4 and 5 are coatings 428B, 428A 428C, 428D and 428E respectively.

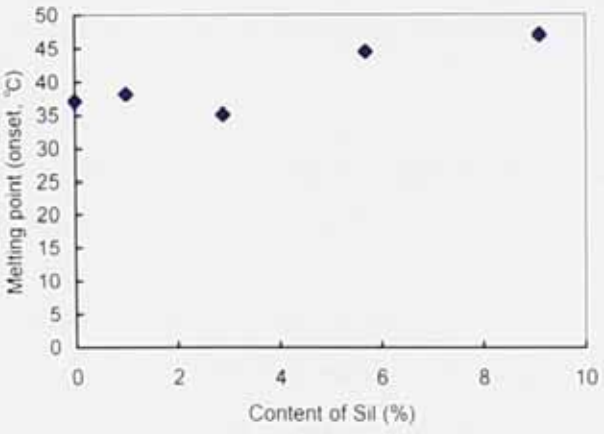

Figure 4.13 Effect of content of **Sil-2** on the melting point of cross-linked coating film

Figure 4.13 shows that overall the onset melting points increase as the content of silica in powder coating increases from 0 to 9.1%, but there is a minimum onset melting point when the content of **Sil-2** is around 2.9%.

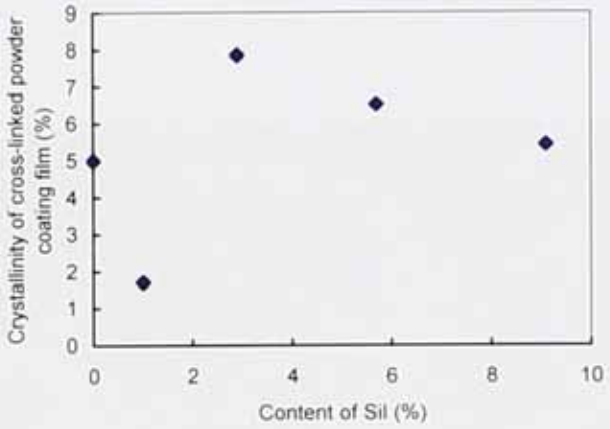

Figure 4.14 Effect of content of **Sil-2** on crystallinity of cross-linked coating film

Figure 4.14 shows the degree of crystallinity of the cross-linked powder coating film. There is a minimum value when the content of **Sil-2** is about 1.0%, but there is also a maximum value when the content of **Sil-2** is about 2.9%.

4.3.3.2 Effect of Nano-scale Silica Particles on the Abrasion Properties of Cross-linked Powder Coating Films

4.3.3.2.1 Abrasion Property Analysis Methods

The SLF 5 test method for wet and dry-rub fastness (detailed described in section 2.2.5) was used to test the abrasion resistance of finished leather samples. The leather samples were powder coated with or without fumed silica in the coating and also powder coated with modified fumed silica **Sil-1** where the surfaces were grafted with acrylate functional groups. The instrument used was a SATRA rub fastness tester, model STM 461.

4.3.3.2.2 Testing Results and Discussion

The dry and wet rub fastness test results are shown in Figure 4.15 and ratings are given in Table 4.7.

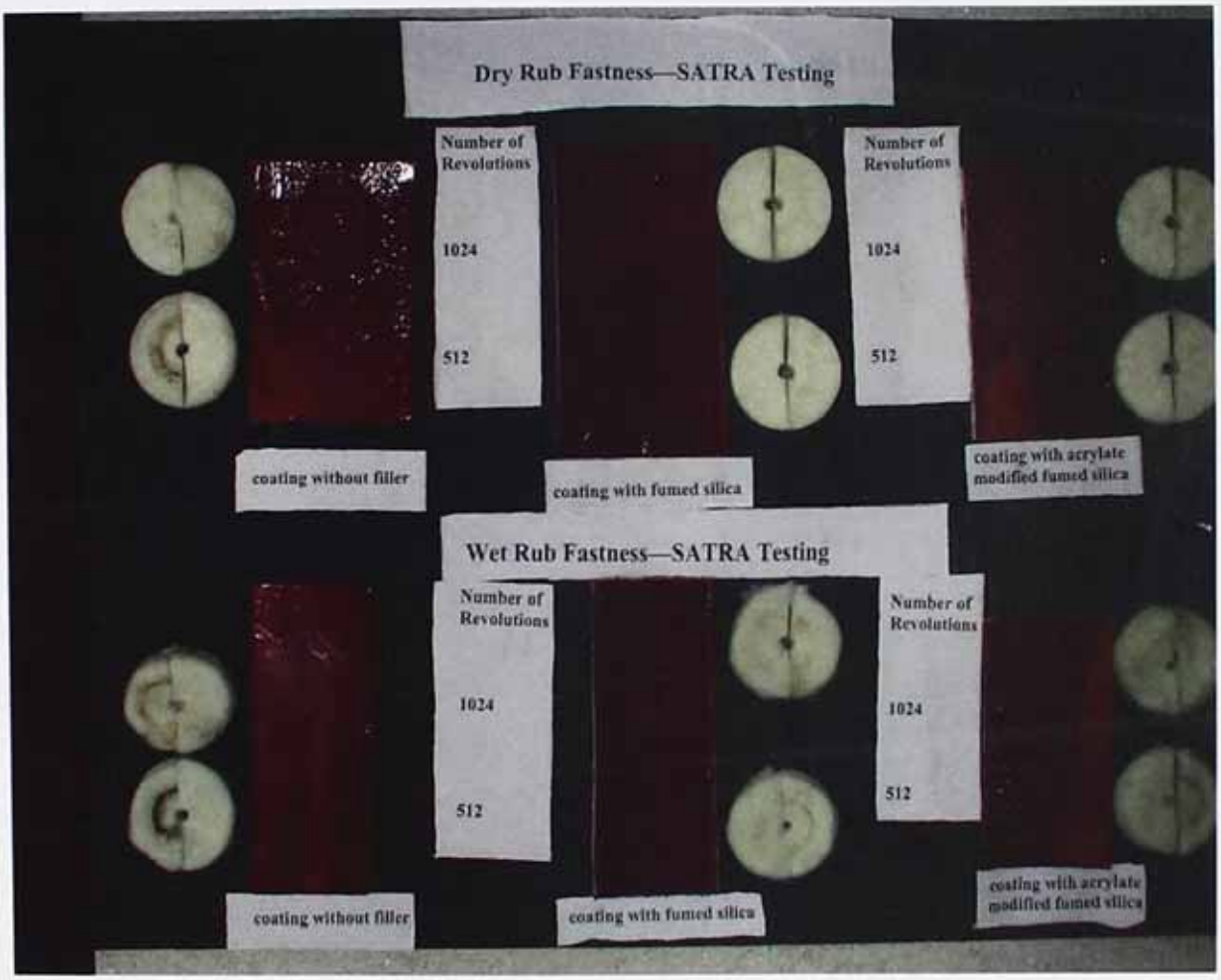

Figure 4.15 Rub Fastness—SATRA testing results of powder coating finished leather

Table 4.7 Ratings for dry and wet rub fastness properties of finished leather samples

Rub fastness test	Dry rub fastness (number of revolutions)		Wet rub fastness (number of revolutions)	
	512	1024	512	1024
Powder coating without filler finished leathers (grey scale)*	1	1	3	3
Powder coating with fumed silica finished leathers (grey scale)	3/4	3/4	4	4
Powder coating with modified fumed silica finished leathers (grey scale)	4	4	5	5

* Note: The Grey Scale has nine possible values: 5, 4-5, 4, 3-4, 3, 2-3, 2, 1-2, 1. and Grey Scale 5 is no visual change (best rating); ----; 1 is a large visual change (worst rating). (See Section 2.2.5)

The rub fastness test results showed that:

- A significant visual change occurred for the leather sample and the rubbing felt after the number of revolutions 512 or 1024 for powder coating without fillers, indicating a poor rub fastness property of coatings without fillers.
- There was little or no visual change for powder coating with fillers (fumed silica or acrylate modified fumed silica **Sil-1**), indicating excellent rub fastness for coatings with fillers.
- The performance of coatings with acrylate modified fumed silica is slightly better than that of coatings with fumed silica.
- Figure 4.15 shows that the powder coating film gloss decreased when formulated with fumed silica, but there was no loss of gloss when the coating was formulated with acrylate modified fumed silica **Sil-1,** indicating a much better or finer dispersion of the nano-particles in the binder resins.

4.3.3.3 Effect of Nano-scale Silica Particles on the Adhesion Properties of Cross-linked Powder Coating Films

4.3.3.3.1 Adhesion Property Analysis Method

The procedure and evaluation of test results was described in Section 2.2.3.

4.3.3.3.2 Adhesion Testing Results and Discussion

The adhesion results for prepared powder coatings formulated with or without nano-scale silica particles are shown in Table 4.8. According to the requirement of the standard DIN EN ISO 11644-2004, the strength of coating adhesion to leather should be ≥2.0N/cm, but during the determination, it is suggested that a reactive hot-melt adhesive film with higher adhesion strength be used. During our tests, the SATRA SLF-11 (described in section 2.2.3) test method was used, and the adhesive was C/70 type Chelsea adhesive (Casewell Co. Ltd., UK). This adhesive is solvent based although the solvent was evaporated before lamination of the finished leather sample with the PVC strip. It was difficult to exceed a cohesive strength of the adhesive of 1.5N/cm.

Table 4.8 Adhesion results of clear UV curable powder coatings finished leather

Type of powder coating used	Without filler		With fumed silica	With silica **Sil-1** *
Type of leather used	Chromium-tanned sheep skin leather with light yellow dyes	Chromium-tanned sheep skin leather with brown yellow dyes	Chromium-tanned cow leather with brown dyes	Chromium-tanned cow leather with brown dyes
Adhesion strength between coating film and leather	> 1.5N/cm	> 1.5N/cm	> 1.5N/cm	> 1.5N/cm
observation	Chelsea adhesive film peeling off or tearing from PVC strips. There was no failure to be observed on the adhesion between coating film and leather.			

* **Sil-1** is fumed silica with surface being grafted with acrylate functional groups.

The results so far show that the porous nano-scale particles did influence physical properties of powder coatings. The DSC results showed that for formulations containing surface modified silica, the melting point of cross-linked powder coating film can be increased by about 10°C. The DMTA results indicated that incorporating **Sil-1** increased the glass transition temperature of coating film, and enhanced mechanical strength as well. The abrasion resistance of powder coatings formulated with nano-scale particles was improved significantly due to the hardness of silica particles.

4.3.4 Effects of Photo-initiator Content on Powder Coating Properties

4.3.4.1 DSC Study of the Effects of Photo-initiator Content on Coating Properties

The PUA resin PUA-1 was subjected to DSC analysis (original DSC curve is given in Appendix C4.3). DSC data was collected from -50 to 150°C at a heating rate of 10 °C/ min. The measured crystallinity is 53.8%, the onset melting temperature is 29.9°C, the peak melting temperature is 96.5°C and the glass transition temperature at midpoint is -29.3°C. The resin was formulated with different contents of the photo-initiator Irgacure® 184. Samples were melted on watch glasses; under IR radiation supplied by the IR equipment described in Section 2.3.2.1 (temperature button was set at 80°C). Samples were mixed uniformly and cross-linked by UV radiation. The UV intensity was about 1.0 J/cm^2 and the sample was exposed for 50seconds. The DSC traces are shown in Appendix C4.4, DSC data were collected from -50 to 150°C at a heating rate of 10°C / min, and the results taken from DSC traces are shown in Figures 4.16, 4.17 and 4.18. The cross-linked resin shows a maximum in crystallinity when the photo-initiator content was between 0.5% and 1% and a maximum glass transition temperature and a minimum melting point when the photo-initiator content is 0.55%. In general, as the photo-initiator content increases, the powder coating resin's melting temperature increases and glass transition temperature decreases. Changes in crystallinity and glass transition temperature with photo-initiator content are, however, very small.

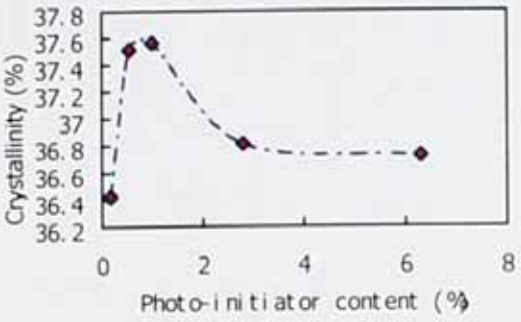

Figure 4.16 Effect of photo-initiator content on crystallinity of the powder coating resin

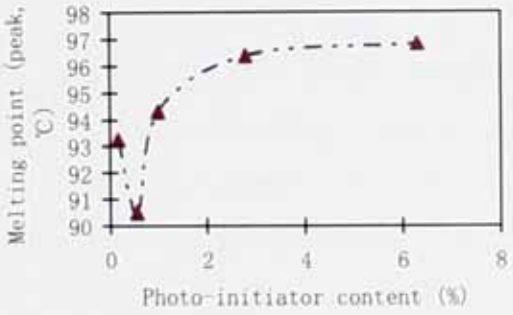

Figure 4.17 Effect of photo-initiator content on melting point of powder coating resin

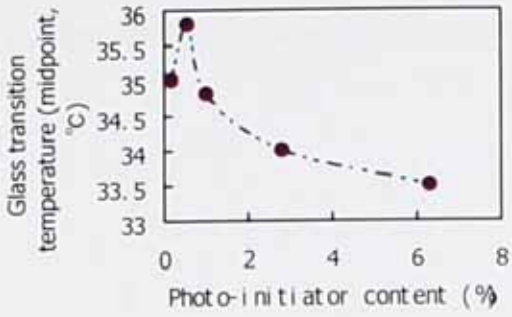

Figure 4.18 Effect of photo-initiator content on
the glass transition temperature of powder coating resin

4.3.4.2 Effects of Photo-initiator Content on the Tensile Properties of Cross-Linked Powder Coating Films

Specimen Preparation:

PUA resin PUA-3, which had a crystallinity of 29.0%, an onset melting temperature of 32.2°C, and peak of 87.5°C and a glass transition temperature of -18.0°C (DSC curve is given in Appendix C4.5), was formulated with different contents of photo-initiator Irgacure® 184 (0.960%, 1.48%, 2.97% and 5.53% by weight). The sample was exposed to IR radiation to melt it and cause it to flow out into a thin film and then it was transferred to the UV radiation region of the conveyor to initiate and develop cross-linking for about 30 seconds. The samples were then left in a conditioned room at 20±1°C, relative humidity 62±1% for 48 hours and then tensile test specimens were cut with a shaped cutter prior to testing the tensile properties.

When the content of photo-initiator was 0.960%, the tensile samples were coded Ia. The original tensile force-distance curves are shown in Appendix C4.6, and were used to give stress (σ) and extension ratio (λ) data. σ was plotted against ($\lambda - \lambda^{-2}$), shown in Figure 4.19 – this relation comes from the theory of rubber elasticity[111] .

Although the plot deviates from a fully linear relation, G was obtained (modulus factor) from the initial slope [128], G= 3.87MPa.

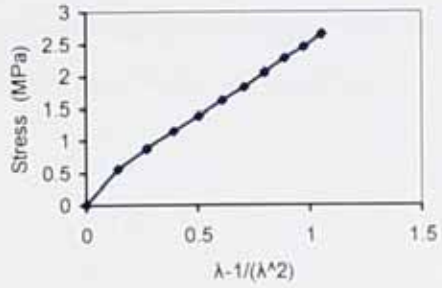

Figure 4.19 Plot of stress (σ) vs. ($\lambda - \lambda^{-2}$) for PUA with 0.096% (w/w) photo-initiator

When the content of photo-initiator in the powder coating was 1.48%, samples were coded Ib. The original tensile force-distance curves are as shown in Appendix C4.7, and these data were used to calculate average σ and λ. Stress (σ) was plotted against ($\lambda - \lambda^{-2}$) to give the curve shown in Figure 4.20. Although the plot deviates from linearity, nevertheless G was again derived from the initial slope [128] to give G= 3.06 MPa.

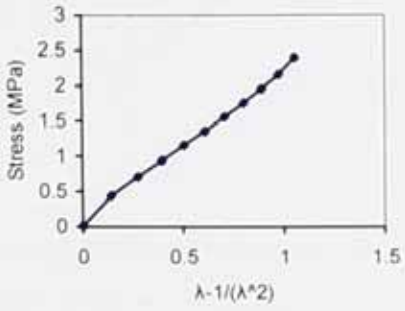

Figure 4.20 Plot of stress (σ) vs. ($\lambda - \lambda^{-2}$) for PUA with 1.48% (w/w) photo-initiator

Similarly stress-strain ratio curves were obtained for film with 2.97% initiator (Fig 4.21, and the original tensile force-distance curves are shown in Appendix C4.8) for which G was 2.94 MPa (derived from the initial slope) and 5.53% initiator (Fig 4.22, and the original tensile force-distance curves are shown in Appendix C4.9) for which G was 4.76 MPa (again derived from initial slope).

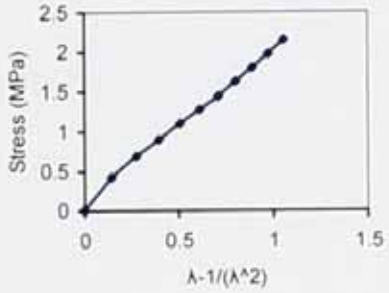

Figure 4.21 Plot of stress (σ) vs. ($\lambda - \lambda^{-2}$) for PUA with 2.97% (w/w) photo-initiator

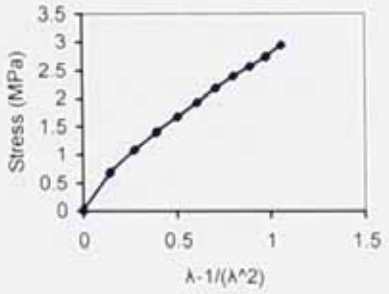

Figure 4.22 Plot of stress (σ) vs. ($\lambda - \lambda^{-2}$) for PUA with 5.53% (w/w) photo-initiator

The effect of Photo-initiator content on elongation at break, modulus factor G and degree of cross-linking for powder coating film are shown in Figures 4.23, 4.24 and 4.25 respectively.

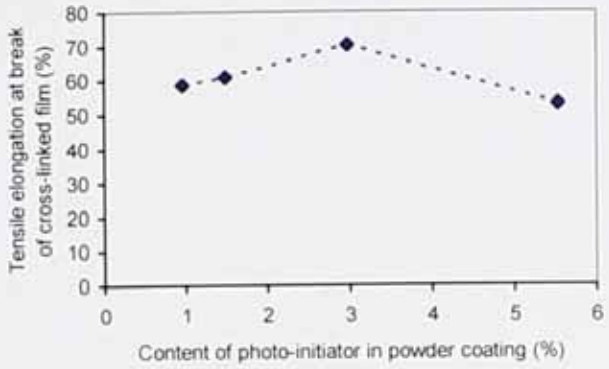

Figure 4.23 Effect of photo-initiator content on elongation at break of cross-linked powder coating film

In Figure 4.23, it can be seen that, as the content of photo-initiator increases from 0.96% to 5.53%, there is no marked change in elongation at break, although there appears to be a maximum in elongation (70.2%) when the content of photo-initiator is about 2.97%.

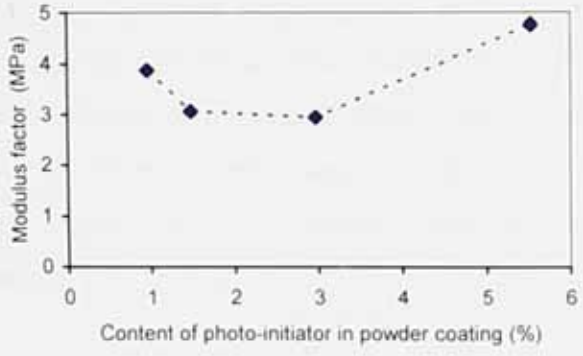

Figure 4.24 Effect of Photo-initiator content on modulus factor of cross-linked powder coating film

In Figure 4.24, it can be seen that, as the content of photo-initiator increases from 0.96% to 5.53% in powder coating, the tensile modulus factor of cross-linked films decreases at first and then increases with the content of photo-initiator.

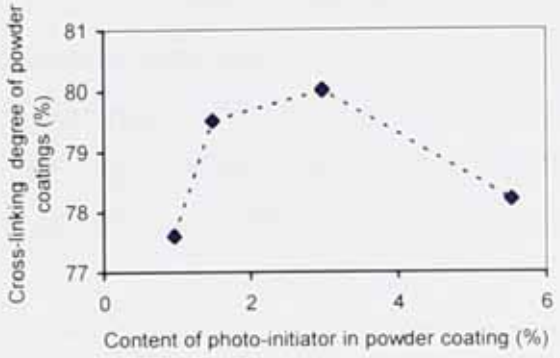

Figure 4.25 Effect of Photo-initiator content on cross-linking degree of powder coatings

In Figure 4.25, it can be seen that, as the content of photo-initiator increases from 0.96% to 5.53%, the cross-linking degree increases at first and then decreases with increasing content of photo-initiator. This indicates that a higher cross-linking degree was obtained when photo-initiator content was between 1.5 to 3.0%. There is a turning point at 3% of photo-initiator content, it shows that the concentration of photo-initiator is too high in the powder coating; most of the UV radiation will be absorbed by photography on the surface which prevents photo-initiator in the deeper layer in the powder coating and results in a lower cross-linking degree of powder coating.

4.3.5 Effect of UV Dose on the Properties of Cross-linked Powder Coating Films

Specimen Preparation:

For PUA resin PUA-3, 15.89g of the material was melted and mixed with 0.31g of photo-initiator Irgacure® 184. It was then poured onto chromium sheep leather with a thin layer of soft paraffin oil on the surface as a releasing agent and then re-melted by exposure to IR radiation. It was left until fully cooled and then removed as solid films. 4 pieces were cut and exposed to IR radiation again and then the powder coating was cross-linked by UV radiation with different UV doses, the respective UV radiation intensities being 1.0J/cm^2, 2.0J/cm^2, 3.0J/cm^2 and 4.0J/cm^2. Afterwards the films were cooled, cleaned with grease-free cotton wetted with petroleum ether (b.p. 40-60℃), and left for 3 days prior to testing their tensile properties.

The plots of stress vs. ($\lambda - \lambda^{-2}$) are shown in Figures 4.26 to 4.29 (original force-extension data are given in appendices C4.12, C4.13, C4.14 and C4.15). Modulus Factor values derived from these curves are given in Figure 4.31.

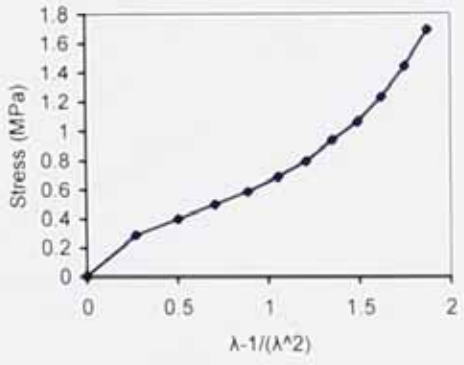

Figure 4.26 Plot of stress (σ) vs. ($\lambda - \lambda^{-2}$) for a Powder coating film cross-linked at a UV intensity of 1 J/ cm^2

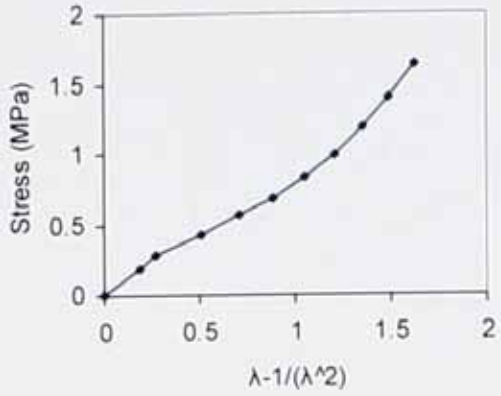

Figure 4.27 Plot of stress (σ) vs. ($\lambda - \lambda^{-2}$) for a Powder coating film cross-linked at a UV intensity of 2 J/ cm^2

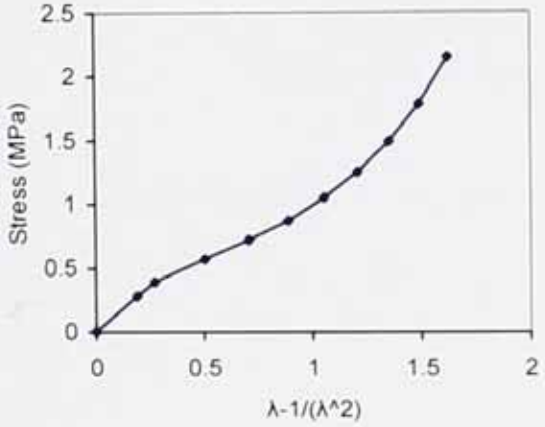

Figure 4.28 Plot of stress (σ) vs. ($\lambda - \lambda^{-2}$) for a Powder coating film cross-linked at a UV intensity of 3J/ cm^2

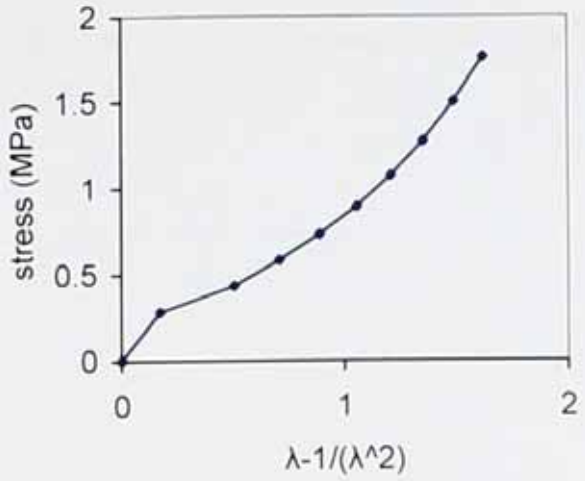

Figure 4.29 Plot of stress (σ) vs. ($\lambda - \lambda^{-2}$) for a Powder coating film cross-linked at a UV intensity of 4J/ cm^2

The UV intensity effect on powder coating film elongation to break, modulus factor G and degree of cross-linking are shown in Figures 4.30, 4.31 and 4.32 respectively.

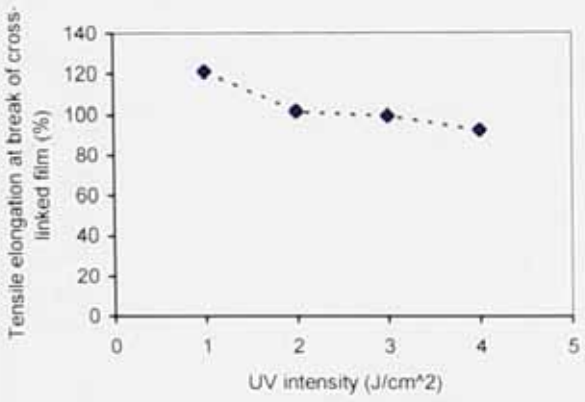

Figure 4.30 Effect of UV intensity on elongation at break of cross-linked film

Figure 4.30 shows that, as the UV intensity used for cross-linking powder coatings increases from 1J/cm^2 to 4J/cm^2, the elongation at break of the cross-linked film decreases gradually from 121% to 92%.

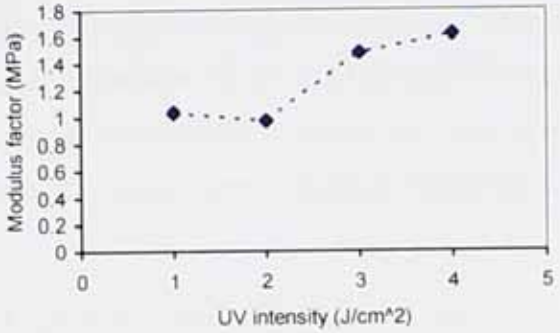

Figure 4.31 Effect of UV intensity on the modulus factor of cross-linked film

Figure 4.31 shows that as the UV intensity used to cross-link the powder coatings increases from 1J/cm^2 to 4J/cm^2, the tensile modulus factor of cross-linked film increased markedly from 1.0 MPa to 1.6 MPa.

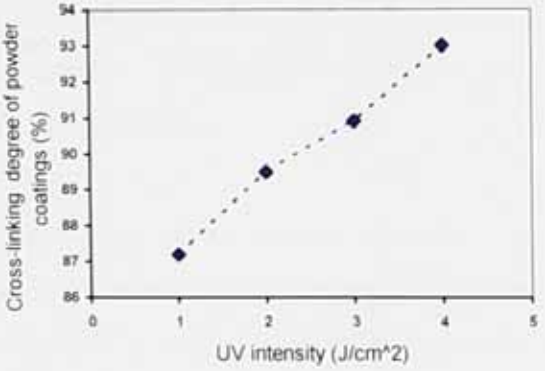

Figure 4.32 Effect of UV intensity on the cross-linking degree of powder coatings

Figure 4.32 shows that as the UV intensity used for cross-linking the powder coatings increases from 1J/cm^2 to 4J/cm^2, the cross-linking degree of the powder coatings show a clear increase from 87.2% to 93.0%. This means that cross-linking tends to become complete as the UV intensity increases. It was found that at the higher intensities (3 to 4J/cm^2) the UV radiation may detrimentally affect film properties, even starting to burn the powder coating film. Clearly in practice the UV intensity used for cross-linking powder coatings should not be too high.

4.4 Results and Discussion on UV Curable Powder Coatings for Leather Application

The experimental results from above sections showed that UV curable powder coating binders made from HDI/DEG/DHBA/BEP, were semi-crystalline polymers, with crystallinities between 12 to 35%, depending on formulations and melting points between 60 and 100 °C; such properties are required for keeping such prepared powder coatings in stable solid state during storage. The resulting powder coating films showed high flexibility when formulated with a photo-initiator and cross-linked. Therefore a polyurethane acrylate based on a HDI/DEG/DHBA/BEP system, was deemed suitable to be investigated as a powder coating binder resin for the finishing of leather. The results of this investigation are discussed in the following sections.

A content of photo-initiator between 1.5 to 3.0% (by weight) was used as it is necessary to ensure that the powder coating film has a sufficient cross-linking degree and the UV radiation intensity was controlled between 1J/cm^2 to 2J/cm^2. Powder coatings formulated with surface modified silica were evaluated since they may result in an improvement of coating film adhesion and rub fastness. In order to compare results with the newly developed system with a commercial system, some results obtained with a commercial product are also given.

4.4.1 Evaluation of a Commercially Available UV Cross-linkable Powder Coating for Finishing of Leather

4.4.1.1 Finishing Leather with Powder Coating Based on Rucote® 7008 Resin

The commercially available powder coating resin Rucote® 7008 was ordered from the Bayer RUCO Polymers Inc. (Columbus, GA, USA). This resin can be thermally or UV radiation cross-linked. The dual curable powder coating resin is an unsaturated resin made from fumaric acid. The powder was sprayed on a crust leather using sieves. The coated sample was fused in an oven with the stoving conditions being 100 °C for 15 minutes (a pre-coated primer was not used). The finished leather sample was cooled to room temperature, and bent double as shown in Figure 4.37. The powder coating film displayed serious cracking even after the sample was bent just one time; the result is shown in Figure 4.33.

Figure 4.33 A leather sample finished with a powder coating based on Rucote® 7008 resin showing cracking after bending.

4.4.1.2 Finishing Leather with Powder Coatings Based on Uvecoat™ 3003 and Uvecoat™ 9010 resins

Commercially available UV curable powder coatings based on Uvecoat™ 3003 and Uvecoat™ 9010 resins were supplied by UCB Company (60 Alle de la Recherche, Brussels,Belgium). These resins can be cross-linked by UV radiation to produce a relatively flexible powder coating finish film and the powder coatings have been developed for the finishing of PVC floor materials. The powder coating was sprayed onto a leather crust by the EMB method. Again finished leather samples were bent as shown in Figure 4.37. When the sample had been bent several times the powder coating film became a little bit crinkled; the result is shown in Figure 4.34. The EMB powder coating finished leather sample was characterized by SEM. The result is shown in Figure 4.35. The top layer seen in the SEM image is the powder coating film; its thickness is between 70-140μm, and it was clearly not uniform. The lower part of the image shows the leather microstructure.

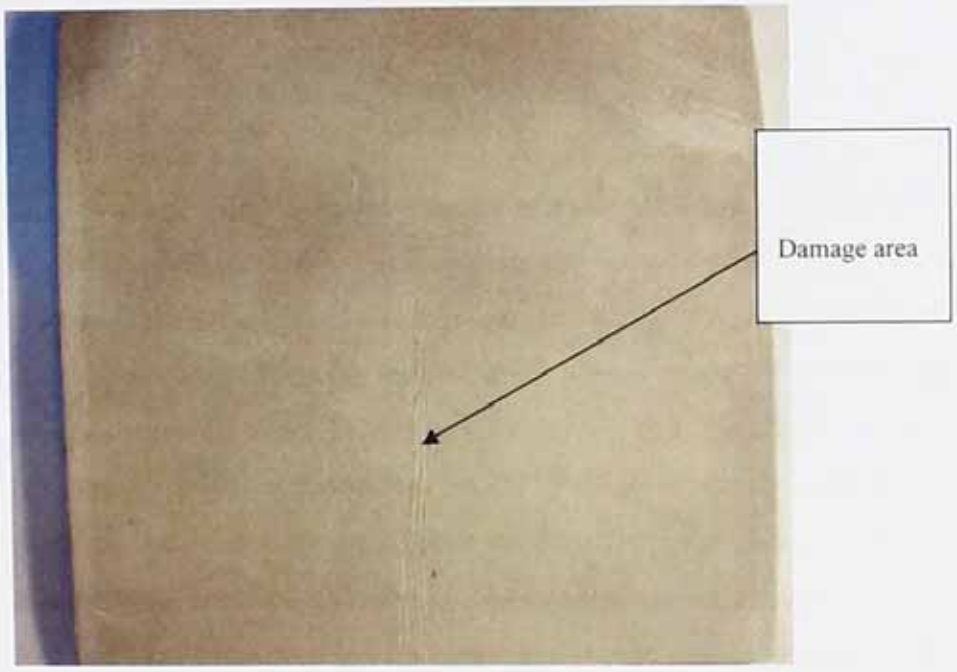

Figure 4.34 A leather sample finished with a powder coating based on both Uvecoat™ 3003 and Uvecoat™ 9010 resins applied by EMB

Figure 4.35 An SEM image of a leather sample finished with a powder coating based on the mixture of UvecoatTM 3003 and Uvecoat™ 9010 resins applied by the EMB finishing method

4.4.2 Studies on UV Curable Powder Coating Resin PUA-2

4.4.2.1 Study on Viscosity of Resin PUA-2

As shown in Figure 4.36, the viscosity of sample PUA-2 was 3710 mPa·s at a speed of 1RPM. For the first measurement, the viscosities went up as the shear rate increased; the sample had been kept between the cone and plate of the viscometer for one hour at 90±0.5°C, for measurement after 1 hour, viscosities went up as the speeds increased from 0.1RPM to 1 RPM, and then kept constant when the measuring speeds increased from 1RPM to 1.6 RPM; for the sample kept in the cone plate of viscometer for two hours at 90±0.5°C, for measurement after 2 hours, viscosities went down as the measuring speeds increased from 0.1RPM to 1 RPM, and then kept constant when the measuring speeds increased from 1RPM to 1.6 RPM. Further study and discussion concerning the changes of sample PUA-2 before and after viscosity measurement will be given in the following section.

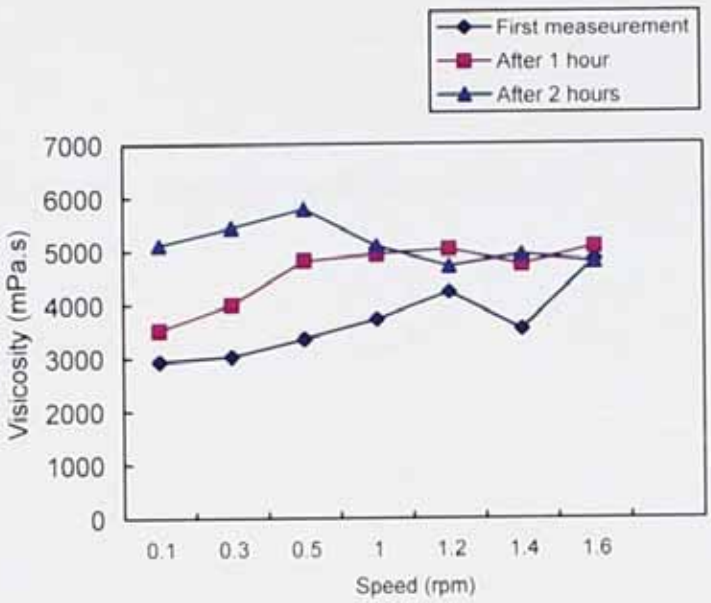

Figure 4.36 Viscosity of PUA-2 at different conditions

4.4.2.2 Characterization of PUA-2 by DSC Analysis

PUA-2 resin samples before and after viscosity measurement at 90^0C for 2 hours have been characterized by DSC, the original DSC curves are given in Appendix C4.10, DSC data was collected from -50 to 150°C at a heating rate of 5°C/min; PUA-2 resin samples before and after curing have been characterized by DSC as well, the DSC curves are attached in Appendix C4.11, DSC data were collected from -50 to 150°C at a heating rate of 5°C/ min; the results are shown in Table 4.9. After viscosity measurement, the crystallinity of PUA-2 is lower than before viscosity measurement. This difference is mainly caused by the crystallization processes. The semi-crystalline resin PUA-2 was transformed into complete amorphous state after curing (no crystalline peak on the DSC curve).

Table 4.9 DSC results for the PUA-2 sample after curing and after viscosity measurement

Sample No.		PUA-2a	PUA-2b	PUA-2c
Sample note		PUA-2	After curing	After viscosity measurement before curing
DSC	Crys. (%)	23.0	----	19.8
	Heat(J/g)	-41.8	----	-36.0
	T_m (°C) onset	28.7	----	26.1
	T_m (°C) peak	67.5	----	60.3
	T_g (°C) onset	----	-23.5	----
	T_g(°C) midpoint	----	-13.2	----

4.4.2.3 Formulation of PUA-2 Resin for Leather Finishing

The semi-crystalline resin PUA-2 was formulated with 1.5% (w/w) photo-initiator Irgacure® 184 (supplied by Ciba Company, Switzerland). The coating was applied to leather and heated and cured by UV radiation at intensity of about 1 J/cm^2 for 20 seconds. The flexibility of the coating is evident when the sample is bent in the fashion as shown in Figure 4.37 and there is no crack or break in the coating.

Figure 4.37 A leather sample finished with a UV-curable powder coating based on polyurethane acrylate resin.

4.4.3 A Study of UV Curable Powder Coated Leather Properties

Details of the UV curable powder coating formulations are listed in Tables 4.10, 4.11, 4.12 and 4.13 and images of tested specimens are shown in Figures 4.38, 4.39, 4.40 and 4.41. The powder coating component materials used were:

PUA resinPUA-3: polyurethane based resin with pendant acrylate functional groups

Pigment: FTX series ASTRAL PINK 1 from Swada Ltd., UK

Sil-2: Surface modified nano-scale fumed silica with 3- (Trimethoxysilyl) propyl methacrylate (ref. Section 4.2.2.5.2)

Photo-initiator: Irgacure® 184 from Ciba Company, Switzerland.

Properties of the powder coating finished leather are given in the following sections, test methods used are discussed in Section 2.2.2 to 2.2.5.

The dry rub fastness test samples of UVPC-1 and UVPC-2 are shown in figure 4.38, UVPC-3 and UVPC-4 are shown in figure 4.39. The martindale abrasion test samples of UVPC-1, UVPC-2, UVPC-3 and UVPC-4 are shown in figures 4.40 and 4.41.

Table 4.10 Powder coating formulation UVPC-1

Component	PUA resin PUA-3	Sil-2	Photo-initiator
Mass (g)	2.78	0.0092	0.0170
(%)	99.06	0.33	0.61

Leather type: Chrome tanned sheepskin leather dyed light yellow

Table 4.11 Powder coating formulation UVPC-2

Component	PUA resin PUA-3	Photo-initiator
Mass (g)	2.90	0.060
(%)	97.97	2.03

Leather type: Chrome tanned sheepskin leather dyed yellow

Table 4.12 Powder coating formulation UVPC-3

Component	PUA resin PUA-3	pigment	Sil-2	Photo-initiator
Mass (g)	1.37	0.223	0.0046	0.0092
(%)	85.26	13.88	0.29	0.57

Leather type: Chrome tanned cow crust

Table 4.13 Powder coating formulation UVPC-4

Component	PUA resin PUA-3	Pigment	Sil-2	Photo-initiator
Mass (g)	9.44	1.93	0.305	0.266
(%)	79.06	16.16	2.55	2.23

Leather type: Chrome tanned cow crust

Figure 4.38 Dry rub fastness samples of UVPC-1 and UVPC-2 (the number of rotations of the pad are indicated on the left of the figure)

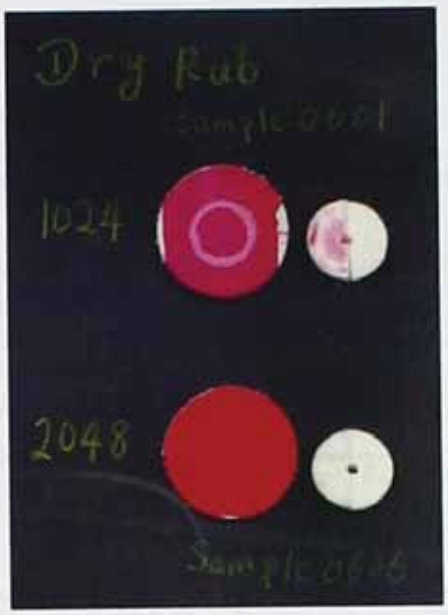

Figure 4.39 Dry rub fastness samples of UVPC-3 and UVPC-4 (the number of rotations of the pad are indicated on the left of the figure)

Figure 4.40 Appearance of Martindale abrasion test samples before testing: formulations UVPC-1, UVPC-2, UVPC-3 and UVPC-4

Figure 4.41 Appearance of Martindale abrasion test samples after testing: formulations UVPC-1, UVPC-2, UVPC-3 and UVPC-4

Table 4.14 Properties of UV Curable powder coatings

Powder coating formulation		UVPC-1	UVPC-2	UVPC-3	UVPC-4
Flex resistance	200 flexes	no change	no change	no change	no change
	280 flexes	no change	crazing of finish	crazing of finish	crazing of finish
Adhesion strength (N/cm)		1.5	----	----	3.5
Dry rub fastness (grey scale)		4/5	3	1	5
Martindale abrasion (10K cycles)		no change of finish	no change of finish	no change of finish	no change of finish

Table 4.14 shows that formulating the powder coatings with a surface modified nano-scale silica (formulations UVPC-1 and UVPC-4) results in a significant improvement of the rub fastness of powder coating than that of without formulating filler (formulation UVPC-2). Compared to dry rub fastness results between UVPC-3 and UVPC-4, it is indicating that abrasion property obviously improves as the silica filler content increases.

The developed UV curable powder coating finish films show high flexibility and good rub fastness.

The finish adhesion strength of UVPC-4 is higher than that of the ISO standard requirement (A finish adhesion strength 2.0N/cm is satisfactory according to ISO 11644 [129]).

Chapter V Conclusions

Up to now, most of the commercially available UV curable powder coatings give hard and brittle coating films; even the commercial products developed by the UCB Company, which are intended to be flexible enough for the finishing of PVC flooring, still lack sufficient flexibility for very flexible substrates such as leather and paper-like materials. Novel UV curable powder coatings have therefore been developed for the finishing of leather during this study [130, 131]. Some of the powder coating formulations developed produce finished films with high flexibility and good rub fastness and adhere well to leather.

5.1 Novel UV Curable Powder Coating Binder Systems

- A series of UV curable powder coating binder resins based on polyurethanes pendant with functional acrylate groups have been synthesized and samples, before curing and after curing, have been characterized by DSC method. The results indicate that semi-crystalline polyurethane resin prepared from HDI/DEG/DHBA/BEP is very suitable for use as a flexible powder coating binder.
- The optimal reactant molar ratios are: diisocyanates to diols either 2:3 or 1.1:1 (depending on molecular weight). DHBA to (DHBA+BEP) in the range 0.35 to 0.6565 and (DHBA+BEP) to total diols in the range 0.35 to 0.65.

5.2 Semi-crystalline Polyurethane Powder Coating Binders

- A semi-crystalline polyurethane preparation can be obtained by formulating hexamethylene diisocyanate (HDI) with different molecular weight polycaprolactone (PCL) diol oligomers. The melting points of prepared polyurethanes only change by 6°C.
- Partially replacing PCL diol with a diol containing side chain 2-butyl-2-ethyl-1,3-propandiol (BEP) during the preparation of semi-crystalline

polyurethane, results in polyurethane crystallinity decreasing significantly, but melting point changing very little.

- Preparing semi-crystalline polyurethanes with pendant carboxylic groups will result in decreasing or eliminating crystallinity following cross-linking.
- Semi-crystalline polyurethanes prepared with pendant hydroxyl groups will also result in decreasing or eliminating crystallinity following cross-linking.

5.3 The Hot Plating Process

- By hot plating treatment, the appearance of powder coating finished leather is improved.
- Powder coating fusion temperature can be as low as 100°C when a hot plating process is used.
- Plated powder coating finished leather tends to be thinner as the hot plating time becomes longer.
- Silicone paper is most suitable as a release agent during hot plating process.

5.4 Filler Effect on Developed Powder Coatings

Surface modified nano-scale silica can significantly improve powder coating rub fastness without affecting appearance.

5.5 Synthesized the Dihydroxymethyl Butylacrylte Monomer

- With the synthetic method I, the yield of DHBA based on TMP is low (about 12%), so it is difficult to obtain a large quantity of DHBA.
- With the synthetic method II, the yield of DHBA based on TMP is high (about 69%). Method II is a more complex synthesis process, the results of this research suggest it is a viable option.

- The functional monomer DHBA can be used to affect molecular architectural design to prepare novel polyurethane powder coating binder resins with pendant acrylate groups.

The powder coatings developed in this work, which give flexible coating films and can be cross-linked at relatively low temperatures, potentially could be used for other heat sensitive, flexible substrate applications, such as powder coatings for cables and paper-like substrates.

The successful synthesis approach developed may also apply to guide the development of polymer architecture design for other powder coatings as well as hot melt adhesives and hot melt pressure sensitive adhesives etc.

References

[1] Tozan, M., Ding, J.-F., and Attenburrow, G.E., *Journal of the Society of Leather Technologists and Chemists*, 2000, **84**:187-191.

[2] Zeno W.W., *Organic Coatings*. John Wiley & Sons, Inc., 1999: 491.

[3] David M.H., *Powder Coatings*, volume (I). John Wiley and Sons, Inc. 2002: 11-12.

[4] Zeno W.Wicks JR., Frank N.Jones and Pappas S.Peter, *Organic Coatings: Science and Technology*. Volume II: Applications, Properties, and Performance. John Wiley & Sons, Inc., 1994: 249.

[5] Zhenfa Chen and Shiyue Zhou, *Coating Process of Powder Coatings*. Shanghai Science&Technology Document Press Ltd., China, 1997: 147.

[6] T. A. Misev, *Powder Coatings Chemistry and Technology*, Chapter 6, powder Application Techniques, 1991.

[7] Powder coating Application Methods
http://cage.rti.org/altern_data.cfm?id=powder&cat=App_Meth

[8] Electrostatic powder coating.
http://www.alu-info.dk/Html/alulib/modul/A00325.htm

[9] Tribostatic powder coating.
http://www.alu-info.dk/Html/alulib/modul/A00326.htm

[10] Twigt Fredd and Vander Linde Robert, EP0636669, 1995.

[11] Bocchi, G.J., *Modern Paints and Coatings*, 1986, **76**:44.

[12] Christian, D.F., Developments in Solventless Coil Coating, presentation, Steel Research Laboratories, BHP Steel. November 17, 2003.

[13] Eduardo C. Escallon, US 5279863, 1994.

[14] Eduardo C. Escallon, US 4582718, 1986.

[15] Wang Robert, US 4568569, 1986.

[16] David M. Howell, *Powder Coatings—The Technology, Formulation and Application of Powder Coatings*. Vol. (I), 2002: 6-10.

[17] M.uminski and L.M.Saija, *Surface Coatings International*, 1995, **6**:244.

[18] Dehai Wang, Ling Jiang. *UV curable materials---theory and application*. Science publisher of China, 2001: 215.

[19] Udding Louwrier S., Baijards RA, de Jong ES. *Journal of Coatings Technology*. 2000, **72,** 904:71-75.

[20] Paul Mills. *Focus on Powder Coatings*. September 2003: 2-3.

[21] "Uvecoat^{TM}--- Resins for UV powder coatings", the brochure of UCB Chemicals.

[22] *Focus on Powder Coatings*, 2002, 9: 3.

[23] Misev Ljubomir, O. Schmid, S. Udding Louwrier and R. Bayard, *Journal of Coating Technology*, 1999, **71**, 891:37.

[24] Shelby F. Thames and James W.Rawlins, A research overview of UV-curable powder coatings from the University of Southern Mississippi, www.pcoating.com/articles/archive/08

[25] Jeno Muthiah, Andrew T. Daly, Richard P. Haley and Joseph J. Kozlowsk, US 6017640, 2000.

[26] Andrew T. Daly, Jeno Muthiah, Richard P. Haley and Joseph J. Kozlowsk, US 6005017, 1999.

[27] McGinniss Vincent D., US4129488, 1978.

[28] McGinniss Vincent D., US4163810, 1979.

[29] Muthiah Jeno and Daly Andrew T., US5922473, 1999.

[30] Blum Rainer and Hilger Christopher, US6106905, 2000.

[31] T.A.Misev. *Powder Coatings*. John Wiley & Sons. 1991:1.

[32] Paul Mills. *Metal Finishing*. January 1998: 38-41.

[33] Wei, J. and Jing, Y. Z., *UV Curable Coatings*. Chemical Industry Press Ltd., Beijing, China. 2005: 9.

[34] www.dsmcoatingresins.com

[35] Mark Drukenbrod. UV Curable Powder Coating System Goes Online. June 26, 2002. www.PaintandCoatings.com

[36] Biller Kevin M. and MacFadden Ben A., US5789039, 1998.

[37] Biller Kevin M. and MacFadden Ben A., US5935661, 1999.

[38] Richard A. Bayards, Martijn M.G. Antonisse, Erik Meij DSM Coating Resins, The Netherlands. Effect of coating composition on UV curable powder coatings. www.radcurenet_de - rte 2001 papers.htm

[39] Saskia Udding-Louwrier, Richard A. Baijards, E. Sjoerd de Jong, and Paul H,G.Binda, 'UV-curable Powder Coatings – Applying UV-curable powder coatings on paper like substrates'. (DSM Coating Resins)
www.pcoating.com/info/contact.html

[40] Abhijit Dutta and Giuseppe Pisi. Leather Finishing. *The Leather Manufacturer*. September 2001: 16.

[41] E. Heidemann. *Fundamentals of Leather manufacture*. By Eduard Roether KG., 1993: 604.

[42] Peter R. Buechler and Benjamin B. Kine, US3048496, 1962.

[43] M.khabir Uddin, Mubarak A.Khan and K.M.I.Ali . Improvement of Leather surface by UV curing. *Polym.-Plast. Technol. Eng.* 1995, **34**, 3: 447.

[44] Rock John D. and Garnett John L., US4268580, 1981.

[45] Johansson, M., Malmstrom, E., Jansson, A., and Hult, A., *J. Coat. Tech.*, 2000, **72**: 49-54.

[46] Johansson, M., Falken, H., Irestedt, A., and Hult, *J.Coat. Tech.*, 1998, **70**:57-62.

[47] Saskia Udding_Louwrier, S., Baijards, R.A., and Sjoerd de Jong, E., *J.Coat. Tech.*, 2000, 72:71.

[48] Decker, C., Morel, F., and Decker, D., *J. Oil & Color Chem. Asso.- Surface Coat. International*, 2000, 83:173.

[49] Decker, C., *Polymer International*, 1998, 45:133.

[50] Zeno W.Wicks, JR. , Frank N.Jones and Pappas S.Peter. *Organic Coatings: Science and Technology*. Volume II: Applications, Properties, and Performance. John Wiley & Sons, Inc., 1994:249.

[51] T. A. Misev. , *Powder Coatings Chemistry and Technology*, 1991: 194.

[52] K. Grundke, S. Michel and M. Osterhold, *Progress in Organic Coatings*, 2000, **39**:101.

[53] M. Wouters and B. de Ruiter, *Progress in Organic Coatings*, 2003, **48**:207.

[54] S. E. Orchard, *Appli. Sci. Res.*, 1965 (A11): 451.

[55] Zhenfa Chen and Shiyue Zhou. *The Coating Process of Powder Coatings*. Shanghai Science& Technology Document Publisher, China, 2000:297.

[56] Kris Buysens, Yves Souris. UV-POWDER: A new coating system for MDF. www.woodfinishing.it/uk/temp/UV_MDF.htm

[57] David M Howell. *Powder Coatings*, volume (I). John Wiley and Sons, 2002: 204.

[58] Joseph V. Koleske . Radiation Curing of Coatings. ASTM International. p.101

[59] David M Howell. *Powder Coatings*. Volume (I). John Wiley and Sons, 2002: 205.

[60] Dehai Wang, Ling Jiang. *UV curable materials---theory and application*. Science publisher of P.R.China, 2001:2.

[61] J. V. Crivello. *Nucl. Instr. And Meth. In Phys. Res., 1999,* B151:8.

[62] Zuren Pan. *Polymer Chemistry*. Chemical Industry Publisher of China, 1988:127

[63] Malcolm P. Stevens, *Polymer Chemistry,* Oxford University Press, Inc., 1999: 79-83.

[64] R. J. Young and P. A. Lovell, *Introduction to Polymers*, Cambridge University Press Ltd., UK, 1991: 248-290.

[65] X. Chen, G. Hou and Y. Chen, *Polymer Testing*, 2007, 26 (2):144-153.

[66] D. C. Bassett, *Principles of Polymer Morphology*. Cambridge University Press Ltd., UK, 1981: 54-166.

[67] David M. Howell. *The Technology, Formulation and Application of Powder Coatings*. Volume I. C Phys M Inst P. John Wiley & Sons Ltd., 2000:206.

[68] Daly Andrew T., Haley Richard P. and Reinheimer Eugene, US6348242, 2002.

[69] Luc Moens, Kris Buysens and Nele Knoops, US6790876, 2004.

[70] Blum Rainer and Prieto R. Jorge, US6541535, 2003.

[71] Misev Tosko A. and Belder Eimbert G., US5763099, 1998.

[72] Freriks Jan and Kooijmans Petrus, US5811198, 1998.

[73] Daly Andrew T. and Muthiah Jeno, US6136882, 2000.

[74] C. li, R.M.Nagarajan, C.C.Chiang and S.L. Cooper, *Polymer Engineering and Science*, 1986, **26,** 20:1442.

[75] Zeno W. Wick, JR., Frank N. Jones and S. Peter Pappas. *Organic Coatings*. bublished by John Wiley & Sons, 1999:181-183.

[76] Denis Couvret, and Jean-Claude Brosse, *Eur. Polym. J.*, 1991, **27**, 2:193.

[77] Wenning Andreas, Franzmann Giselher and Spyrou Emmanouil, US6747070, 2004.

[78] Milocco Claudio and Filippetti Mario, US5525161, 1996.

[79] Moens, L., Loutz, J.M., Maetens, D., Loosen, P., and Van Kerckhove, M., US 5639560, 1997.

[80] M.Johansson, T.Glauser, A. Jansson and E. Malmstrom, *Progress in Organic Coatings*, 2003, **48**, 2:194.

[81] Fink, D. and Brindopke, G. *European Coatings Journal*, 1995, 9:606.

[82] Daly Andrew T. and Haley Richard P., EP1129788, 2001.

[83] www.industrialheating.com/CDA/ArticleInformation/coverstory

[84] Wenning. A,. *Macromolecular Symposi.*, 2002, 187:597.

[85] David M. Howell. *The Technology, Formulation and Application of Powder Coatings.* Volume I . John Wiley & Sons Ltd., 2000:208.

[86] A.Valet and D.Rogez . *Surface Coatings International*, 1999, 6:293.

[87] Jiuzhuo LV, YaXian Xu and Guang Yuan, *Journal of Petrochemical Universities of China*, 2001, **14**, 2:44-49.

[88] Douglas Richart. The role of additives in powder coatings. www.iA[A[magazine.com/powderRD/issue1/

[89] www3.dsm.com/~data/hierarchie.pl

[90] Joseph V. Koleske . Radiation Curing of Coatings. ASTM International. p.190.

[91] http://www.chemistry.ccsu.edu/glagovich/teaching/472/qualanal/tests/ceric.html

[92] http://www.finishing.com/325.42.shtml

[93] http://www.rohmhaas.com/powdercoatings/tech/technical_briefs/techbriefs_solventrub.html.

[94] G.G.Sward. Paint Testing Manual. ASTM Special Technical Publication 500. 1972:181-187.

[95] Manual of Brookfield Viscometers--- More Solutions to Sticky Problems, p.13-18.

[96] Official Methods of Analysis 1996. The Society of Leather Technologists and Chemists, Northampton, UK

[97] G.G.Sward. Paint Testing Manual. ASTM Special Technical Publication 500. 1972:314-332.

[98] Christopher Tronche, Jeff C. Ubert and Chander P. Chawla. DSM Desotech, USA. Evaluation of some parameters influencing the properties of UV curable coatings.

[99] Frank Bauer, Horst Ernst and Ulrich Decker, *Macromolecular: Chemistry and Physics*, 2000, **201,** 18:2654.

[100] Luke Groholl. Coatings. *Chemfiles.* Sigma-Aldrich Corp. 2005, **5**, 3:5.

[101] Haining Ji, Nobuyuki Sato, William k. Nonidez and Jimy W. Mays, *Polymer,* 2002, 43:7119.

[102] W. Clark Still, Michael Kahn, and Abhijit Mitra, *J. Org. Chem.*, 1978, **43,** 14: 2923-2925.

[103] Laurence M. Harwood, and Christopher J. Moody, *Experimental Organic Chemistry-Principles and Practice,* Blackwell Scientific Publications, 1989:180-188.

[104] Horbart H. Willard, Lynne L. merritt, JR., John A. Dean and Frank A.Settle, JR. *Instrumental methods of analysis*, Chapter III. Published by D. Van Norstrand Company. 1981: 69.

[105] G. Tong. Instrument Analysis Application in Modern Coatings. Chemical Industry Press Ltd., Beijing, China, 2006: 275.

[106] W.J.Macknight, M. Yang and T. Kajiyama. *ACS Polymer Preprints,* 1968, 9: 860.

[107] G. Tong, *Instrument Analysis Application in Modern Coatings.* Chemical Industry Press Ltd., Beijing, China, 2006: 236-239.

[108] Erjun Tang, Guoxiang Chang, Qing Shang and Xiaolu Ma, *Progress in Organic Coatings,* 2006, **57,** 3:282.

[109] W. TU, *Water Bourne Coatings.* Chemical Industry Press Ltd., Beijing, China, 2005: 514.

[110] Wang Xingye. *Composite Mechanics Analysis and Design.* Guofang Science and Technology Publisher. 1999: 101-103.

[111] W. L. Vandoolaeghe and E. M. Terentjev. *The Journal of Chemical Physical.* 2005, **123,** 034902.

[112] R.Mafi, S.M.Mirabedini, M.M.Attar and S.Moradian, *Progress in Organic Coatings,* 2005, **54,** 3:164-169.

[113] V.S.Reddy, W.J. Weikei and J. Arbaugh, *Polymer,* 1996, **37,** 20:4653.

[114] Iglesias MT, Guzman J, Riande E., *Journal of Polymer Science Part A—Polymer Chemistry*, 1994, **32,** 13:2565.

[115] Francis R. Galiano, Gerald J. Mantell, and David Rankin, US3210327, 1965.

[116] Francis R. Galiano, Gerald J. Mantell, and David Rankin, FR1366079, 1964.

[117] Sigma-aldrich Handbook—Fine Chemicals, 2005.

[118] Tsuyoshi Kiyotsukuri, Tsuyoshi Masuda and Naoto Tsutsumi, *Polymer,* 1994, **35,** 6:1274.

[119] Organic Division, Chemistry Department of Lanzhou University and Fudan University. *Organic Chemistry Experiment*. Published by High Education Press, 1988:359.

[120] Imre Bucsi., Anlta Meleg., Arpad Molna and Mihaly Bartok, *Journal of Molecular Catalysis A: Chemical,* 2001, 168:47.

[121] Shubham P. Chopade. *Reactive Functional Polymers,* 1999, 42: 201.

[122] Sugiyama Shigesada, Hamayoshi Shigeyuki and Nagami Shingo, JP 2004183011, 2004.

[123] Sugiyama Seiji and Koura Katsuhiko, JP 2004099953, 2004.

[124] Yajima Hiroyuki; Nishisaka Tomoaki and Tsuchida Hisafumi, JP 2004176155, 2004.

[125] Liu Junliang. Study on manufacture processes of bamboo strengthening single-layer laminated composite. *Science and Technology in China,* 2006, 2:Part V.

[126] Nabeen K. Shrestha and Tetsuo Saji, *Surface and Coatings Technology,* 2004, **3,** 186:444.

[127] John Dingle. Manufacturing Leather from Chicken Skin. RIRDC Publication No 01/154, 2001. http://www.candccentral.co.uk/en-us/dept_70.html

[128] Translated by Bai Rulin. J.M.Hodkinson. *Mechanical Testing of Advanced Fibre Composites.* Chemical Industry Press. Beijing. 2005: 52.

[129] ISO 11644, Test for adhesion of finish, 2004

[130] G. Attenburrow, J. Ding and X. Jiang. WO 2006/082080 A1, 2006.

[131] X. Jiang, J. Ding and G. Attenburrow. GB 2423770 A, 2006.

Appendix

Appendix C3.1
DSC curves of polyurethane sample with pendant carboxylic acid groups before and after cross-linked

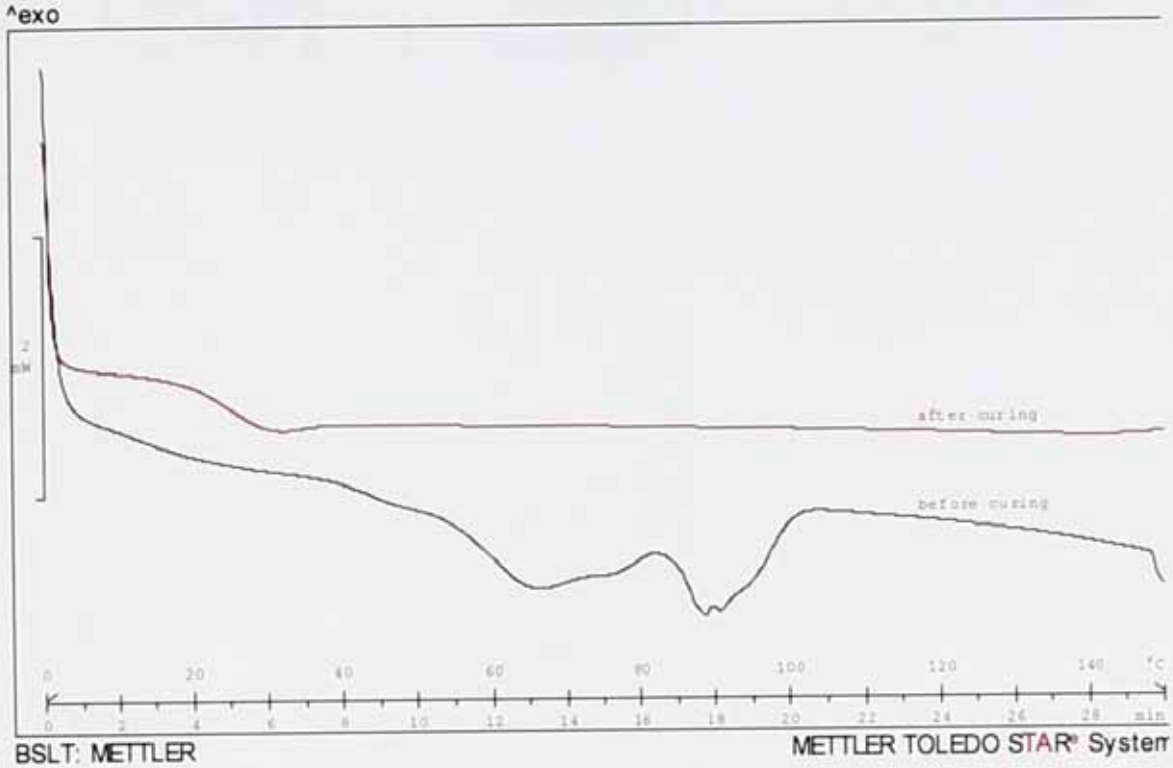

Appendix C3.2
Original Developed TLC Plate

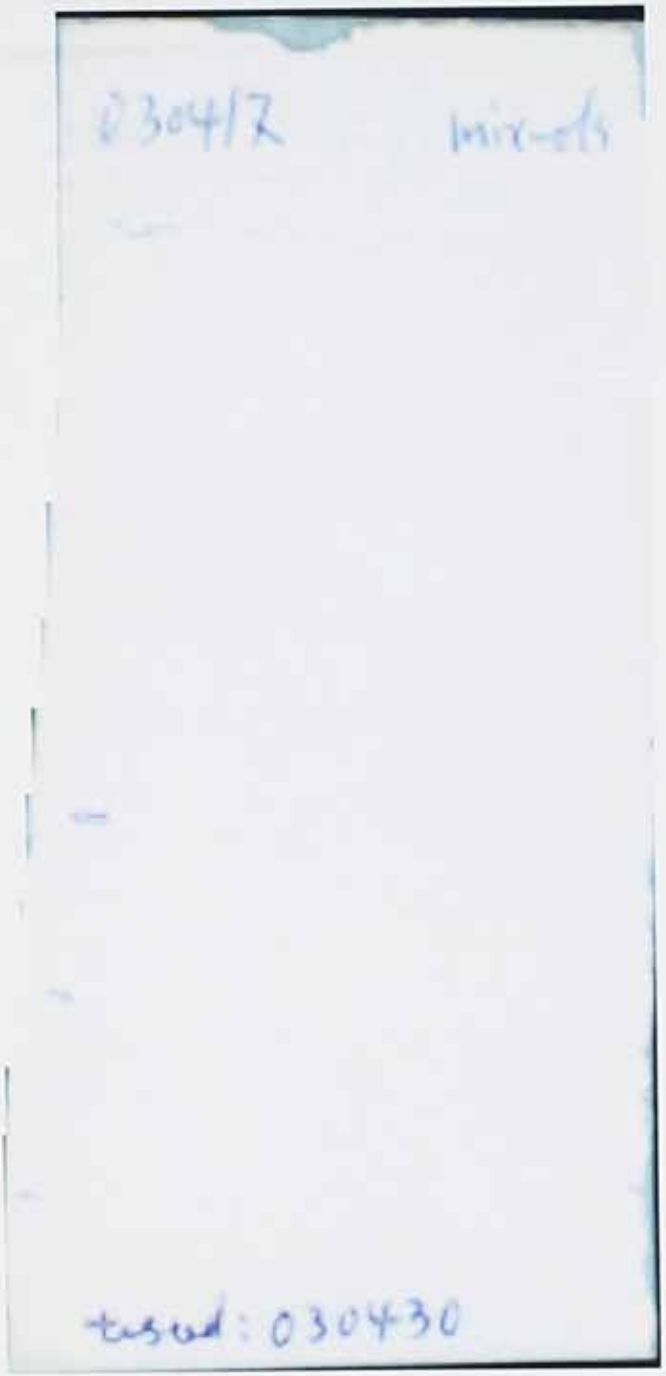

Appendix C3.3
Original Developed TLC Plate

Appendix C3.4
DSC curves of samples PCL-1250, PU-1 and PU-2. The detailed information on samples pu-1 and pu-2, please see Section 3.3.1, Figure 3.9.

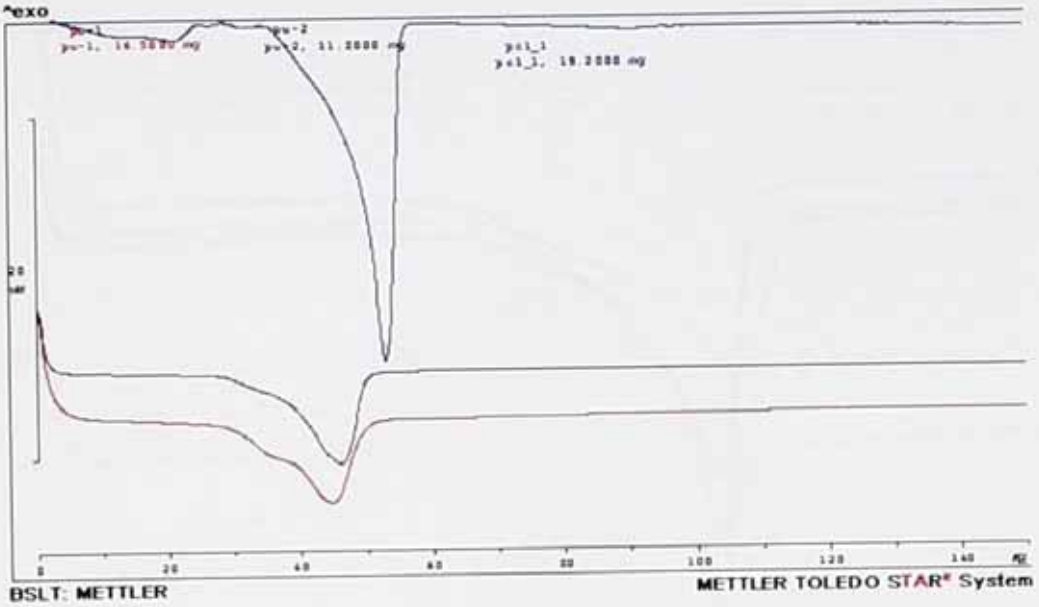

Appendix C3.5
DSC curves of samples pu-4a, pu-4b and pu-4c. Detailed information of theses samples, please see Section 3.3.1, Figure 3.10.

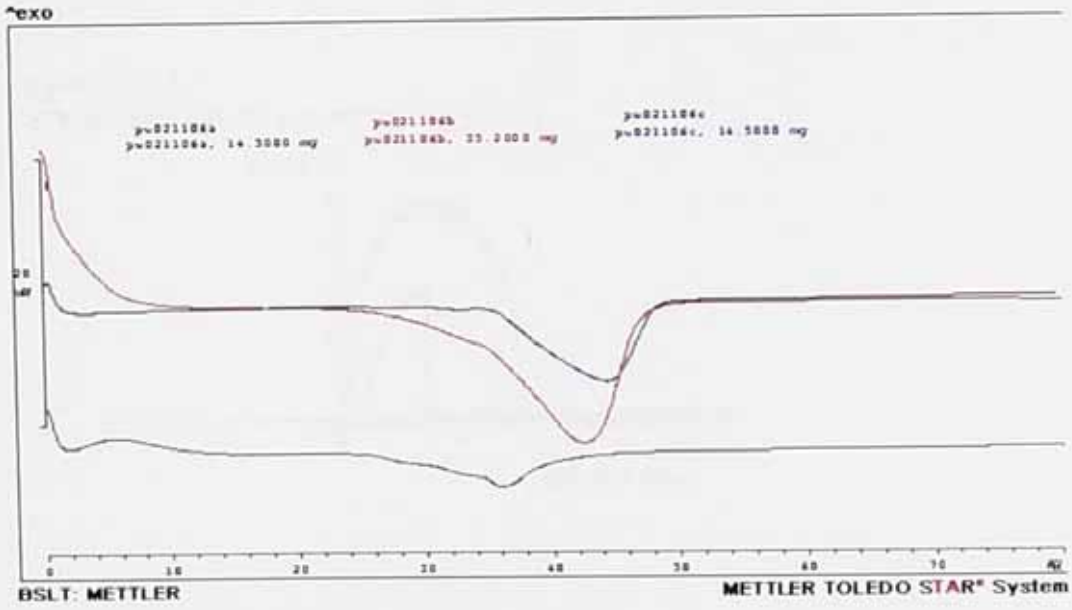

Appendix C3.6
DSC curves of samples pu-3d, pu-3a, pu-3b and pu-3c. Detailed information of theses samples, please see Section 3.3.1, Figure 3.11.

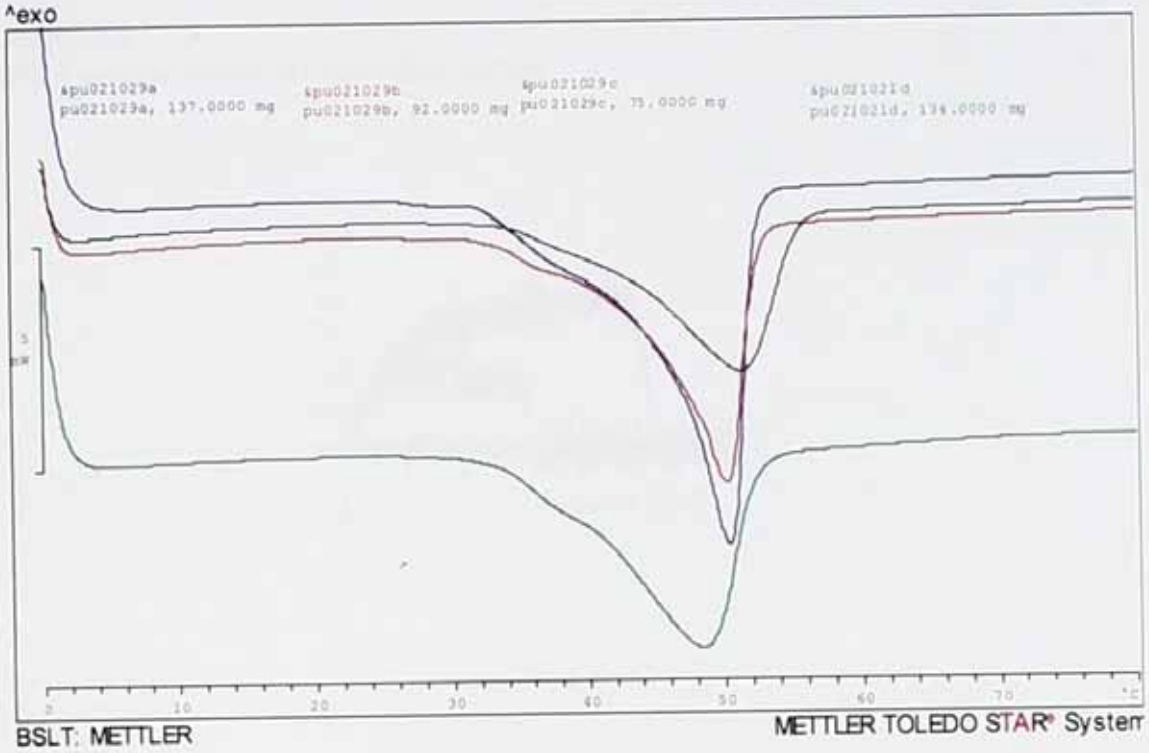

Appendix C3.7
PU-6 sample tensile test recording curves

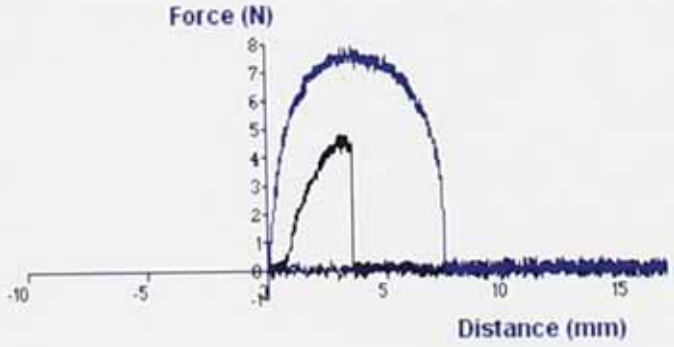

Appendix C3.8
PU-7 sample tensile test recording curves

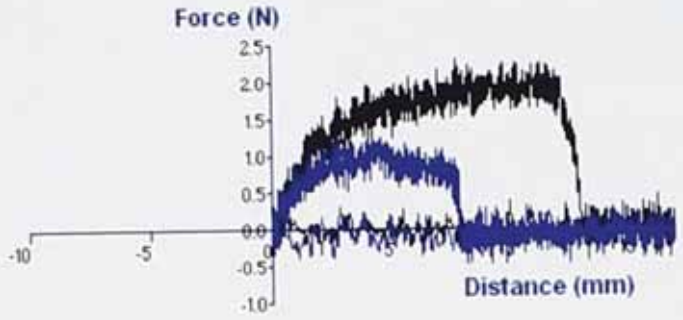

Appendix C3.9
Original Developed TLC Plate

Appendix C3.10
Samples before curing, mole fraction of monomer DHBA in the mixture of DHBA and BEP No. 1 is 0%; No. 2 is 27.1%; No. 3 is 51.2%; No. 4 is 74.2%; No. 5 is 100%

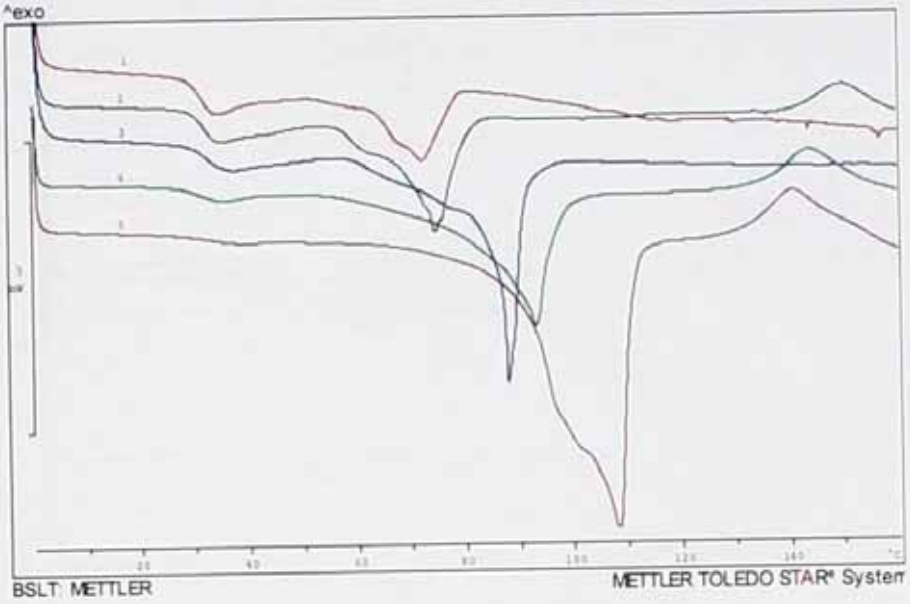

Appendix C3.11
Samples after curing, mole fraction of monomer DHBA in the mixture of DHBA and BEP No. 1 is 100%; No. 2 is 74.2%; No. 3 is 51.2%; No. 4 is 27.1%; No. 5 is 0%

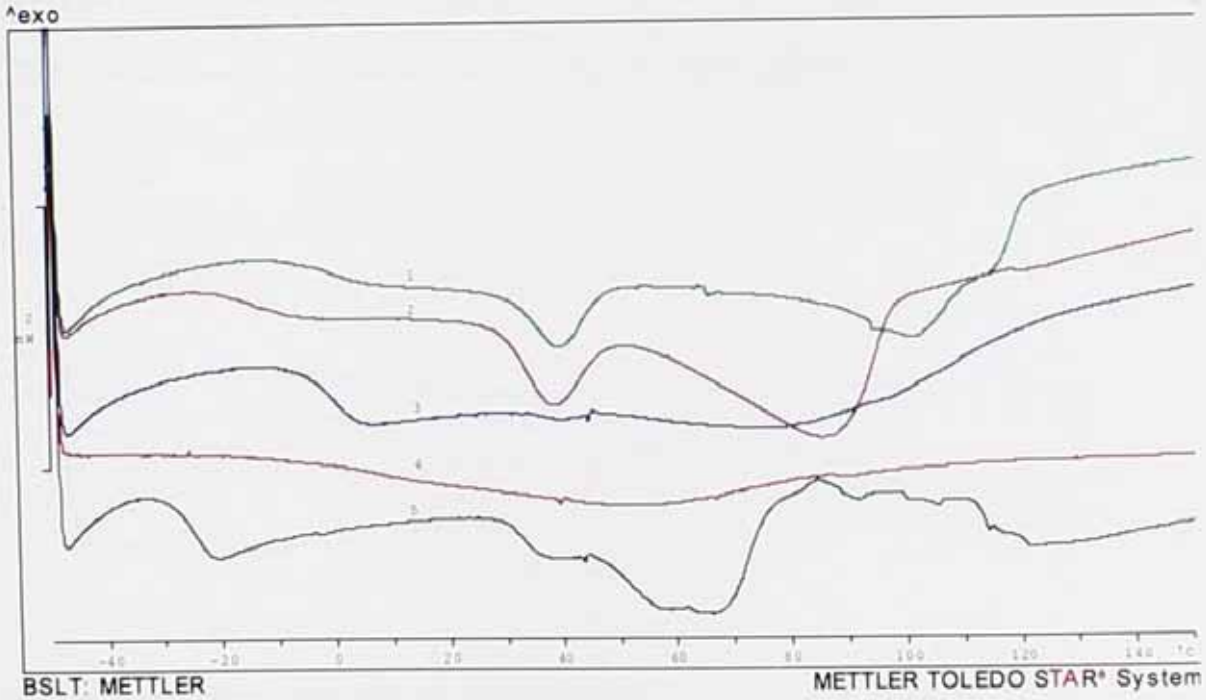

Appendix C3.12

Samples before curing, mole fraction of monomer DHBA in the mixture of DHBA and BEP No. I 100%; No. II is 73.2%; No. III is 51.4%; No. IV is 28.6%; No. 5 is 0%

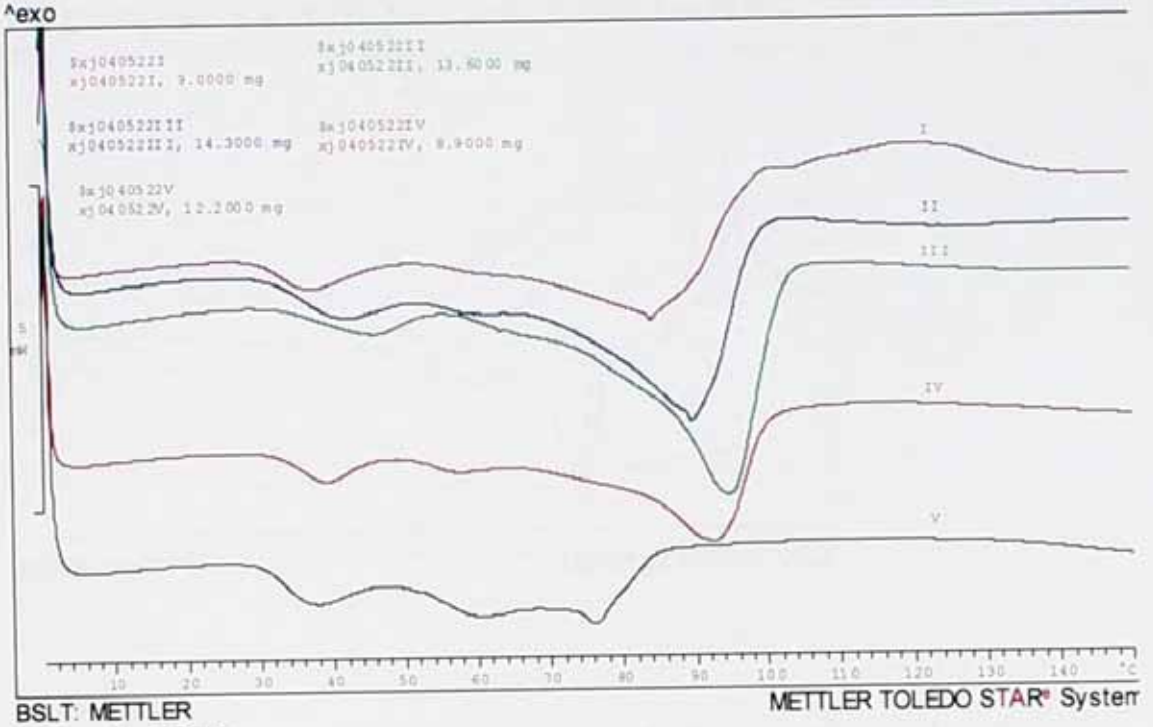

Appendix C3.13

Samples after curing, Mole fraction of monomer DHBA in the mixture of DHBA and BEP No. I 100%; No. II is 73.2%; No. III is 51.4%; No. IV is 28.6%; No. 5 is 0%

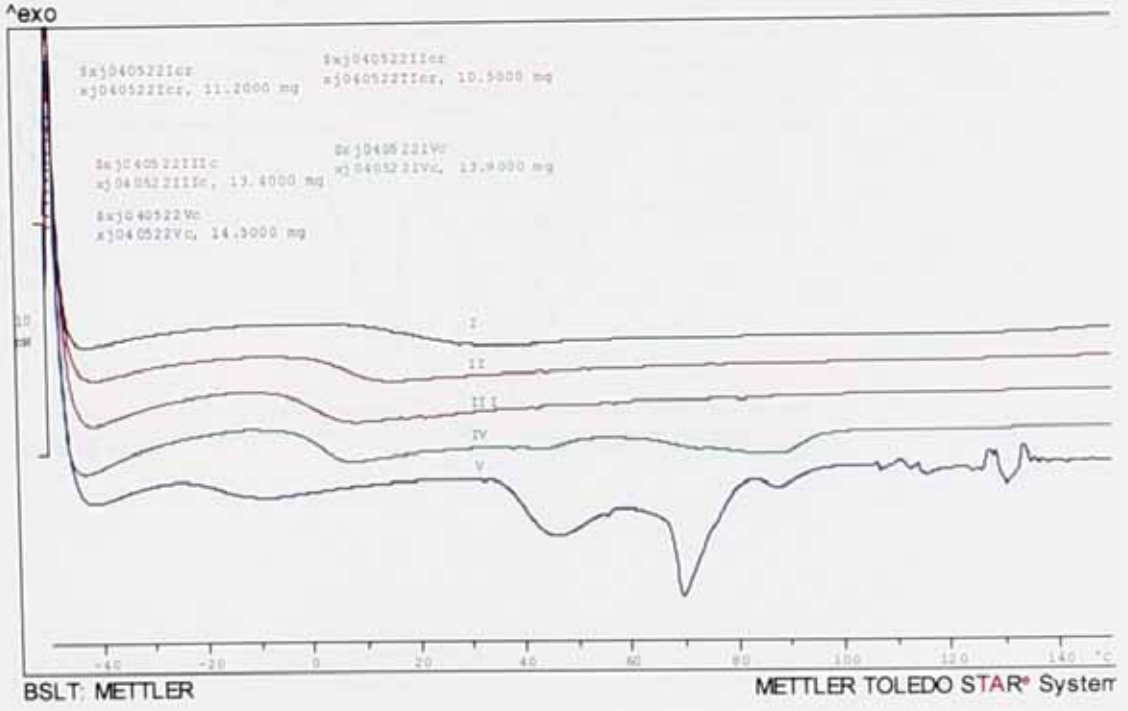

Appendix C3.14
Samples before curing, mole fraction of monomer DHBA in diols No. 1 is 0%; No. 2 is 21.3%; No. 3 is 39.7%; No. 4 is 60.3%; No. 5 is 79.9%

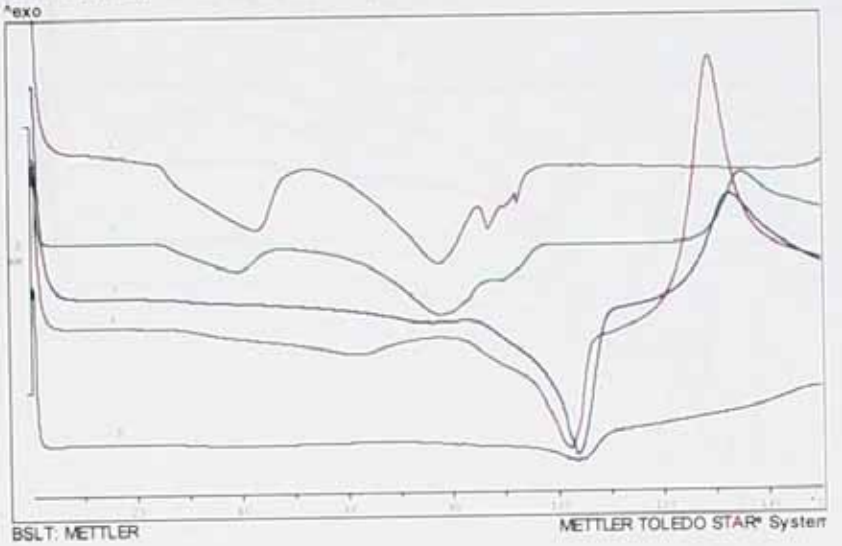

Appendix C3.15
Samples after curing, mole fraction of monomer DHBA in diols No. 1 is 79.9%; No. 2 is 60.3%; No. 3 is 39.7%; No. 4 is 21.3%; No. 5 is 0%

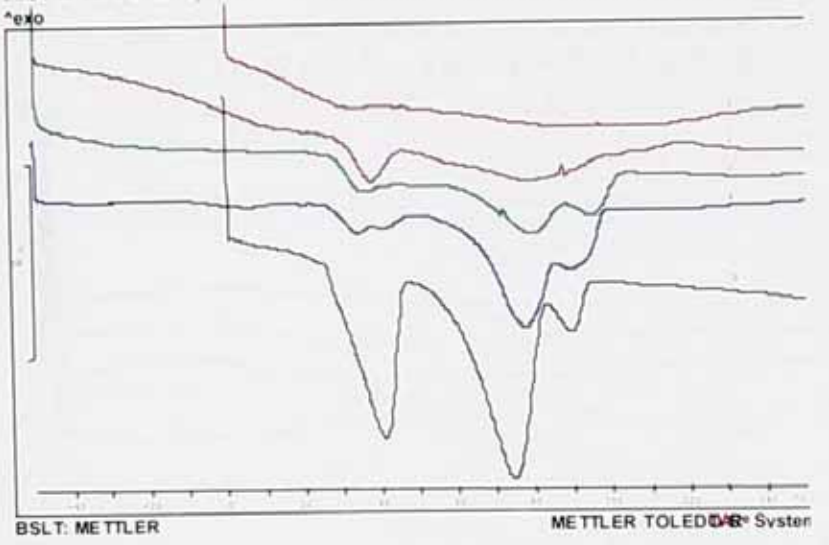

Appendix C3.16
Samples before curing, mole fraction of monomer DHBA in diols No. 1 is 0%; No. 2 is 20.5%; No. 3 is 39.6%; No. 4 is 59.6%; No. 5 is 79.1%

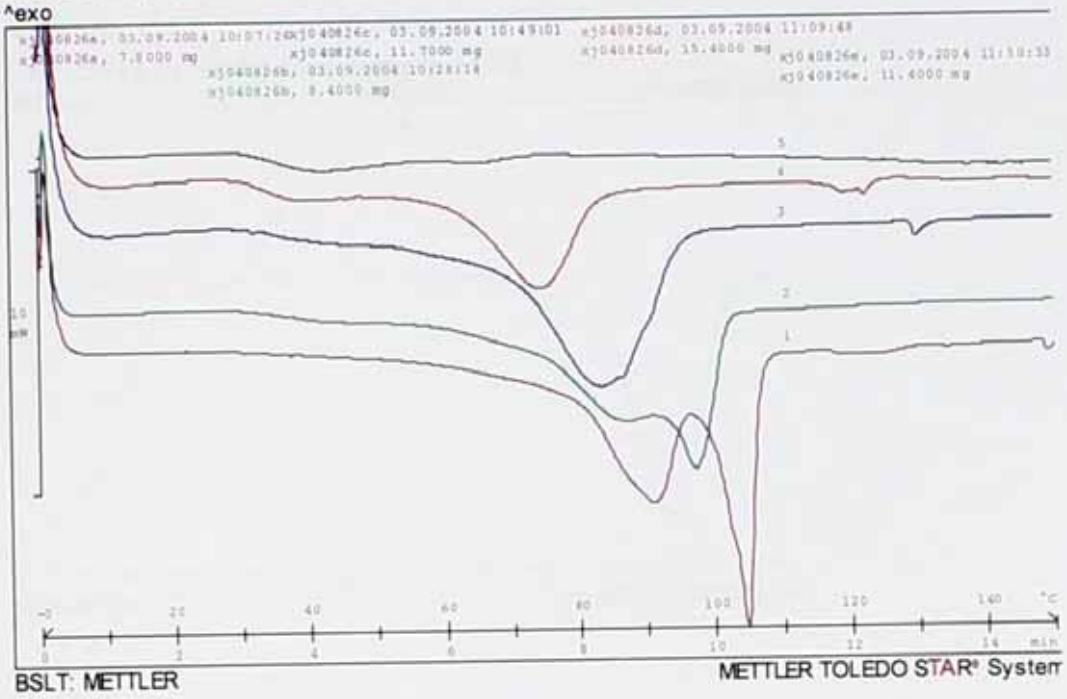

Appendix C3.17
Samples after curing, mole fraction of monomer DHBA in diols No. 1 is 0%; No. 2 is 20.5%; No. 3 is 39.6%; No. 4 is 59.6%; No. 5 is 79.1%

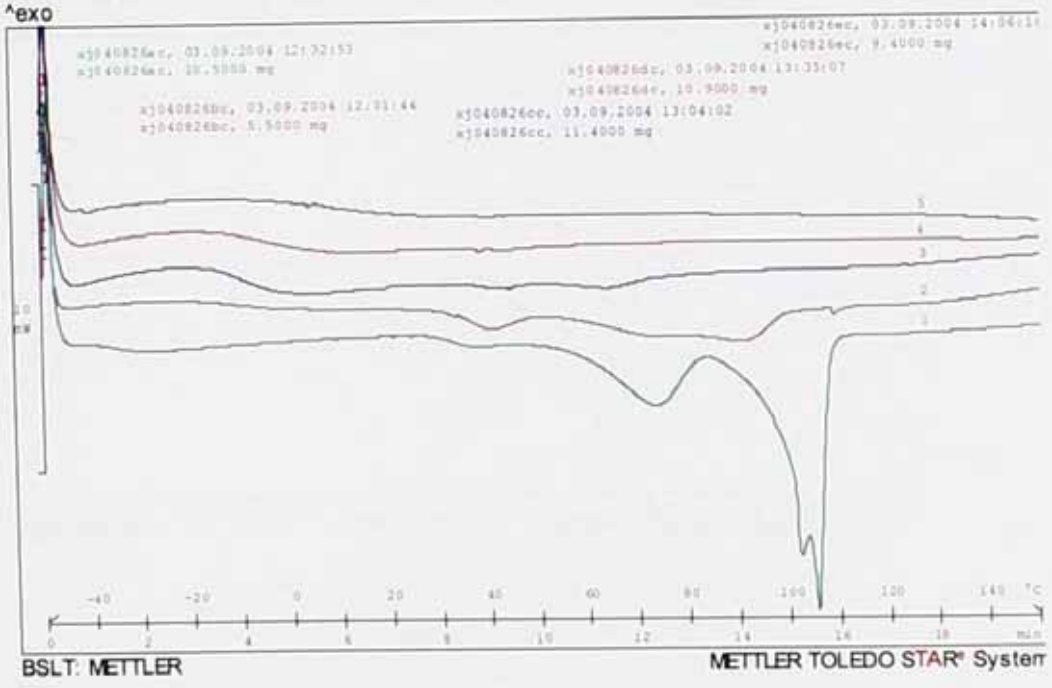

Appendix C4.1
DSC curve of binder resin sample 512B

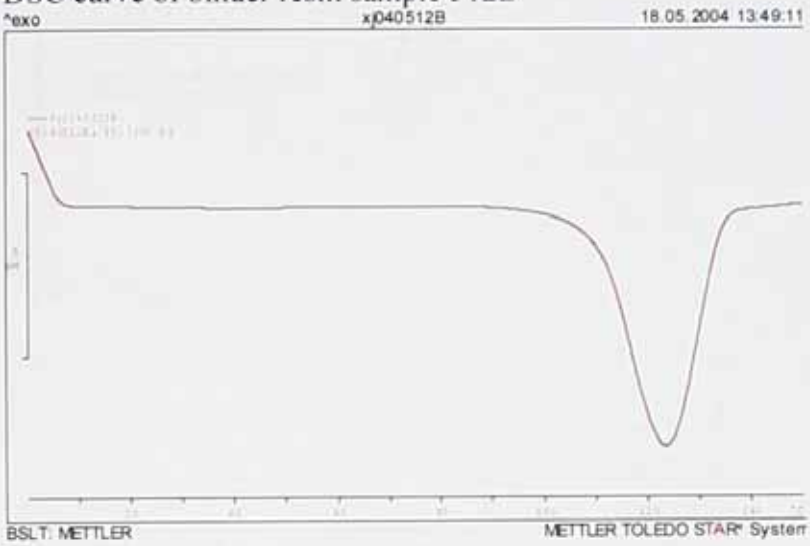

Appendix C4.2
DSC curve of binder resin sample 512E

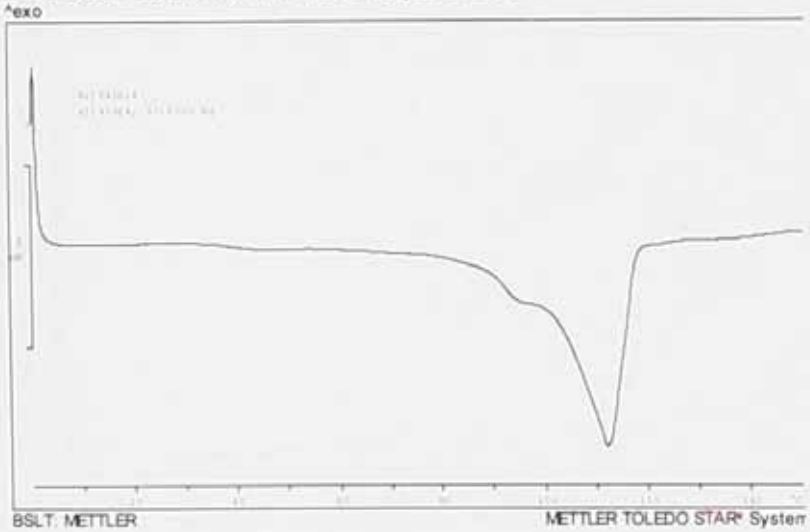

Appendix C4.3
PUA resin PUA-1 DSC curve

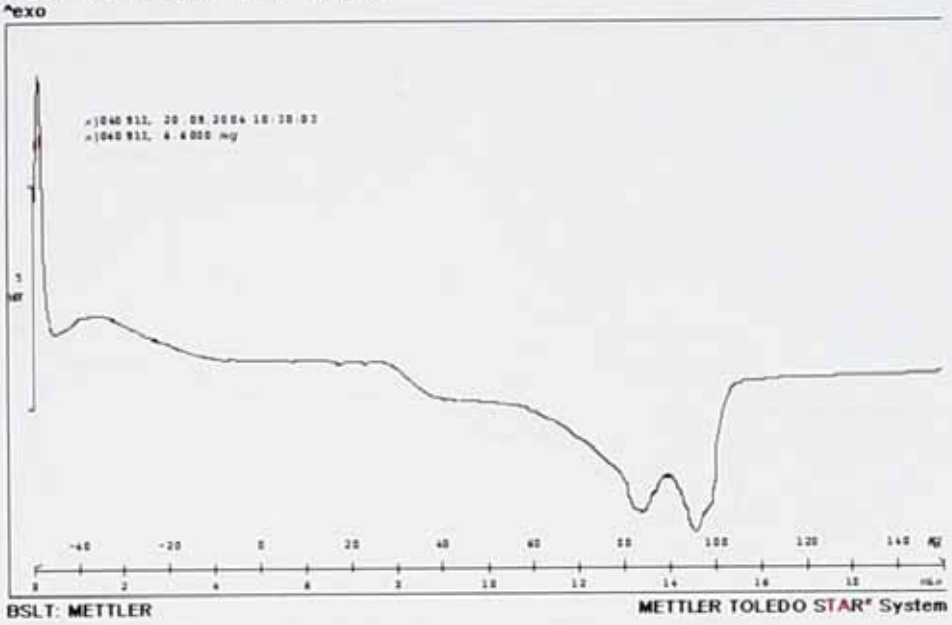

Appendix C4.4
DSC curves of cured powder coating sample PUA-1 with different photo-initiator content

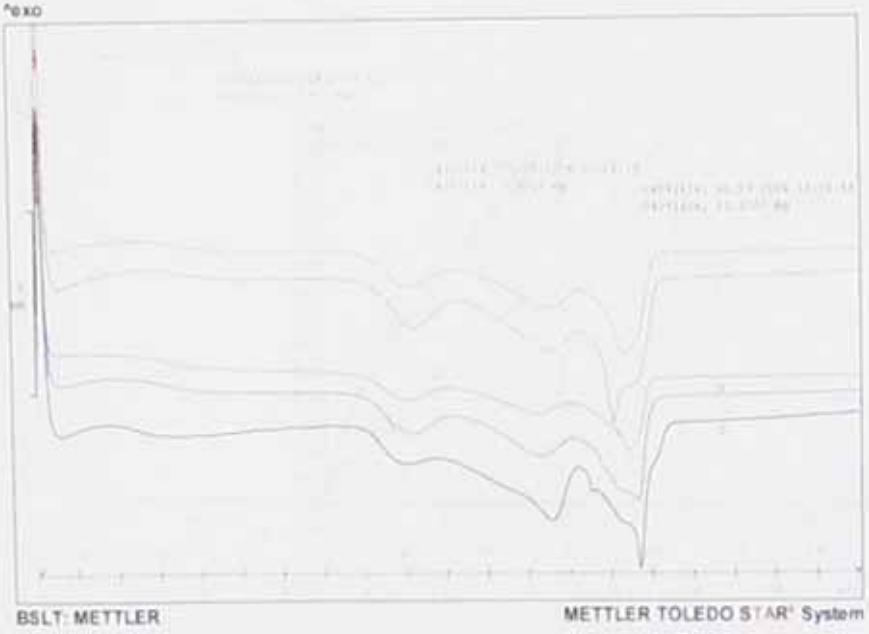

Appendix C4.5
PUA resin PUA-3 DSC curve

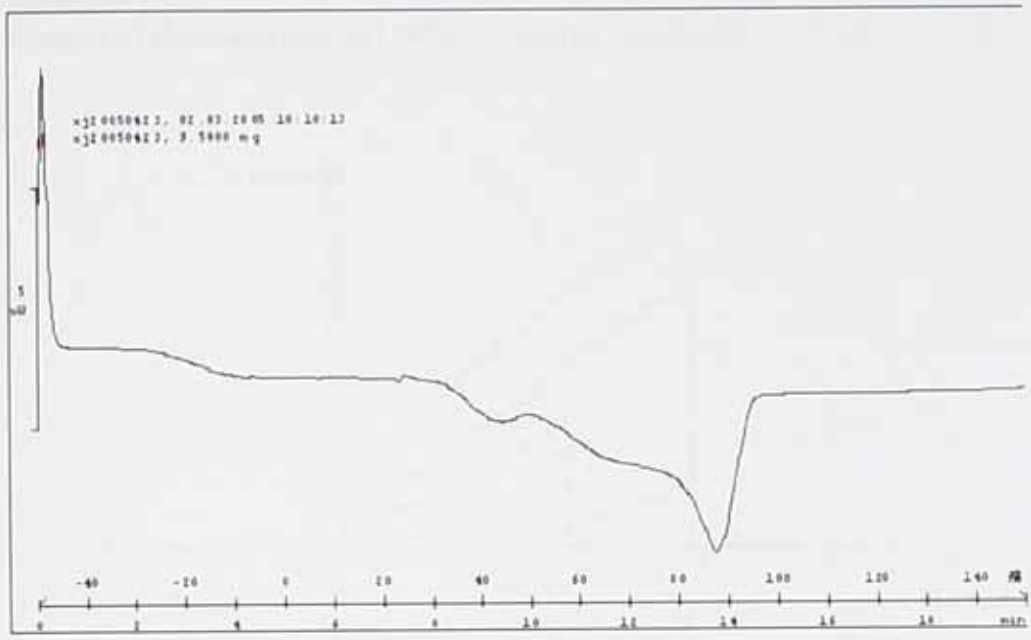

Appendix C4.6
Content of photo-initiator is 0.960%, the tensile samples are la

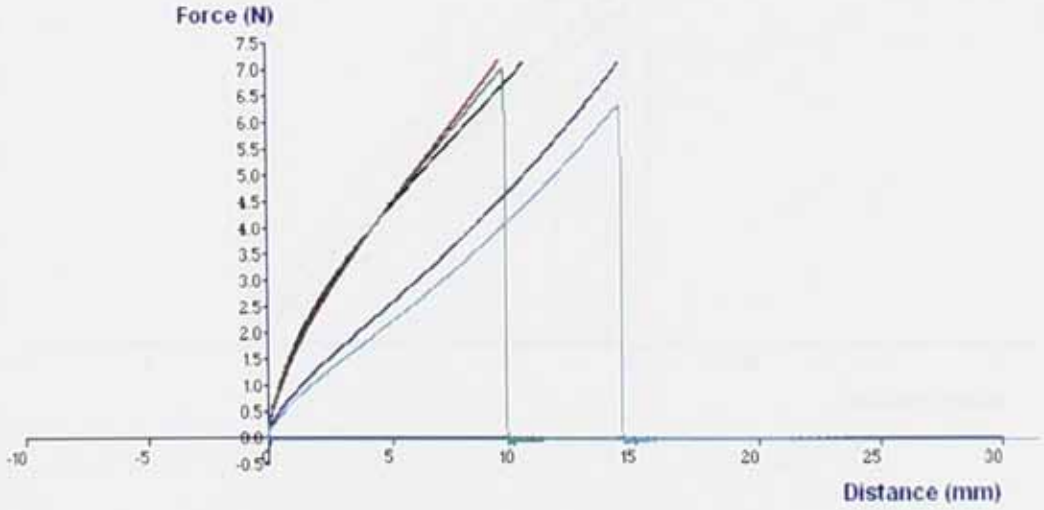

Appendix C4.7
Content of photo-initiator is 1.48%, the tensile samples Ib

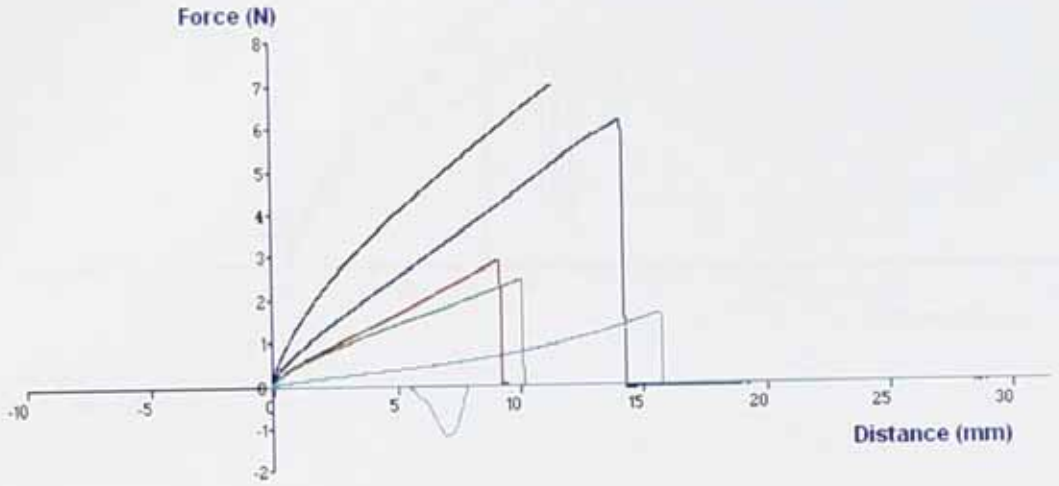

Appendix C4.8
Content of photo-initiator is 2.97%, the tensile samples are Ic

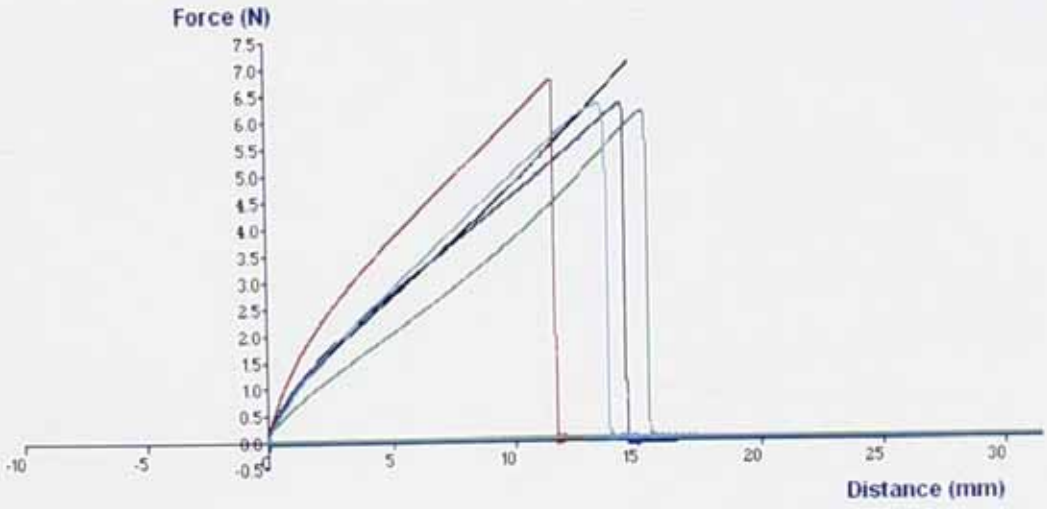

Appendix C4.9
Content of photo-initiator is 5.53%, the tensile samples are Id

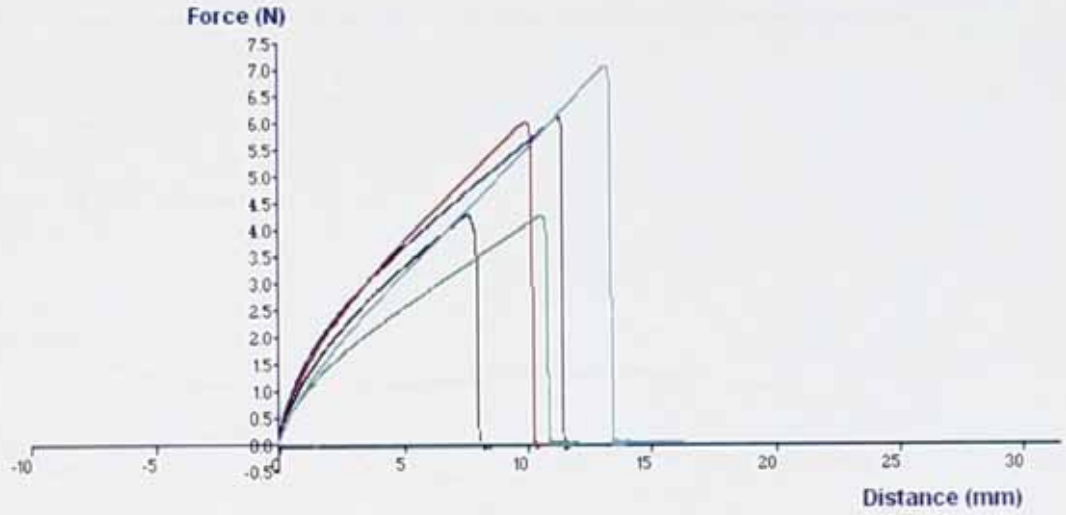

Appendix C4.10
DSC curve a is PUA-2 before viscosity measurement sample PUA-2a

DSC curve b is PUA-2 after viscosity measurement sample PUA-2c

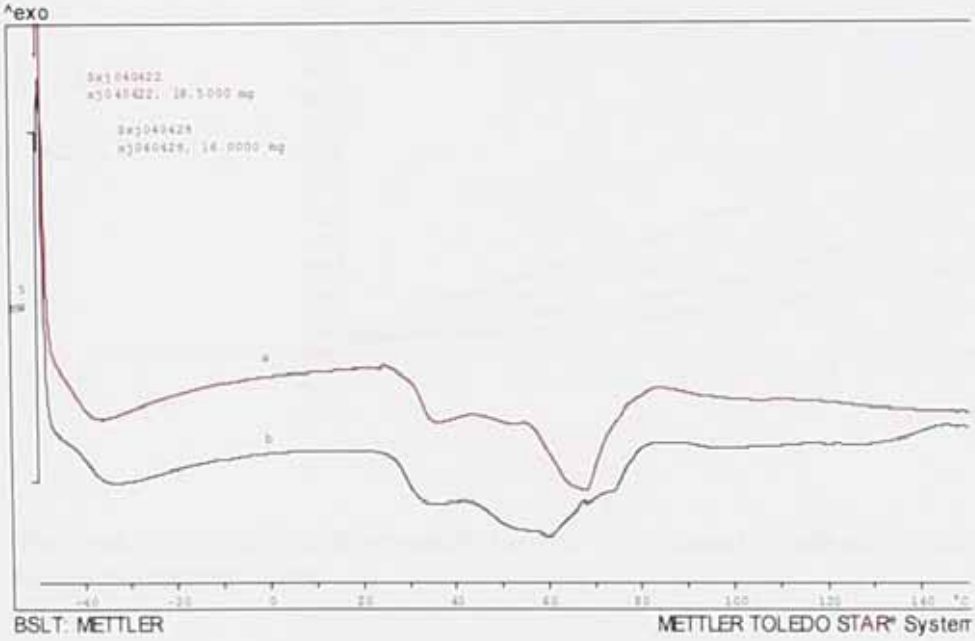

Appendix C4.11
DSC curve PUA-2a is PUA-2 sample before curing

DSC curve PUA-2b is PUA-2 sample after curing

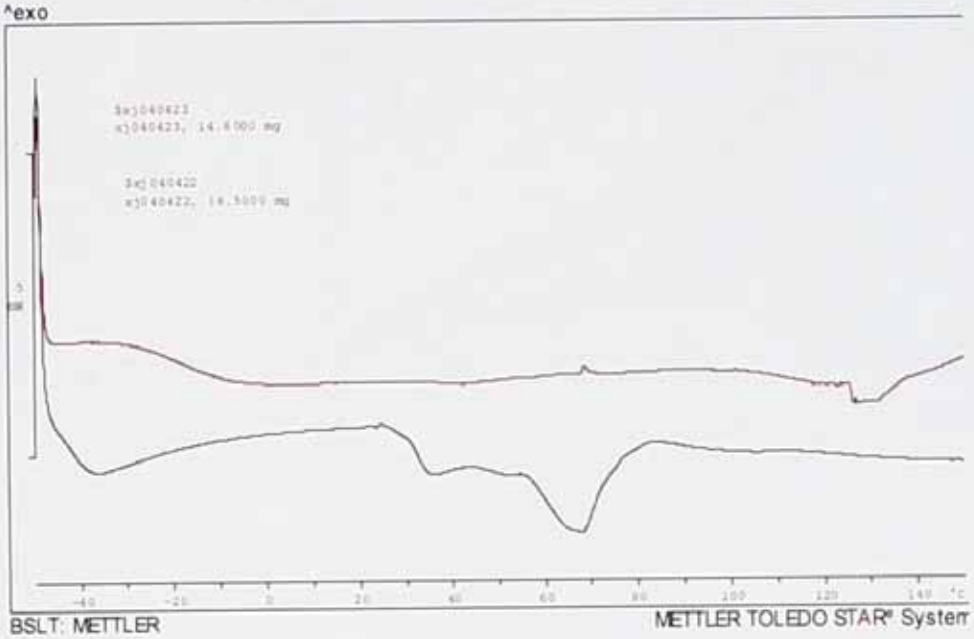

Appendix C4.12
UV radiation intensity is about 1J/cm^2, the tensile samples are Ra

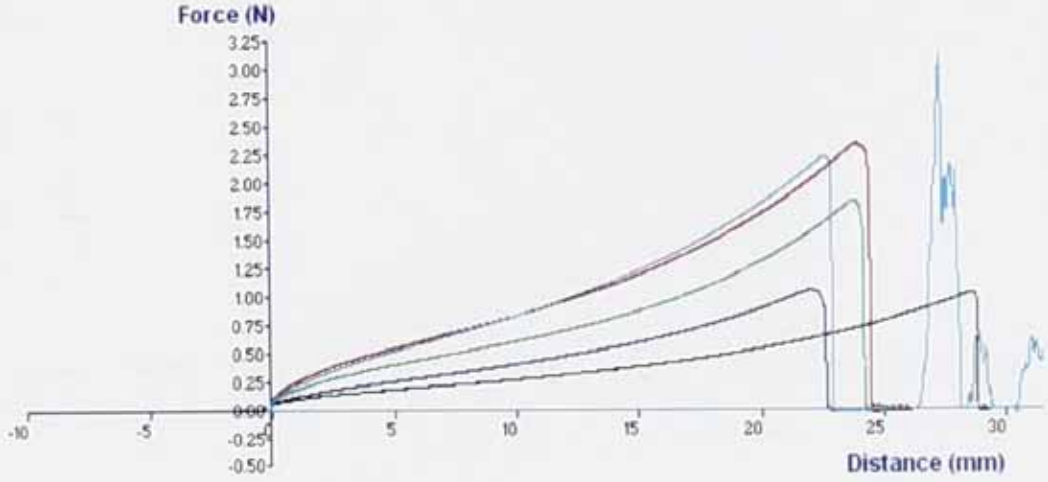

The peaks in the picture after sample broken were caused by removing the specimens before the testing finish.

Appendix C4.13
UV radiation intensity is about 2J/cm^2, the tensile samples are Rb

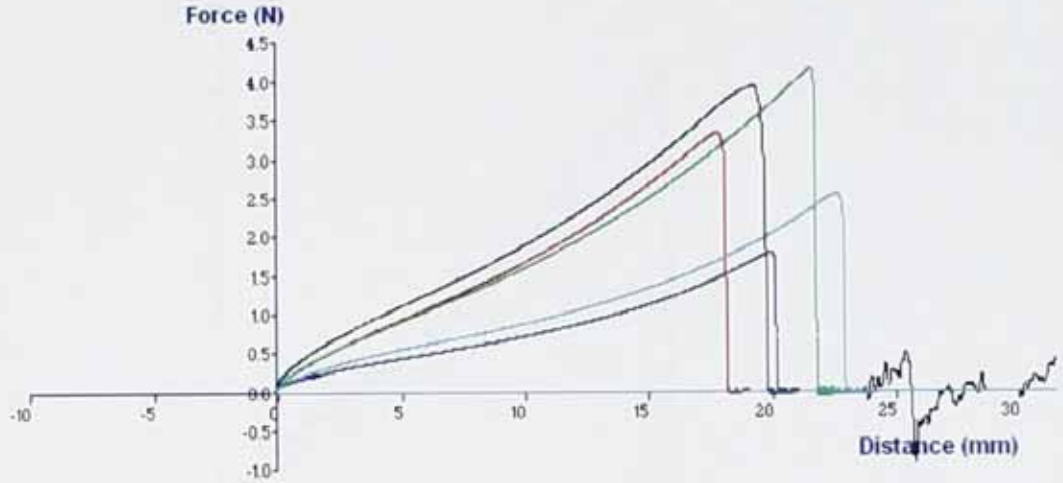

Appendix C4.14
UV radiation intensity is about 3J/cm^2, the tensile samples are Rc

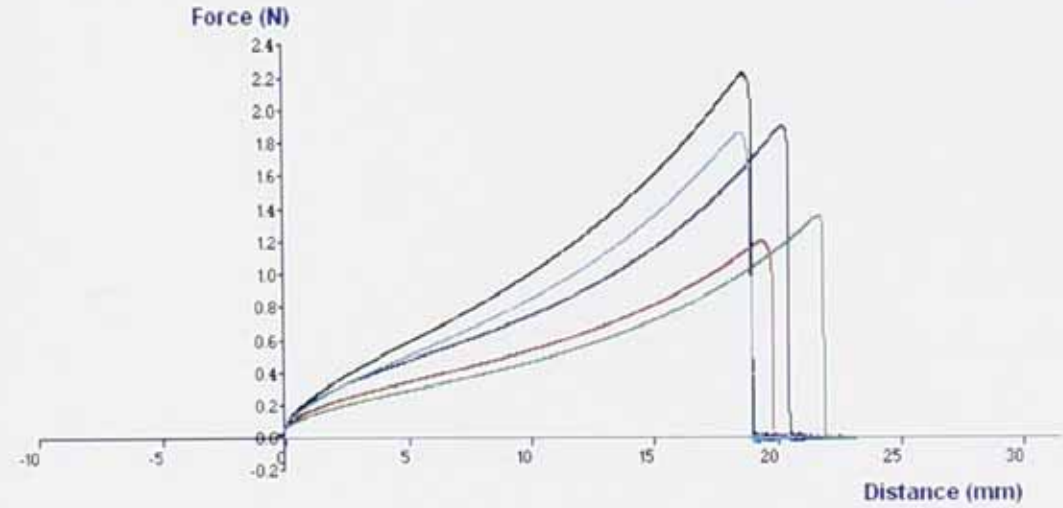

Appendix C4.15
UV radiation intensity is about 4J/cm^2, the tensile samples are Rd

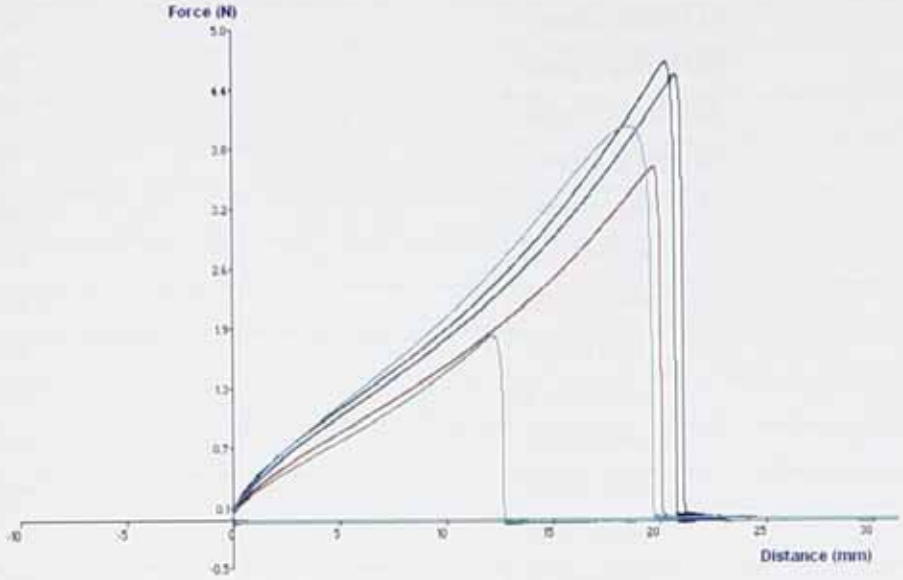

Appendix of Codes

Equivalent New Code	Original Code
512A	Sample xj040512A
512B	Sample xj040512B
512C	Sample xj040512C
512D	Sample xj040512D
512E	Sample xj040514
PU-3a	PU021021d
PU-3b	PU021029b
PU-3c	PU021029c
PU-3d	PU021021d
PU-4a	PU021106a
PU-4b	PU021106b
PU-4c	PU021106c
PU-5a	PU030106a
PU-5b	PU030106b
PU-5c	PU030113c
PU-5d	PU030113a
PU-5e	PU030113b
PU-6	PU041206a
PU-7	PU041217
PUA-1	040913
PUA-2	422
PUA-2a	Xj040422
PUA-2b	Xj040423
PUA-2c	Xj040428
PUA-3	20050423
PUA-4	50428
Ia	20050408Ia
Ib	20050408Ib
Ic	20050408Ic
Id	20050408Id
Ra	20050408Ra
Rb	20050408Rb
Rc	20050408Rc
Rd	20050408Rd

Sil-1	Sil716
Sil-2	Sil315
UVPC-1	0527
UVPC-2	YS
UVPC-3	0601
UVPC-4	0606